Analysis of the role of CDK and ubiquitin E3 ligase activity in regulation of CIZ1 proteostasis

Louise Caprani

Division of Biomedical and Life Sciences

Faculty of Health and Medicine

Lancaster University

A thesis submitted to Lancaster University in fulfilment of the requirements for the degree MSc by Research Biomedical Science

September 2021

Declaration

This dissertation is the result of my own work and has not been previously submitted, in part or whole, for the award of a higher degree qualification at this University or elsewhere.

Louise Caprani

Acknowledgements

I would like to thank my supervisor Dr Nikki Copeland for all of his advice and support throughout the research and writing experience. I would also like to thank my secondary supervisor Dr Sarah Allinson for her support in the lab and advice during lab meetings.

I would like to thank my friends in the lab and outside. Special thanks to Freya Ferguson, James Tollitt and Olivia Iwanowytsch for their technical help and support throughout the research experience. Beyond labmates I would like to thank Megan Dooley and Lauryn Buckley-Benbow for their friendship and all of the support in every step of the way.

I would like to thank my partner, Kane Harding, for all of his support. I would like to give a massive thank you to my parents Claire Caprani and Darren Brown for their continuous support and motivation, I couldn't have done it without you.

List of figures

List of tables

Abbreviations

APC/C	Anaphase promoting complex/ cyclosome
APS	Ammonium persulfate
BSA	Bovine serum albumin
CAPS	3-(Cyclohexylamino)-1-propanesulfonic acid
CDC20	WD-40-domain-cell division cycle protein 20 of APC/C
Cdc25	Cell division cycle 25 phosphatase
Cdc45	Cell division cycle 45
Cdc6	Cell division cycle 6
Cdh1	WD-40 domain substrate adaptor protein of APC/C
CDK	Cyclin dependent kinase
CDKIs	Cyclin dependent kinase inhibitors
Cdt1	Chromatin licensing and DNA replication factor 1
CIZ1	Cip1-interacting zinc finger protein
CMG	Cdc45, Mcm2-7, GINS replicative DNA helicase complex
DAPI	4',6'-diamidino-2-phenylindole
DDK	Dbf4 dependent kinase Cdc7-Dbf4)
DMEM	Dulbecco's Modified Eagles Media
DMSO	Dimethyl Sulfoxide
DNA	Deoxyribonucleic acid
DPBS	Dulbecco's Phosphate-Buffered Saline
DTT	Dithiothreitol
DUB	De-ubiquitinating enzymes
E1	Ubiquitin activating enzyme
E2	Ubiquitin conjugating enzyme
E2F	E2 factor family of transcription factors
E3	Ubiquitin ligase
EDTA	Ethylenediaminetetraacetic acid
EdU	Ethynyl deoxyuridine
ER	Oestrogen receptor
FBXO38	F-box only protein 38

GFP	Green fluorescent protein
GINS	Go Ichi Ni San
HECT E3	Homologous to the E6AP carboxyl terminus ubiquitin ligase
HER2	Human epidermal growth factor receptor 2
LB	Lysogeny broth
MCM2-7	Minichromosome Maintenance Proteins 2-7
MEFs	Murine embryonic fibroblasts
NSCLC	Non-small cell lung cancer
ORC	Origin recognition complex
PCNA	Proliferating cell nuclear antigen
PD	Palbociclib (PD0332991) Isethionate
PFA	Paraformaldehyde
PHA	PHA-767491
PI	Propidium iodide
PMSF	Phenylmethane sulfonyl fluoride
Pre-IC	Pre-initiation complex
Pre-RC	Pre-replication complex
PVDF	Polyvinylidene fluoride
Rb	Retinoblastoma protein
RBR E3	RING between RING ubiquitin ligase
RING E3	Really Interesting New Gene ubiquitin ligase
RNA	Ribonucleic acid
SCF	Skp, Cullin, F-box containing complex
SCLC	Small cell lung cancer
SDS	Sodium dodecyl sulfate
SDS-PAGE	Sodium dodecyl sulfate polyacrylamide gel electrophoresis
shRNA	Short hairpin ribonucleic acid
siRNA	Small interfering ribonucleic acid
Skp2	S-phase kinase-associated protein 2
TAZ	WW domain conjugating transcription regulator 1
TEAD	TEA domain

TEMED	Tetramethylethylenediamine
UBE2O	E3-idenependent E2 ubiquitin-conjugating enzyme E2 O
UBR5	Ubiquitin-protein ligase E3 component n-recognin 5
UPS	Ubiquitin proteasome system
Xist	X-inactive specific transcript
YAP	Yes associated protein

Abstract

Cip1 interacting Zinc finger protein 1 (CIZ1) is a nuclear matrix protein and coordinates the activity of cyclin A- cyclin dependent kinase 2 (CDK2) for efficient initiation of DNA replication. The overexpression of CIZ1 has been associated with tumorigenesis in several common cancers including breast, prostate, colorectal, gall bladder and hepatocellular carcinoma, this suggests that CIZ1 may be a viable target for therapeutic intervention in CIZ1-dependent cancers. The working model for CIZ1 regulation suggests that CIZ1 protein levels are regulated by DDK/CDK2 mediated phosphorylation which protects from ubiquitin proteasome system (UPS) mediated degradation. Furthermore, inhibition of DDK/ CDK2 may facilitate the UPS-mediated degradation of CIZ1. The UPS-mediated degradation of CIZ1 would be dependent on a functional UPS, therefore the E3 ligases that target CIZ1 may represent biomarkers for patient stratification when determining which patients would respond to CDK inhibitors as a way of reducing CIZ1 levels. Further characterisation of the molecular pathways that regulate CIZ1 levels could provide potential avenues for reducing CIZ1 in cancer. Here, the efficacy of small molecule CDK/DDK inhibitors to reduce CIZ1 levels was evaluated in murine fibroblasts. Furthermore, three E3 ligases (UBR5, FBXO38 and UBE2O) that potentially target CIZ1 were transfected into 3T3 cells in order to characterise their potential role in regulating CIZ1 protein levels. In this study, inhibition of CDK4/6, DDK and CDK2 resulted in a non-significant reduction in CIZ1 levels during G1/S. Furthermore, inhibition of CDK1 resulted in a non-significant reduction in CIZ1 levels later in the cell cycle. Inhibition of DDK/CDK2 potentially facilitates the UPS mediated degradation of CIZ1, inhibition of the proteasome using MG132 prevented CIZ1 degradation with concomitant inhibition of DDK or CDK2. For E3 transfection experiments, there was difficulty validating E3 expression in the 3T3 cells. Nevertheless, there was a non-significant reduction in CIZ1 levels in cells transfected with UBR5-GFP or FBXO38-FLAG. Together the findings suggest that manipulation of CIZ1 regulators could provide an avenue to reduce CIZ1 levels, however the findings are preliminary and further validation of the findings is required in future work.

Table of contents

Chapter 1: Introduction

1.1. Introduction

Cip1 interacting Zinc finger protein 1 (CIZ1) has diverse activities in the regulation of the cell cycle, X chromosome inactivation and epigenetic maintenance in healthy cells (Copeland *et al.,* 2010; Copeland *et al.,* 2015; Coverley *et al.,* 2005; Ridings-Figueroa *et al.,* 2017; Stewart *et al.,* 2019). However, in cancer CIZ1 has been associated with tumourigenesis and has been found to be required for tumour growth in several xenograft models (Den Hollander *et al.,* 2006; Higgins *et al.,* 2012; Liu *et al.,* 2015; Wu *et al.,* 2016; Zhang *et al.,* 2015). This suggests that CIZ1 may be a viable target in cancer. There are at present no direct approaches to therapeutically target CIZ1. In this project, the signalling pathways that regulate CIZ1 protein levels will be investigated and the efficacy of reducing CIZ1 levels by modulation of the cyclin dependent kinase activity and the proteasome will be evaluated. The targeting of these post-translational regulatory pathways may be of clinical benefit for the treatment of cancer. This review will describe the role of CIZ1 in cell cycle regulation, define its role in tumourigenesis and describe the role of cyclin dependent kinase activity and the proteasome in cell cycle regulation and their potential role in the regulation of CIZ1 protein levels.

1.2. Cip-1 interacting zinc-finger protein (CIZ1) structure

CIZ1 was discovered as a binding partner of the CDK2 inhibitor protein $p21^{Cip1/Waf1}$ (Mitsui *et al*., 1999). Human CIZ1 is 842 amino acid residues in length and has an estimated 70% homology with murine CIZ1. (Coverley *et al.,* 2005), therefore murine systems are often used to study CIZ1 (Ainscough *et al.,* 2007; Copeland *et al.,* 2010; Copeland *et al.,* 2015; Coverley *et al.,* 2005; Nishibe *et al.,* 2013; Mitsui *et al.,* 1999). The domain structure of CIZ1 includes two glutamate-rich domains, three zinc finger domains, an acidic domain and matrin 3-homologoug domain 3 (MH3) (Ainscough *et al.,* 2007; Coverley *et al.,* 2005; Mitsui *et al.,* 1999; Warder and Keherly, 2003). The zinc finger domain has a role in binding DNA and the acidic domain has a role in protein interaction (Gin *et al.,* 2008; Klug, 2010). The C-terminal domain of CIZ1 interacts with the nuclear matrix (Ainscough *et al.,* 2007) and the N terminal has binding sites for cell division cycle 6 (Cdc6) and cyclin A-CDK2 (Copeland *et al.,* 2015; Pauzaite *et al.,* 2016).

1.3. The role of CIZ1 in the initiation of DNA replication

CIZ1 is a nuclear protein and biochemical analysis has demonstrated interaction of CIZ1 with p21 (Mitsui *et al.,* 1999). It has been proposed that CIZ1 could bind and sequester the CDK2 inhibitor p21, thereby providing a mechanism for the increase in CDK2 activity in G1 of the cell cycle. However, a study has shown that the expression of CIZ1 in p21 null murine embryonic fibroblasts (MEFs) stimulates DNA synthesis demonstrating that the role of CIZ1 in the initiation of DNA replication is not dependent on modulating p21 activity (Coverley *et al.,* 2005). CIZ1 has a role in the initiation of DNA replication (Figure 1.1) (Copeland *et al.,* 2010; Copeland *et al.,* 2015; Coverley *et al.,* 2005), this is dependent on the ability of CIZ1 to bind cyclin E and cyclin A and facilitate the timely localisation of cyclin A-CDK2 to origins of replication. CIZ1 binds cyclin E then cyclin A in a two-step process to provide spatio-temporal control of cyclin activity during the initiation of DNA replication (Copeland *et al.,* 2010; Copeland *et al.,* 2015). In early G1 of the cell cycle, CIZ1 is able to bind to cyclin E and this is followed by Cdc6 recruitment and subsequent pre-replication complex formation (Copeland *et al.,* 2015). In late G1 the expression of cyclin A increases leading to the displacement of cyclin E by cyclin A-CDK2 (Copeland *et al.,* 2010). CIZ1 contains 16 putative phosphorylation sites and Cyclin A-CDK2 phosphorylates CIZ1 on residues T144, T192 and T293, this prevents binding of cyclin A-CDK2 and the replication activity of CIZ1 is reduced (Copeland *et al.,* 2015). Cyclin A-CDK2 also mediates Cdc6 phosphorylation, phosphorylation of Cdc6 leads to its cytoplasmic localisation (Delmolino *et al.*, 2001). The subsequent recruitment of proliferating cell nuclear antigen (PCNA) and DNA polymerase α allows DNA replication to be initiated (Bell and Dutta, 2002).

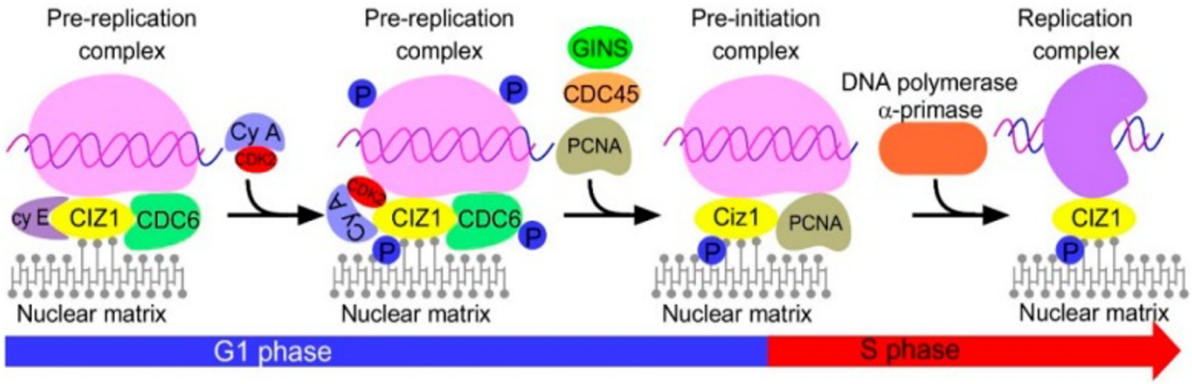

Figure 1.1. The role of CIZ1 in the initiation of DNA replication. In early G1, CIZ1 is able to bind cyclin E and Cdc6 resulting in the assembly of the pre-replication complex (Copeland et al., 2015). The increase in cyclin A levels during late G1 results in cyclin E being displaced by cyclin A-CDK2 (Copeland et al., 2010). CIZ1 and Cdc6 are subsequently phosphorylated and Cdc6 is replaced by PCNA (Copeland et al., 2015). Recruitment of GINS and Cdc45 allows assembly of the pre-initiation complex (Liu et al., 2016). Binding of DNA polymerase completes the replication complex. Abbreviations: Cdc45: Cell division cycle 45; Cdc6: Cell division cycle 6; GINS: Go Ichi Ni San; PCNA: Proliferating cell nuclear antigen. Figure from Liu et al., (2016).

CIZ1 may have a role as a kinase sensor and this prevents the re-replication of DNA. At low kinase levels during late G1, CIZ1 is hypophosphorylated and able to interact with cyclin A-CDK2 to facilitate the localisation to chromatin. As kinase levels increase, CIZ1 becomes hyperphosphorylated and unable to interact with cyclin A-CDK2 preventing DNA replication, thereby preventing the re-replication of DNA (Copeland *et al.,* 2015). As CIZ1 acts as a kinase sensor and involved in regulating the threshold of CDK activity at which DNA replication can occur, CIZ1 may contribute to tumourigenesis by allowing DNA replication to occur at high CDK level that would usually be non-permissive for DNA replication thereby leading to DNA replication stress (Pauzaite, *et al.,* 2016).

1.4. The role of CIZ1 in tumourigenesis

Overexpression of CIZ1 or alternative splice variants of *CIZ1* transcript can drive tumour growth. CIZ1 is associated with common cancers including breast, prostate, colorectal, hepatocellular carcinoma, gall bladder cancer and small cell (SCLC) and non-small cell lung cancer (NSCLC) (Den Hollander and Kumar, 2006; Den Hollander *et al.,* 2006; Higgins *et al.,* 2012; Lei *et al.,* 2016; Liu *et al.,* 2015; Wang *et al.,* 2014; Wu *et al.,* 2016; Yin *et al.,* 2013; Zhang *et al.,* 2015) where CIZ1 contributes to the hallmarks of cancer as described by Hanahan

and Weinberg, (2011). Importantly, CIZ1 is non-essential for murine development, an *in vivo* study found mice lacking CIZ1 grew with no developmental abnormalities during embryonic development and postnatal growth (Nishibe *et al.,* 2013), this suggests that CIZ1 is non-essential for murine development providing the basis that CIZ1 may be a viable therapeutic target. There is some evidence that CIZ1 has a tumour-suppressor function as CIZ1 (-/-) MEFs are susceptible to viral oncogenesis (Nishibe *et al.,* 2013). Dysregulation of CIZ1 can also contribute to lymphoproliferative disorders, CIZ1 has a role in the localisation of Xist at the inactive X chromosome and in CIZ1 null mice the localisation of Xist is disrupted in activated lymphocytes (Ridings-Figueroa *et al.,* 2017; Stewart *et al.,* 2019). Together the findings highlight the importance of normal CIZ1 levels. However, there is evidence demonstrating CIZ1 differential splicing, overexpression and transcriptional regulation contribute to tumourigenesis.

1.4.1. The role of CIZ1 alternative splice variants in cancer

The *CIZ1* gene contains 18 exons (Liu *et al.,* 2016). Variant CIZ1 with the alternative splicing of exon 4 is found in Ewing's tumour cells, omission of exon 4 affects the nuclear distribution of CIZ1 and the organisation of DNA replication (Rahman *et al*., 2007). Alternative splicing between exon 14 and 15 leads to the production of b-variant CIZ1 identified in small cell lung cancer (SCLC) and non-small cell lung cancer (NSCLC) and is restricted to tumour cells. Targeting the b-variant CIZ1 using short hairpin (sh)RNA reduces tumour growth in a xenograft model of SCLC (Higgins *et al.,* 2012). A further CIZ1 spice variant leading to truncation of CIZ1 is called CIZ1-F variant and is elevated in early-stage colon and breast solid tumours (Swarts *et al.,* 2018). CIZ1 splice variants could be used as diagnostic biomarkers in cancer, a quantitative immunoassay has been developed for the detection of the CIZ1 b-variant, a lung cancer biomarker (Coverley *et al.,* 2017).

1.4.2. The role of CIZ1 overexpression in cancer

The overexpression of CIZ1 has been liked to tumourigenesis in breast, prostate, colorectal, gall bladder and hepatocellular carcinoma (Den Hollander and Kumar, 2006; Den Hollander *et al.,* 2006; Lei *et al.,* 2016; Liu *et al.,* 2015; Wu *et al.,* 2016; Yin *et al.,* 2013; Zhang *et al.,* 2015), in all cases CIZ1 was found to promote proliferation. CIZ1 overexpression can promote

migration and invasion (Wu *et al.,* 2016; Zhang *et al.,* 2014; Zhou *et al.,* 2018) and can contribute to evasion of tumour suppressors (Den Hollander and Kumar, 2006). Studies investigating the role of CIZ1 in cancer demonstrate that small interfering (si)RNA mediated depletion of CIZ1 can reduce proliferation and migration *in vitro* (Higgins *et al.,* 2012; Lei *et al.,* 2016; Liu *et al.,* 2015; Yin *et al.,* 2013; Wu *et al.,* 2016; Zhang *et al.,* 2015) and inhibit tumour growth in several xenograft models (Higgins *et al.,* 2012; Liu *et al.,* 2015; Wu *et al.,* 2016; Zhang *et al.,* 2015). In addition, CIZ1 levels can provide information on the stage of cancer. In colorectal tumours CIZ1 expression has been shown to be increased in tumour tissue in comparison to adjacent healthy tissue and CIZ1 expression levels correlated to the stage of colon cancer (Wang *et al.,* 2014).

1.4.3. The role of CIZ1 in oncogenic transcriptional regulation

CIZ1 has also been shown to contribute to tumourigenesis based on its role in oncogenic transcriptional regulation. In breast cancer, CIZ1 can promote oestrogen receptor (ER) transactivation by facilitating the recruitment of ER to the promoter region of oestrogen-responsive genes. *CIZ1* is an oestrogen-responsive gene as demonstrated in MCF7 and ZR-75 breast cancer cell lines. A positive feedback loop is formed as CIZ1 sensitizes breast cancer cells to oestrogen, subsequent ER signalling leads to CIZ1 expression and further sensitisation of the cells to oestrogen leading to oestrogen hypersensitivity in breast cancer. The overexpression of CIZ1 increased the proliferation of ZR-75 human breast ductal carcinoma cells demonstrating a role of CIZ1 in promoting tumourigenesis in breast cancer (Den Hollander *et al.,* 2006). CIZ1 is also able to interact with oestrogen receptor (ER) coactivator Dynein Light Chain 1 (DLC1) and translocate to the nucleus, ultimately sequestering p21 and subsequently leading to an increase in CDK2 activity and progression of the cell cycle (Den Hollander and Kumar, 2006).

CIZ1 has an oncogenic role in hepatocellular carcinoma (HCC) as CIZ1 is able to activate (Yes-associated protein/ Transcriptional co-activator with PDZ-binding motif (YAP/TAZ) signalling. YAP and TAZ function as transcriptional regulators, this requires interaction with TEA domain family member (TEAD) transcription factors (Lin *et al.,* 2017). YAP/TAZ-TEAD signalling regulates the expression of cyclin E and connective tissue growth factor (CTGF), therefore

activation of YAP/TAZ signalling by CIZ1 enhances growth and migration which contributes to tumourigenesis (Lei *et al.,* 2016; Wu *et al.,* 2016). The siRNA-mediated depletion of CIZ1 can reduce the expression of genes that are regulated by YAP (Lei *et al.,* 2016). Furthermore, the knockdown of CIZ1 in HepG2 and Huh-7 hepatocellular carcinoma cell lines inhibited growth and migration (Wu *et al.,* 2016).

CIZ1 levels are found to be higher in gall bladder cancer tissue samples in comparison to adjacent healthy tissue (Zhang *et al.,* 2015). The overexpression of CIZ1 in human gall bladder cancer cell lines has been shown to promote tumourigenesis. The role of CIZ1 in promoting tumourigenesis in gall bladder cancer is potentially mediated through the ability of CIZ1 to activate beta-catenin/ T- cell factor (TCF) signalling in gall bladder cancer cells, this pathway can lead to the transcription of oncogenes including cyclin D (Zhang *et al.,* 2015). Together the findings demonstrate an oncogenic role of CIZ1 when overexpressed.

An understanding of the signalling networks that regulate CIZ1 protein levels may provide avenues for targeting CIZ1 in cancer. The activity of CIZ1 during the initiation of DNA replication is regulated by CDK-mediated phosphorylation (Copeland *et al* 2010; Copeland *et al.,* 2015). Preliminary work suggests a role of CDK-mediated phosphorylation and UPS-mediated degradation in the regulation of CIZ1 protein levels (Pauzaite, 2019). CDK and UPS activity regulates cell cycle progression, and the dysregulation of their activity can contribute to tumourigenesis (Bochis *et al.,* 2015; Peyressatre *et al.,* 2015).

1.5. The role of cyclin-CDKs in the cell cycle

The cell cycle consists of four ordered phases including growth phase 1 (G1), DNA replication (S), growth phase 2 (G2) and mitosis (M) (Bajar *et al.,* 2016; Vermeulen *et al.,* 2003). In G1 the cell prepares for DNA replication and the length of G1 can vary dependent on external conditions, if the external conditions are unfavourable the cell can enter a non-replicative quiescent state (G0) until extracellular conditions are favourable (Grant and Cook, 2017). In S phase the genome is replicated and in G2 the DNA is checked to ensure faithful replication. In M phase the chromosomes are segregated equally between two daughter cells (Vermeulen *et al.,* 2003).

Cyclin-dependent kinases (CDKs) are considered 'master regulators' of the cell cycle and there are over 20 members of the CDK family in the mammalian genome. CDKs are serine/ threonine kinases and are inactive in the monomeric form. Interaction of CDKs with cognate regulatory subunits, cyclins, activates the kinase activity of CDKs and subsequent phosphorylation of proteins involved in cell cycle progression (Ding *et al.,* 2020). The mammalian genome contains approximately 30 cyclins, but only cyclins A, B, D and E have major roles in coordinating the cell cycle (Malumbres, 2014). Cyclin binding to its cognate CDK binding partner induces a physical conformational change. For CDK1 and 2 this facilitates phosphorylation by CDK-Activating Kinase (CAK) on threonine (T160) that greatly enhances its catalytic activity (Li *et al.,* 2015). In addition, CDK is also controlled via phosphorylation of residues threonine (Thr14) and tyrosine (Tyr15) that inhibit its catalytic activity (Baldwin, 2009). Phosphorylation at these sites are removed by the cell division cycle 25 (Cdc25) family of protein phosphatases (Boutros *et al.,* 2006). As the activity of CDKs must be precisely regulated there is also inhibitor proteins that associate with specific cyclin-CDK complexes. These proteins are collectively called CDK inhibitors (CDKIs) and include inhibitors of CDK4 (INK4) proteins ($p16^{INK4a}$, $p15^{INK4b}$, $p18^{INK4c}$, $p19^{INK4d}$) that inhibit both CDK4 and CDK6 and CDK-interacting protein/ Kinase inhibitory protein (Cip/Kip) ($p21^{CIP1}$, $p27^{INK4}$, $p57^{KIP2}$) which inhibit cyclin-CDK1/2 complexes (Quereda *et al.,* 2015).

The activity of CDKs is controlled by the temporally regulated transcription and degradation of cyclins. This leads to oscillation of cyclin-CDK activities which is important in maintaining the unidirectionality of the cell cycle (Benanti, 2012). In early G1 cyclin D is expressed, this is followed by cyclin E during mid-G1, cyclin A during late G1 and cyclin B at late G2 (Figure 1.2) (Gérard and Goldbeter, 2009; Malumbres, 2014; Peyressatre *et al.,* 2015). The sequential activation of cyclin-CDK complexes promotes a smooth increase in kinase activity throughout the cell cycle that is represented by the quantitative model of CDK activity that defines CDK thresholds required for G1/S transition and G2/M transition (Stern and Nurse, 1996).

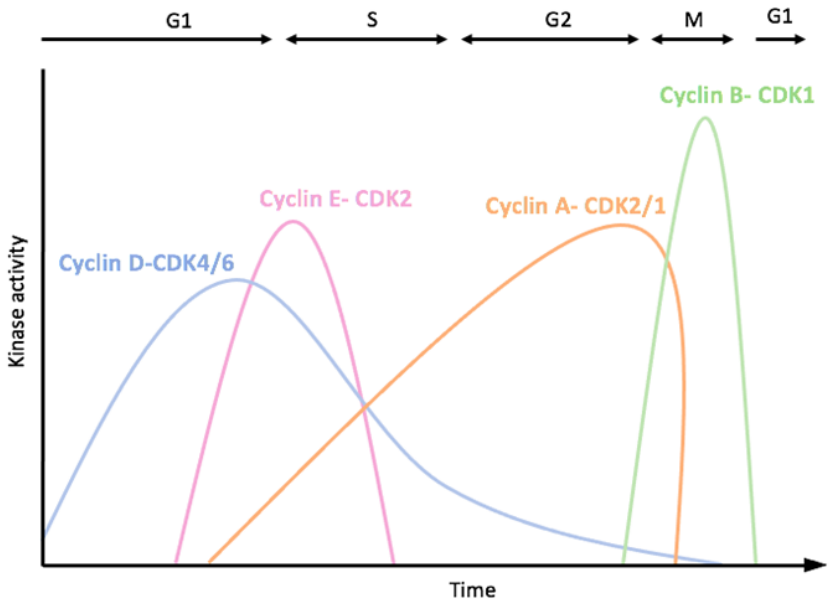

Figure 1.2. The sequential expression of cyclins. The oscillation of cyclin-CDK activities drives progression through the cell cycle phases. Cyclin D activates CDK4/6 (early G1), cyclin E activates CDK2 (mid G1), cyclin A activates CDK2 (late G1) and CDK1 (G2). Cyclin B activates CDK1 (late G2). Gérard and Goldbeter, (2009).

In early G1, cyclin D is expressed. Cyclin D1-3 bind to either CDK4 or CDK6, the activation of cyclin D-CDK4/6 leads to the mono-phosphorylation of retinoblastoma (Rb) (Narasimha *et al*., 2014). Rb phosphorylation and release of E2F transcription factor leads to transcription of cyclins E and A that phosphorylate Rb. Hyperphosphorylation of Rb allows cells through restriction point (G1 checkpoint) (Moser *et al.,* 2018), the point in which cells commit to the cell cycle and cell division becomes independent from mitogens (Blagosklonny and Pardee, 2002; Moser *et al.,* 2018). Cyclin E-CDK2 promotes the initiation of DNA replication and cyclin A with CDK2 or CDK1 continues S phase and entry into mitosis (De Boer *et al.,* 2008). Cyclin B-CDK1 drives mitosis including spindle assembly, chromosome condensation and breakdown of the nuclear envelope (Gavet and Pines,2010; Jackman *et al*., 2020).

Recent data raised the idea that cells possess more than one restriction point (Spencer *et al.,* 2013; Moser *et al.,* 2018). The first restriction window (R1) at the end of the cell cycle can regulate the fate of cells after the completion of mitosis based on mitogen signals and p21 levels. Cells with low p21 enter the next cell cycle in G1 with intermediate CDK2 activity ($CDK2^{inc}$ cells) and hyperphosphorylated Rb, these cells are committed to the cell cycle. Cells with high p21 levels enter a CDK2 low ($CDK2^{low}$) state after mitosis and enter a quiescence-

like state. As CDK2^{low} cells have hypophosphorylated Rb they are dependent on mitogen signals. CDK2^{low} cells can commit to the cell cycle by progression through restriction window two (R2). The ability of cells to enter a CDK2 low state enables cells to respond to metabolic stress and DNA replication/ mitosis errors (Spencer *et al.,* 2013). The findings demonstrate that cells can be born into G1 with residual CDK2 activity or a G0-like state with no residual CDK2 activity based on p21 levels at the end of the previous cell cycle (Figure 1.3).

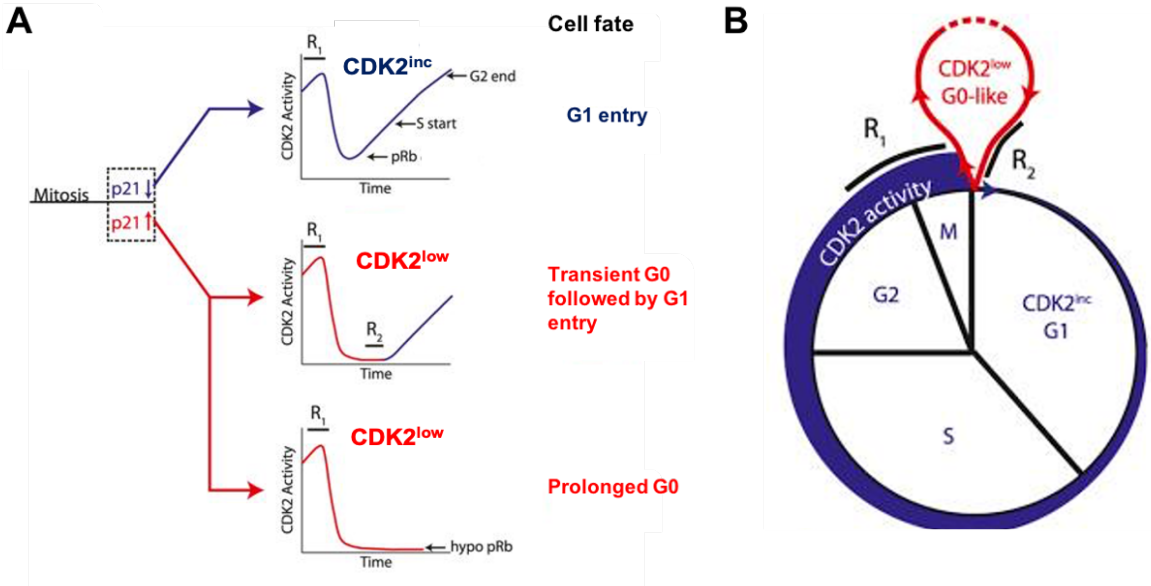

Figure 1.3. A model for cell cycle commitment based on two restriction windows. (A) Restriction window 1 (R1) regulates CDK2^{inc} and CDK2^{low} fates determined by low and high p21 levels, respectively. CDK2^{inc} cells can commit to the cell cycle. CDK2^{low} cells enter a quiescent-like state that can be followed by commitment to the cell cycle based on progressing through restriction window 2 (R2). CDK2 activity can increase once R2 has been passed (Spencer *et al.,* 2013). **(B)** The quiescence-proliferation decision. The location of R1 and R2 are shown, R1 regulates CDK2^{low} and CDK2^{inc} fates. CDK2^{low} cells that pass R2 can commit to the cell cycle. Figure adapted from Spencer *et al.,* (2013).

1.5.1. The role of CDK activity in replication licensing and initiation of DNA replication

CDKs have an important role in the initiation of DNA replication. DNA replication is highly orchestrated to ensure DNA replication occurs once per cell cycle (Parker *et al.,* 2017). The stages of DNA replication can be divided into origin licensing, helicase loading/ activation and replisome formation (Figure 1.4) (Tanaka and Araki, 2013; Symeonidou *et al.,* 2012).

Origin licensing begins in G2-M with the origin recognition complex (ORC) binding to putative origins of replication (Bell and Stillman, 1992; Wang *et al.,* 2019). ORC is made up of six sub-units (ORC1-6) and initiates the formation of the pre-replication complex (pre-RC) (Lee and

Bell, 1997; Sun *et al.,* 2012). ORC is bound by cell division cycle 6 (Cdc6) and this is followed by the recruitment of chromatin licensing and DNA replication factor 1 (Cdt1) and minichromosome maintenance (Mcm2-7) protein complex (Fragkos *et al.,* 2015; Randell *et al.,* 2006). This is followed by the recruitment of a second Mcm2-7 hexamer which leads to the formation an Mcm2-7 double hexamer which encircles double-stranded DNA. Cdc6, ORC and Cdt1 are released from the double hexamer (Evrin *et al.,* 2009). These events can occur only in early G1 phase, when CDK activity is low, and is inhibited post-restriction point in mid to late G1 phase due to the increase in CDK activity (Takeda and Dutta, 2005).

The binding of pre-initiation complex (pre-IC) proteins leads to the activation of Mcm2-7 (Evrin *et al.,* 2009). Pre-IC formation requires the activity of Dbf-4 dependent kinase (DDK) and cyclin E-CDK2 which are kinases active at the G1/S transition. These kinases are required for the loading of cell division cycle 45 (Cdc45) and Go Ichi Ni San (GINS) to form the Cdc45-Mcm2-7-GINS (CMG) complex which has robust helicase activity (Riera *et al.,* 2017). Formation of the CMG complex results in the separation of the two Mcm2-7 hexamers and subsequent activation of helicase activity (Sun *et al.,* 2014). Replisome formation requires the CDK-mediated recruitment of processivity factor proliferating cell nuclear antigen (PCNA) and DNA polymerases (Fragkos *et al.,* 2015). DNA polymerase α has a role in the initiation of DNA replication, polymerase ε and polymerase δ are involved in leading and lagging strand synthesis (Zhou *et al.,* 2019).

CIZ1 has an important role in the initiation of DNA replication. The C-terminal domain of CIZ1 interacts with the nuclear matrix and CIZ1 directly interacts with the pre-RC protein Cdc6, this facilitates contact between chromatin and the nuclear matrix (Copeland *et al.,* 2010; Copeland *et al.,* 2015). CIZ1 directly interacts with cyclin E and cyclin A in a two-step process and facilitates the localisation of cyclin A-CDK2 to chromatin for the efficient initiation of DNA replication. In mid-G1, CIZ1 interacts with cyclin E and this leads to the formation of the pre-RC. As cyclin A expression increases during late G1, cyclin E is replaced by cyclin A leading to

subsequent phosphorylation of proteins that are involved in the process of DNA replication (Copeland *et al.,* 2010).

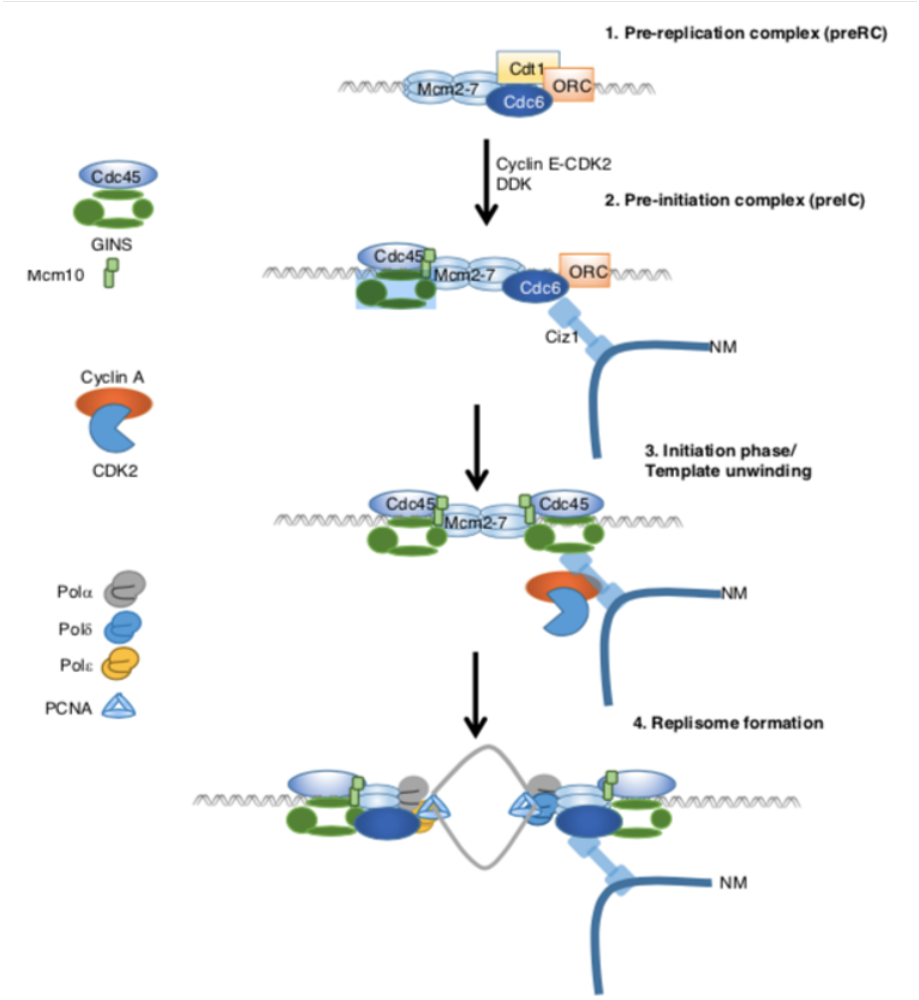

Figure 1.4. Initiation of DNA replication. Pre-replication complex (pre-RC) formation requires the recruitment of Cdc6, Cdt1 and MCM2-7 to ORC. Recruitment of a second Mcm2-7 hexamer leads to formation of a Mcm2-7 double hexamer (Evrin *et al.,* 2009; Fragkos *et al.,* 2015). CIZ1 associates with the nuclear matrix (NM) and directly with Cdc6 to facilitate contact between the nuclear matrix and chromatin (Copeland *et al.,* 2015). Pre-initiation complex (pre-IC) formation requires both Db4-dependent kinase (DDK) and cyclin E-CDK2 activity for the recruitment of Cdc45-Mcm2-7-GINS (CMG) complex (Heller *et al.,* 2011; Tanaka *et al.,* 2011). CIZ1 facilitates localisation of cyclin A-CDK2 for efficient initiation of DNA replication (Copeland *et al.,* 2010). Replisome assembly includes the recruitment of DNA polymerases and PCNA (Fragkos *et al.,* 2015). Abbreviations: Cdc6: cell division cycle 6; Cdc45: Cell Division Cycle 45; Cdt1: chromatin licensing and DNA replication factor 1; GINS: Gp Ichi Ni San; Mcm2-7: minichromosome maintenance 2-7; ORC: origin recognition complex; PCNA: proliferating cell nuclear antigen. Figure adapted from Pauzaite *et al.,* (2016).

1.5.2. The role of CDK activity in the prevention of re-replication

The quantitative model of CDK activity was developed by Stern and Nurse, (1996) and demonstrates that different levels of kinase activity co-ordinates progression through cell cycle stages. Rising CDK activity is fundamental for the regulation of DNA replication and separates origin licensing from origin firing, this ensures that replication occurs once per cell cycle. The re-replication of DNA can result in genome instability which is a hallmark of cancer (Hanahan and Weinberg, 2011).

Replication licensing is restricted to late mitosis and G1 phase of the cell cycle when CDK activity is low and is inhibited mid- to late-G1 when CDK activity rises. Licensing factors are regulated by CDK-mediated phosphorylation to prevent re-replication (Takeda and Dutta, 2005) (Figure 1.5). During S phase, cyclin A-CDK2 mediated phosphorylation of Cdc6, Orc1 and Cdt1 prevents re-replication of DNA as phosphorylated Cdc6 localises to the cytoplasm and phosphorylated Orc1 and Cdt1 are polyubiquitinated and subsequently degraded at the proteasome (Delmolino *et al.,* 2001; DePamphilis *et al.,* 2012; Liu *et al.,* 2004; Méndez *et al.,* 2002). In addition, Cdt1 binds PCNA through PCNA-Interacting Peptide (PIP) leading to the polyubiquitylation of Cdt1 by $CRL4^{Cdt2}$ and proteasomal degradation (Abbas and Dutta, 2011). During late S and G2 phase, Cdt1 activity is inhibited by geminin which prevents Cdt1-MCM association (Yanagi *et al.,* 2002). Together, CDK-mediated phosphorylation and UPS-mediated degradation regulate DNA licensing factors to prevent re-replication of DNA.

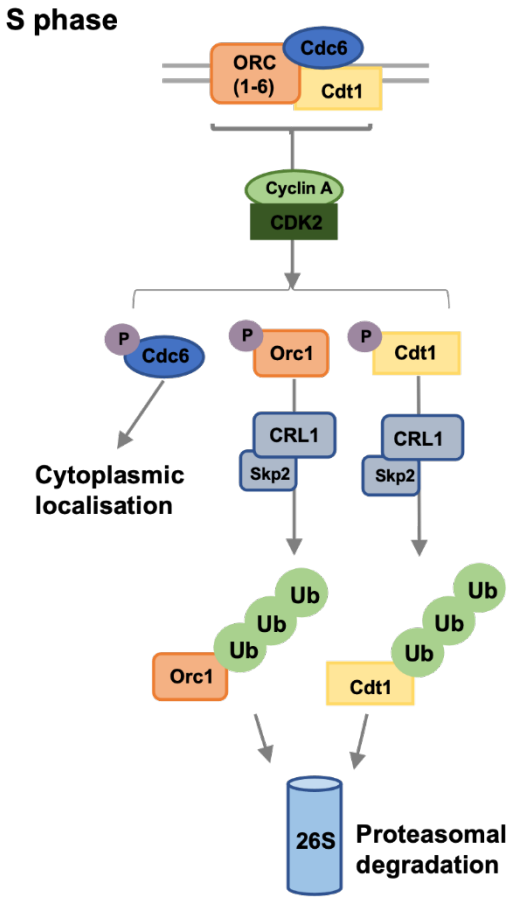

Figure 1.5. Mechanisms involved in the prevention of DNA re-replication. During S phase the re-replication of DNA is prevented by a number of different mechanisms. Cyclin A-CDK2 mediated phosphorylation of Cdc6 leads to cytoplasmic localisation. Cyclin A-CDK2 mediated phosphorylation of Orc1 and Cdt1 results in subsequent ubiquitination by cullin-RING ubiquitin ligase, $CRL1^{Skp2}$, and proteasomal degradation at the 26S proteasome.

The role of CIZ1 in the initiation of DNA replication is mediated by CDK activity. At low kinase levels CIZ1 interacts with cyclin A-CDK2 to promote the efficient initiation of DNA replication and at high kinase levels CIZ1 is hyperphosphorylated and unable to interact with cyclin A-CDK2, this prevents the localisation of cyclin A-CDK2 to chromatin and prevents re-replication (Copeland *et al.,* 2010; Copeland *et al.,* 2015). CIZ1 protein levels may be regulated by CDK-mediated phosphorylation and UPS-mediated degradation to keep CIZ1 levels under tight regulation (Pauzaite, 2019).

1.6. The ubiquitin proteasome system

The ubiquitin proteosome system (UPS) is a protein degradation system and plays an important role in regulating the cell cycle. The UPS degrades proteins that are misfolded,

damaged or no longer needed (Thibaudeau and Smith, 2019). For example, cyclins are degraded when no longer needed and this is necessary to ensure that there is oscillation of cyclin-CDK activity (Benanti, 2012). Ubiquitin (Ub) is a 8.5KDa protein and is covalently linked to lysine residues of target proteins and the polyubiquitylation of proteins leads to proteasomal degradation (Deng *et al.,* 2020; Xu and Jaffrey, 2013). In addition to UPS-mediated degradation, ubiquitination of proteins can also affect their localisation and activity depending on the ubiquitin linkage formed (Xu and Jaffrey, 2011).

The attachment of ubiquitin to target proteins involves activities of E1 ubiquitin-activating enzymes, E2 ubiquitin-conjugating enzymes and E3 ubiquitin ligases (Figure 1.6) (Stewart *et al.,* 2016). The E1 enzyme utilises its cysteine residue to form a high energy thioester bond with C-terminal glycine-76 of ubiquitin, this is an ATP-dependent reaction (Streich and Lima, 2014). The next step of the process involves the transfer of ubiquitin from the E1 enzyme directly to the E2, this is a transthiolation reaction (Stewart *et al.,* 2016). The next step involves the covalent attachment of ubiquitin to the target protein through an isopeptide bond catalysed by E3 ubiquitin ligase which brings the E2 enzyme and substrate together for ubiquitin transfer from E2 to substrate (Ullah *et al.,* 2018). Addition of further ubiquitin's can lead to the formation of ubiquitin chains, ubiquitin is linked to one of seven lysine residues, K6, K11, K27, K29, K33, K48 and K63 of another ubiquitin molecule (Morimoto and Shirakawa, 2016). Substrates can be monoubiquitinated or polyubiquitinated, this determines substrate fate; monoubiquitylation can regulate subcellular localisation of proteins and K48-linked polyubiquitylation targets proteins for proteasomal degradation (Grice and Nathan, 2016).

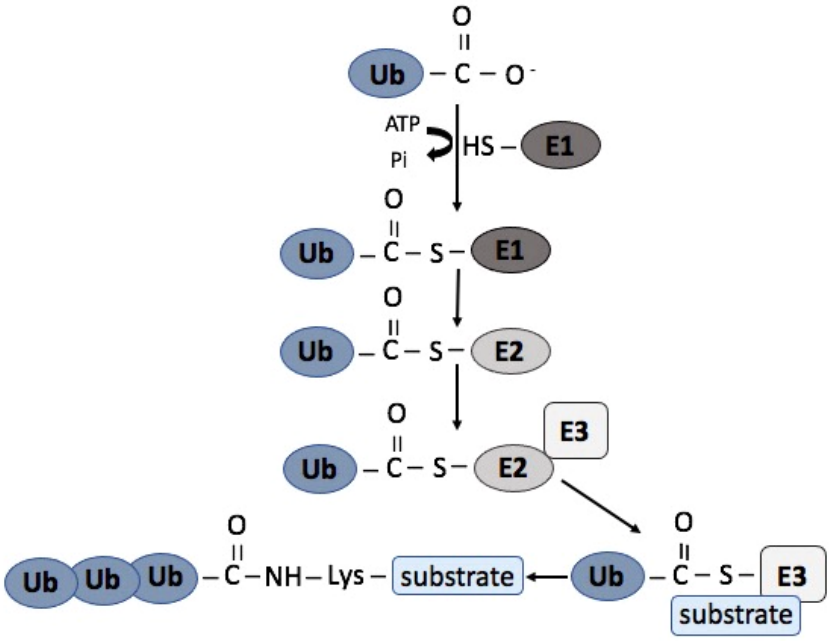

Figure 1.6. The role of ubiquitin activating enzyme (E1), ubiquitin conjugating enzyme (E2) and ubiquitin ligases (E3) in the ubiquitination of substrates. E1 forms a thioester bond with ubiquitin then ubiquitin is transferred to E2 forming a thioester bond and ubiquitin is transferred to the substrate forming an isopeptide bond catalysed by E3. Ubiquitin transfer to the substrate can be repeated to form a polyubiquitin chain (Stewart et al., 2016).

Finally, the E3 ligase determines substrate specificity. In humans, there are approximately 600-700 E3 ligases and they are categorised into three groups (Figure 1.7) including RING (really interesting new gene), HECT (homologous to the E6-AP carboxyl terminus) and RBR (RING between RING fingers) E3 ligases (Liu *et al.,* 2017; Rubenstein and Hochstrasser, 2010).

RING E3 ligases are the largest group. RING finger domain is a Zn^{2+} coordinating domain that has a role in facilitating direct ubiquitin transfer from the E2 enzyme to the target protein (Metzger *et al.,* 2014). The multi-subunit E3 ubiquitin ligase Skp, Cullin, F box- containing (SCF), also known as Cullin-RING ligase (CRL), promotes degradation of approximately 20% of UPS-degraded proteins (Soucy *et al.,* 2009). In SCF complexes, substrate specificity is determined by the F-box protein (Skaar *et al.,* 2013; Skaar *et al.,* 2014). F-box proteins are categorised based on protein interaction domains into F-box and WD40 domain (FBXW), F-box and Leu-rich repeat (FBXL) and F-box only (FBXO) which have a conserved homology not present in many F-box proteins (Jin *et al.,* 2004). SCF E3 ligase substrates are involved in cell cycle regulation and DNA replication (Abbas and Dutta, 2017). The multi subunit E3 ligase APC/C (anaphase promoting complex or cyclosome) is considered to be the most

sophisticated RING E3 ligase and has a role in cell cycle regulation by engaging with Cdc20 (cell division cycle 20) or Cdh1 (CDC20-like protein 1) (Alfiere *et al.,* 2017).

HECT E3 ligases are the second largest group of E3s. The catalytic HECT domain contains an N-terminal lobe and a C-terminal lobe which are connected together by a flexible hinge region. The mechanism of action for HECT E3s involves a two-step process in which there is the transfer of ubiquitin to the catalytically active cysteine of the E3 ligase followed by the transfer of ubiquitin to the substrate (Rieser *et al.,* 2013). HECT E3s are involved in cell growth and proliferation, apoptosis, DNA damage and the immune response as well as regulation of Notch, transforming growth factor-β (TGF-β) and Wnt signalling (Scheffner and Kumar, 2014). RBR E3 ligases consist of RING1, in-between RING and RING2. RBRs are characterised by a RING-HECT hybrid mechanism (Cotton and Lechtenberg, 2020) and have a role in cell cycle regulation (Deng *et al.,* 2020).

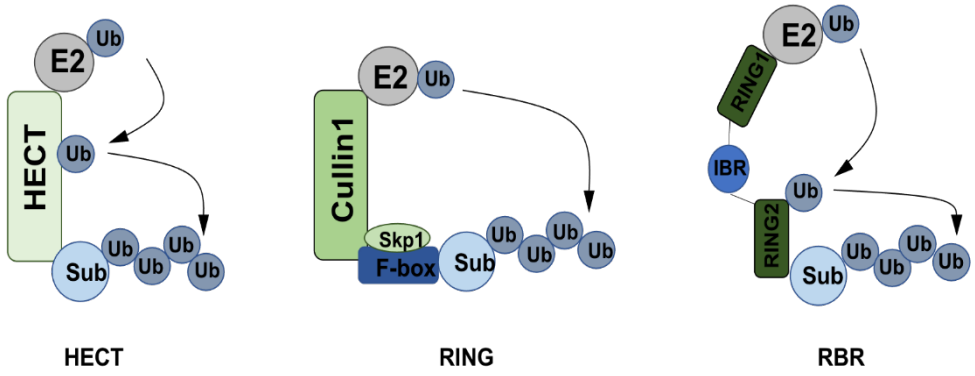

Figure 1.7. The different classes of E3 ligases include RING (really interesting new gene), HECT (homologous to the E6-AP carboxyl terminus) and RBR (RING-between-RING) E3s. HECT E3 mechanism is a two-step process that first involves the transfer of ubiquitin to a cysteine residue of the E3 ligase and the formation of a thioester bond, the second step involves the transfer of ubiquitin to the substrate. RING E3 mechanism is a direct process which involves the transfer of ubiquitin to the substrate by providing close proximity between E2 and target substrate. RBR E3 mechanism involves a two-step process, first is the transfer of ubiquitin to the RING2 domain, second is the transfer of ubiquitin to the substrate (Rieser *et al.,* 2013). Abbreviations: IBR: in-between RING; Sub: substrate; Ub: ubiquitin. Image adapted from Deng *et al.,* (2020).

Substrates that are polyubiquitinated are marked for degradation by the proteasome. The 26S proteasome is composed of a 20S proteolytic core particle capped by a 19S regulatory subunit (Bard *et al.,* 2018; Tanaka, 2009). Proteins targeted for degradation are recognised by the 19S regulatory subunit then subsequently translocated to the 20S proteolytic core

particle in which the protein is degraded (Tanaka, 2009). The 19S subunit can recognise proteins through Ub receptors such as Rpn10 and Rpn13 (Grice and Nathan, 2016; Schrader *et al.,* 2009). The 19S subunit has a role in deubiquitylation of the substrate by deubiquitylating enzymes (DUBs) including Usp14, Uch37 or Rpn11 (De Poot *et al.*, 2017). The 20S proteolytic core contains the peptidases that degrade proteins to a mixture of peptides which are further hydrolysed to amino acids (Tanaka, 2009).

1.7. The role of CDKs and the UPS in cell cycle regulation

The activity of the cyclin-CDK complexes and cell cycle regulatory ubiquitin ligases are intricately linked. The temporal control of the cell cycle requires both CDK and UPS activity. The oscillation of cyclin-CDK activities which drives unidirectionality of the cell cycle requires UPS-mediated degradation of cyclins when no longer needed (Dang *et al.,* 2020). SCF and APC/C are multi-subunit cullin RING E3s and are involved in the regulation of cell cycle events (Bochis *et al.,* 2015) (Figure 1.8). SCF and APC/C activity oscillate during the cell cycle with SCF being active from late G1 to early mitosis and APC/C being active mid-mitosis to the end of G1 phase (Bassermann *et al.,* 2014; Kernan *et al.,* 2018).

In early G1 phase, APC/C^{Cdh1} targets mitotic proteins including cyclin A and cyclin B for degradation (Li and Zhang, 2009). The APC/C^{Cdh1}-mediated Skp2 degradation stabilises the activity of p21 and p27, this maintains low levels of CDK activity (Qiao *et al.,* 2010). In late G1, APC/C^{Cdh1} activity is inactivated, one way this is achieved is through autoubiquitylation mediated by Cdh1 (Choudhury *et al.,* 2016). The increase in activity of S-cyclin/CDK2 results in the phosphorylation of Cdh1 which prevents interaction with APC/C, in S phase SCF mediates the degradation of Cdh1 (Bassermann *et al.,* 2014). APC/C^{Cdh1} is also inhibited by early mitotic inhibitor 1 (Emi1) which is an E2F target gene (Cappell *et al.,* 2018). The increase in CDK activity during late G1 occurs due to the inactivation of APC/C^{Cdh1} and the accumulation of Skp2 (Nakayama and Nakayama, 2005). SCF^{Skp2} mediates the proteasomal degradation of p21 and p27 which leads to an increase in cyclin E-CDK2 activity and cell cycle progression through S phase (Lu and Hunter, 2010). Cyclin E-CDK2 and cyclin A-CDK2 are involved in S phase progression and cyclin A-CDK2 phosphorylates Cdh1 which contributes to the inhibition of APC/C^{Cdh1} (Bassermann *et al.,* 2014). The CDK2-mediated phosphorylation of cyclin E leads

to subsequent degradation by SCF^{FBW7}, this provides a negative feedback mechanism for the regulation of cyclin E levels (Koepp *et al.,* 2001).

During early G2 of the cell cycle, SCF^{Skp2} mediates the degradation of CDK inhibitor proteins p21 and p27 in order to maintain the activity of cyclin A-CDK1/CDK2 (Bassermann *et al.,* 2014). In late G2, SCF^{Skp2} mediates p21 and p27 degradation and CDK1 is activated by the $SCF^{B\text{-}TrCP}$ mediated degradation of the CDK1 inhibitor, Wee1 (Chow and Poon, 2012). For Wee1 to be targeted by $SCF^{B\text{-}TrCP}$ it needs to be phosphorylated by cyclin B-CDK1 (Watanabe *et al.,* 2004) creating a positive feedback mechanism for the activation of CDK1 (Bassermann *et al.,* 2014). It is important for cyclin B-CDK1 to be strictly regulated as this kinase complex is responsible for timely mitotic entry (Gavet and Pines, 2010).

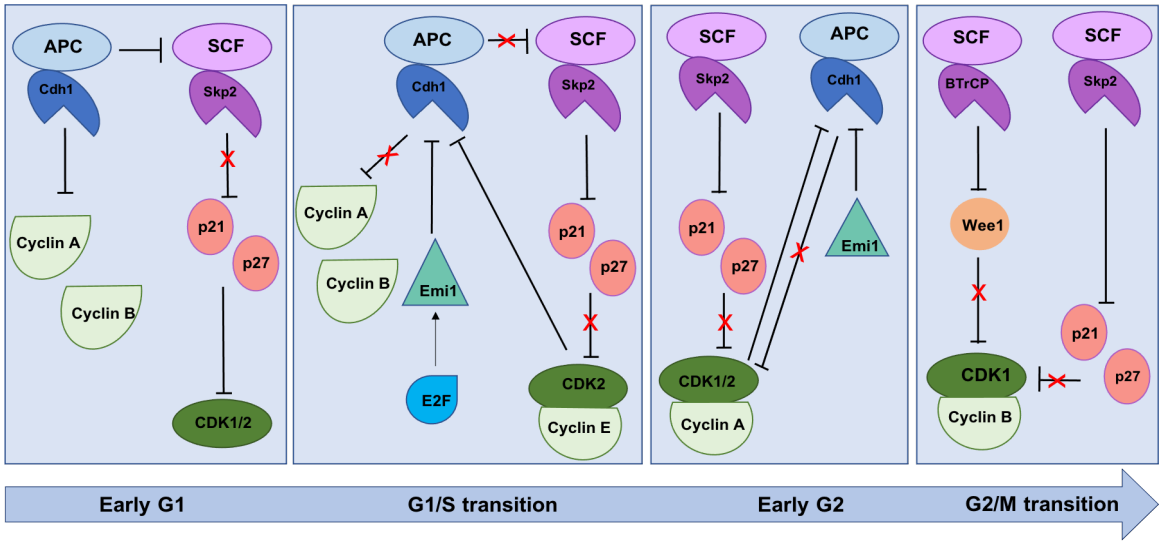

Figure 1.8. The cell cycle is driven by an interplay between CDK and UPS activities. In early G1, CDK activity is kept low by APC/C^{Cdh1} mediated cyclin A and cyclin B degradation (Li and Zhang, 2009) and also APC/C^{Cdh1}-mediated degradation of Skp2, this prevents degradation of CDK inhibitor proteins p21 and p27 (Qiao *et al.,* 2010). During G1/S, APC/C^{Cdh1} is inhibited by both CDK-mediated phosphorylation and the inhibitor Emi1 (Bassermann *et al.,* 2014). This dual inhibition of APC/C^{Cdh1} allows accumulation of Skp2, activating SCF^{Skp2} -mediated degradation of CDK inhibitors p21 and p27 (Lu and Hunter, 2010). This results in cyclin E-CDK2 activation and progression into S phase of the cell cycle where cyclin A levels increase. During early G2, APC/C^{Cdh1} continues to be inactivated and there is SCF^{Skp2}-dependent degradation of CDK inhibitors p21 and p27. At G2/M, SCF^{Skp2}-dependent degradation of p21 and p27 is maintained (Bassermann *et al.,* 2014) and SCF^{BTrCP}-mediated degradation of the CDK1 inhibitor Wee1 leads to activation of cyclin B-CDK1 (Chow and Poon, 2012) and entry into mitosis. Figure adapted from Bassermann *et al.,* (2014).

The progression of cells through mitosis requires the inhibition of APC/C to be removed (Bassermann *et al.,* 2014). APC/C is inhibited by Emi1 and therefore Emi1 must be degraded. This process involves the CDK-mediated phosphorylation of Emi1 by cyclin B-CDK1 which enables SCF^{BTrCP} to target Emi1 for proteasomal degradation (Bassermann *et al.,* 2014; Vordermaier, 2004). The Spindle Assembly Checkpoint (SAC) inhibits the activation of APC/C, this is in place to prevent progression to anaphase. Until SAC has been fulfilled, mitotic proteins such as RubR1, Rub3 and Mad2 are able to bind to Cdc20 and prevent the activation of APC/C^{Cdc20} (Kim *et al.,* 2017; Lara-Gonzalez *et al.,* 2012). In addition, Cdc20 is inhibited by CDK1-mediated phosphorylation (Hein *et al.,* 2021). A small amount of APC/C^{Cdc20} is still active during the activation of SAC, this is important as APC/C^{Cdc20} is able to maintain cyclin B-CDK1 activity by ubiquitylating p21 (Amador *et al.,* 2007). After the attachments of spindles to kinetochores (fulfilment of SAC), SAC is inactivated and the inhibition of APC/C^{Cdc20} is removed and APC/C^{Cdc20} initiates anaphase. Finally, APC/C targets cyclins A and B for degradation to reset low kinase activity (Bassermann *et al.,* 2014). Cell cycle regulation is dependent upon a tight interplay between CDK activity and UPS activity, therefore dysregulation of CDK and UPS activity can lead to cell cycle deregulation (Bochis *et al.,* 2015; Peyressatre *et al.,* 2015).

1.8. Therapeutic targeting of CDKs and the UPS in cancer

Dysregulation of CDKs can occur due to different reasons such as gene amplification, protein overexpression, alternative splicing or problems with inactivation through Cip/Kip inhibitors (Peyressatre *et al.,* 2015). Aberrant activity of CDKs contributes to the increased proliferation of cancer cells (Asghar *et al.,* 2015; Canavese *et al.,* 2012). Examples of the overexpression of CDKs in cancer include the overexpression of CDK1 associated with B lymphoma and advanced melanoma and the overexpression of CDK2 associated with breast cancer (Zhao *et al.,* 2009; Weroha *et al.,* 2010). Cyclin E has been found to be overexpressed in breast, lung, cervical, endometrium and colon cancer. Deregulated proteolysis of cyclin E can occur through loss of function mutations of SCF^{Fbw7}, this ubiquitin ligase targets cyclin E for degradation (Hwang and Clurman, 2005). The overexpression of cyclin D has been linked to the progression of breast cancer, possibly due to deregulation of Fbx4 activity, an F-box protein that mediates cyclin D degradation (Alao, 2007).

First generation CDK inhibitors were relatively non-specific, displaying limited selectivity among CDKs, therefore had limitations with poor efficacy and toxicity (Asghar *et al.,* 2015). More selective inhibitors have been developed such as Palbociclib (PD 0332991; Pfizer). Palbociclib is an FDA approved highly selective CDK4/6 inhibitor used in combination with an aromatase inhibitor for the first-line treatment of advanced post-menopausal oestrogen receptor positive (ER^+), human epidermal growth factor receptor negative ($HER2^-$) breast cancer (Beaver *et al.,* 2015). More recently, the CDK4/6 inhibitors ribociclib (Kisqali) and abemaciclib (Verzenio) received FDA approval for first line therapy of hormone receptor positive (HR^+)/ $HER2^-$ advanced breast cancer when used in combination with an aromatase inhibitor (Piezzo *et al.,* 2020). The increased selectivity of CDK inhibitors allows CDKs to be a viable drug target.

E3 ubiquitin ligase activity is tightly regulated, this is achieved in the form of post-translational modifications such as phosphorylation and ubiquitylation or through auto-inhibitory mechanisms such as dimerisation (Balaji and Hoppe, 2020). The dysregulation of the UPS has been associated with tumourigenesis. The oncogene Skp2 promotes the degradation of CDK inhibitors p21 and p27, the overexpression of Skp2 is associated with a decrease in p27 and poor prognosis in cancers such as colon cancer and breast cancer (Fujita *et al.,* 2008; Zhang *et al.,* 2016). So far, only the proteasome has been successfully targeted as a cancer therapeutic targeted towards the UPS using Bortezomib (Velcade, Millennium Pharmacaeuticals). Bortezomib can inhibit proliferation in tumour cell lines such as multiple myeloma (MM) (Chari *et al.,* 2010; Chen *et al.,* 2011).

Dysregulation of CDK and UPS activity can contribute to tumourigenesis. Preliminary work has suggested CDKs and the UPS may regulate CIZ1 levels (Pauzaite, 2019) and therefore dysregulation of their activity can lead to increased CIZ1 levels and tumourigenesis. It is therefore important to understand how regulators of CIZ1 can be targeted/ manipulated as a strategy to reduce CIZ1 levels in cancer.

1.9. Regulation of CIZ1 by CDKs and the UPS

CIZ1 has a role in promoting the initiation of DNA replication and its activity is regulated by CDK-mediated phosphorylation (Copeland *et al.,* 2010; Copeland *et al.,* 2015). Pauzaite, (2019) investigated the regulation of CIZ1 protein levels and found CIZ1 levels to accumulate during G1 and increase into S in mouse embryonic fibroblasts (3T3) cells. CIZ1 accumulation was found to correlate with cyclin A expression and the phosphorylation of CIZ1 at T293 as well as cyclin E expression and the phosphorylation of CIZ1 at S331 suggesting CDK-mediated phosphorylation could promote CIZ1 accumulation from G1 to S. The study also found that small-molecule CDK inhibitors reduced CIZ1 levels by facilitating UPS-mediated degradation of CIZ1.

The findings made by Pauzaite, (2019) allowed a working model for CIZ1 regulation to be proposed (Figure 1.9). Under normal conditions, CIZ1 protein levels are regulated by DDK/ CDK mediated phosphorylation. The phosphorylation of CIZ1 causes it to be stabilised and thereby allows CIZ1 to accumulate in G1 phase of the cell cycle, this is opposed by UPS mediated degradation providing tight regulation of CIZ1 levels throughout the cell cycle. This model suggests that dysregulation of CIZ1 can occur through aberrant CDK activity leading to hyperphosphorylation of CIZ1 and overaccumulation which can drive forward tumourigenesis. Conversely, loss of function of the regulatory E3(s) that promote the normal degradation of CIZ1 protein can contribute to the increase of CIZ1 levels and tumourigenesis. This model suggests that inhibition of CDK and DDK could provide an avenue for reducing CIZ1 levels by shifting the equilibrium of CIZ1 regulation towards UPS-mediated degradation, this reduction would be dependent on a functional UPS (Pauzaite, 2019).

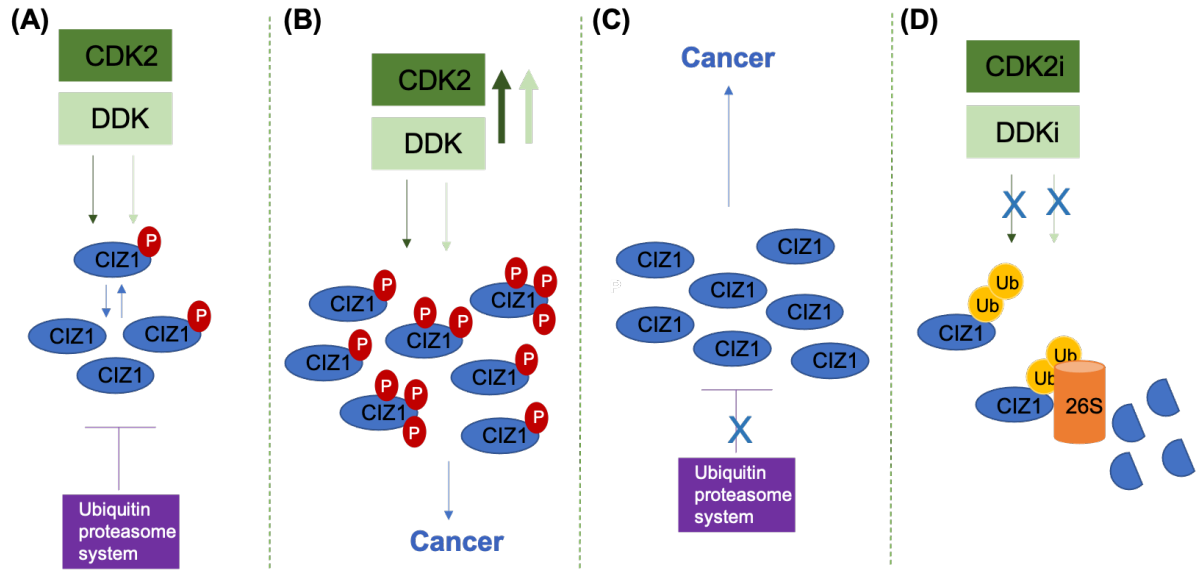

Figure 1.9. The proposed model for the regulation of CIZ1 levels and CIZ1 overexpression in cancer. (A) CIZ1 levels are normally regulated by CDK2 and DDK mediated phosphorylation which leads to CIZ1 stability and accumulation as the phosphorylation is protective against UPS-mediated degradation. Opposing regulation is by the UPS which can degrade CIZ1 at specific points in the cell cycle to keep CIZ1 levels under tight regulation. **(B)** Aberrant CDK and DDK activity can lead to the hyperphosphorylation of CIZ1 and CIZ1 overexpression which can lead to cancer by driving the proliferation of cancer cells. **(C)** Loss of function of the UPS can also lead to CIZ1 overexpression as CIZ1 can no longer be degraded, this can also contribute to tumourigenesis. **(D)** CDK2 and DDK inhibitors shift the equilibrium of CIZ1 regulation towards UPS mediated degradation resulting in a reduction in CIZ1 protein levels. Figure adapted from Pauzaite, (2019).

Pauzaite, (2019) then identified three putative E3 ligases that potentially target CIZ1 through *in vitro* ubiquitylation assays using HeLa whole-cell extract as a source of E3 ligase. HeLa whole-cell extract was subject to sequential chromatography steps and the activity of fractions was determined by *in vitro* ubiquitylation assays and western blot analysis to identify polyubiquitylation of CIZ1. Liquid chromatography-mass spectrometry (LC-MS) identified three E3 ligases that potentially polyubiquitylate CIZ1 including F-box only protein 38 (FBXO38), E3-independent E2 ubiquitin-conjugation enzyme (UBE20) and Ubiquitin-protein ligase E3 component n- recognin 5 (UBR5).

FBXO38 is the substrate recognition component of an SCF E3 ligase and is 134KDa. FBXO38 is widely expressed in different tissues and shuttles between the nucleus and cytoplasm (Georges *et al.,* 2019; Sumner *et al.,* 2013). FBXO38 is a coactivator of Krüppel-like factor 7 (KLF7), a transcription factor expressed in the nervous system with a role in neuronal projection (Sumner *et al.,* 2013). FBXO38 also interacts with programmed cell death protein

1 (PD-1) and mediates its polyubiquitylation (Meng *et al.,* 2018; Serman and Gack 2019), this demonstrates FBXO38 has a role in regulating T-cell mediated immunity. As F-box proteins typically target phosphorylated proteins, further investigation is required to determine the interplay between CIZ1 phosphorylation and CIZ1 stability and degradation.

UBE2O is an E3-independent E2 and is 141KDa. UBE2O is widely expressed but the highest levels are found in the brain, heart and lung and UBE2O is predominantly cytoplasmic (Ullah *et al.,* 2018). UBE2O targets include 5'-AMP-activated protein kinase catalytic subunit a2 (AMPKα2), mixed-lineage leukaemia (MLL) protein and SMAD family member 6 (SMAD6) (Hormaechea-Agulla *et al.,* 2018). UBE2O mediates monoubiquitination (involved in protein signalling), multi-ubiquitination (involved in protein localisation) and polyubiquitination (involved in proteasomal degradation) (Ullah *et al.,* 2018). *UBE2O* amplification, mutations and deletions have all been associated with gastric and lung cancers (Ullah *et al.,* 2018) making it unclear on an oncogenic or tumour suppressive role of UBE2O.

UBR5 is a HECT E3 ligase and is over 300KDa. UBR5 has widespread tissue expression and has predominantly nuclear localisation (Shearer *et al.,* 2015). UBR5 domain structure is outlined in Figure 1.10 and includes two nuclear localisation sequences (Shearer *et al.,* 2015). As CIZ1 is a nuclear protein (Coverley *et al.,* 2005), UBR5 could target CIZ1 in the nucleus.

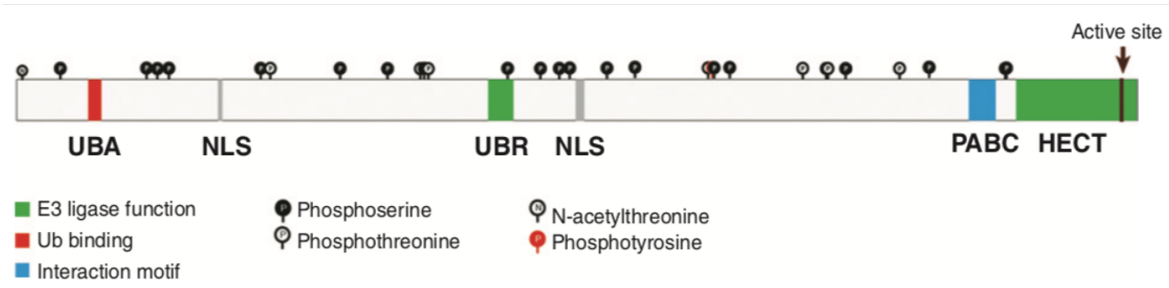

Figure 1.10. The structure of UBR5. The HECT domain contains the catalytic cysteine residue, the other domains include the homologous to the C-terminal region of Poly-Adenylation Binding Protein (PABC/MLLE) domain, nuclear localisation sequence (NLS), Ubiquitin Recognition Box (UBR) and Ubiquitin activation (UBA). The post-translational modifications of UBR5 are also shown. Shearer et al., (2015).

UBR5 interacts with a variety of proteins with roles in a range of processes including the cell cycle such as E2F1 (Cipolla *et al.,* 2019; Munoz *et al.,* 2007) and Katanin p60 (ATPase-containing) subunit A1 (KATNA1) (Shearer *et al.,* 2015). Amplification of *UBR5* has been

associated with breast and ovarian cancer. *UBR5* has been shown to be coamplified with *MYC* in MYC-driven cancers; MYC overexpression can sensitise cells to apoptosis and UBR5 has been shown to suppress MYC-induced apoptosis in breast cancers cells (Qiao *et al.,* 2020). UBR5 is overexpressed in serous ovarian carcinoma and mediates therapeutic resistance (O'Brien *et al.,* 2008). Recently, UBR5 has been associated with lung adenocarcinoma, shRNA targeted towards UBR5 reduces tumour volume in nude mice (Saurabh *et al.,* 2020). Loss of function mutations of *UBR5* have been linked to tumourigenesis. Nonsynonymous mutations of *UBR5* are found in 18% of mantle cell lymphoma (MCL) cases, frameshift mutations are predicted to affect the conserved cysteine residue located in the HECT domain and thereby disrupt the catalytic activity of UBR5 (Meissner *er al.,* 2013). UBR5 overexpression and loss of function mutations of *UBR5* have been associated with tumourigenesis, therefore the literature on UBR5 makes it unclear if UBR5 falls under oncogene or tumour suppressor.

The working model for CIZ1 regulation suggests that inhibition of DDK/ CDK2 can reduce CIZ1 levels and this is dependent on a functional UPS. Therefore, the E3(s) that target CIZ1 could provide an avenue for patient stratification, this is based on the idea that functional activity of the E3s would be required for the patient to respond beneficially to CDK inhibitors as a way of reducing CIZ1 levels. Further characterisation of the role of CDK and UPS activities on the regulation of CIZ1 levels would be beneficial in understanding how CIZ1 could potentially be therapeutically targeted. Identification of which putative E3(s) target CIZ1 for degradation is yet to be determined.

1.10. Aims

The aims of the current work are to investigate the use of CDK and DDK inhibitors to reduce CIZ1 levels. The efficacy of CDK and DDK inhibition to reduce CIZ1 levels will be assessed using CDK4/6, CDK2, DDK, and CDK1 small molecule inhibitors in asynchronous and synchronous populations of 3T3 cells with the aim of determining the role of CDK-mediated phosphorylation on CIZ1 levels across all phases of the cell cycle. Overexpression of the putative E3s in 3T3 cells by transfection will work towards the aim of characterising the E3s that target CIZ1 for degradation. Finally, the ability of CDK and DDK to induce apoptosis and

cell death in cancer cell lines will be evaluated with the aim of determining if the effect of the small molecule inhibitors can translate to the prevention of cancer cell survival.

Chapter 2: Materials and Methods

2.1. Tissue culture

2.1.1. Culturing 3T3 fibroblasts

Mouse embryonic fibroblasts (3T3 cells) were cultured in Dulbecco's Modified Eagles Media (DMEM) (Gibco) supplemented with 10% (v/v) foetal bovine serum (FBS) (Labtech) and 1% (v/v) penicillin-streptomycin-glutamine (Gibco) in a humidified incubator at 37 °C, 5% CO_2 (Copeland *et al.,* 2015). The cells were cultured in 15 cm NUNClon Delta coated cell culture plates in 30 ml of media. The cells were passaged every 24 to 48 hours to maintain 50-60% confluence. To passage the cells, the media was removed, and the cells washed in 10 ml 1x Dulbecco's Phosphate-Buffered Saline (DPBS) (Gibco). The cells were dissociated from the culture dish by incubating the cells in 9 ml 1x DPBS with 1 ml 0.5% Trypsin-EDTA (Gibco) for 2 minutes. The trypsin was neutralised in an equal volume of media and the cells split onto desired dishes proportionate to surface area of the tissue culture dishes.

2.1.2. Synchronisation of 3T3 fibroblasts

Contact inhibition and serum starvation were used to synchronise 3T3 cells (Copeland *et al.,* 2010; Copeland *et al.,* 2015; Coverley *et al.,* 2002). Cells were grown to 100% confluence and at this point the media was replaced with fresh media and the cells cultured for a further 48 hours. Contact inhibition and serum starvation means the cells enter quiescence (G0). To release the cells from G0, the cells were dissociated from the culture dish by incubating the cells in 9 ml DPBS supplemented with 2 ml 0.5% trypsin-EDTA for 5 minutes. Cells were then split 1 in 4 into fresh media. The release of cells into fresh media at a lower density allows the cells to re-enter the cell cycle in G1 as a synchronised population. Figure 2.1 is a timeline of G0 release highlighting when the cells will enter into S phase.

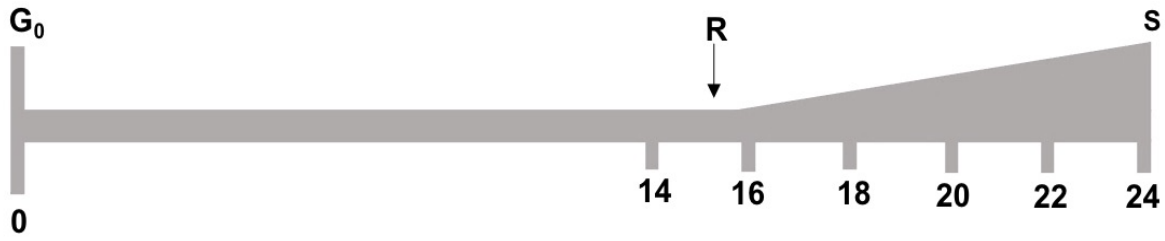

Figure 2.1. The synchronisation of 3T3 cells. The timeline of events of synchronised 3T3 cells after release from G0 to S phase. Restriction point (R) and entry of cells into S phase are shown as demonstrated previously by Coverley *et al.,* (2002).

2.1.3. Culturing cancer cell lines

The human prostate cancer (PC-3) cell line and primary and metastatic human colorectal carcinoma (SW480 and SW620, respectively) cell lines were cultured in DMEM (Gibco) supplemented with 10% (v/v) FBS (Labtech) and 1% (v/v) penicillin-streptomycin-glutamine (Gibco) in a humidified incubator at 37 °C, 5% CO_2. The cells were cultured in 15 cm cell culture plates in 30 ml of media and maintained at 50-60% confluence. The cells were passaged as described in 2.1.1.

2.2. 5-Ethynyl-2'- deoxyuridine (EdU) labelling and fluorescence microscopy

Cell cycle synchronisation of 3T3 cells was measured using the incorporation of the thymidine analogue 5-Ethynyl-2'-deoxyuridine (EdU) into nascent DNA 16-24 hours after G0 release. Synchronised 3T3 cells were cultured in a plate containing autoclaved glass coverslips. EdU at a final concentration of 10 μM (Invitrogen) was added to the culture plate 1 hour prior to removal of the coverslip. The coverslips were washed three times in 1x phosphate buffered saline (PBS), fixed for 15 minutes in 4 % paraformaldehyde (PFA), washed three times in 1x PBS then stored at 4 °C until covalent attachment of Alexa Fluor-azide flurophores.

Coverslips were washed twice in PBS, 1% (w/v) bovine serum albumin (BSA) (VWR) for 5 minutes, cells permeabilised in 0.5% Triton X-100 for 20 minutes, washed twice in PBS, 1% (w/v) BSA for 5 minutes. Cells were fluorescently labelled using Click-iT™ imaging kit (Invitrogen). To the coverslips was added 20 μL of Click-iT™ EdU Cell Proliferation Cocktail (Invitrogen) (17.2 μL of 1x Click-iT™ EdU reaction buffer, 0.8 μL Copper sulphate solution, 0.48 μL Alexafluorazide 555, 2 μL of 1x EdU Additive). The coverslips were incubated in a humidity chamber for 30 minutes at 37 °C, 5% CO_2 then washed three times in PBS. Coverslips were mounted on Vectasheild containing DAPI (Vector Laboratories) and imaged by fluorescence microscopy (Zeiss Scope.A1). DAPI filter set: excitation G365, beamsplitter FT395, emission BP 445/50. Alexa flour 555 filter set: excitation BP 550/25, beamsplitter FT570, emission BP 605/70. Percentage S phase cells was calculated by the following: Percentage S phase cells = (positively stained nuclei (EdU positive)/ total nuclei (total DAPI stained) x 100. Replicate number stated in figure legend. Merged images were generated using the add channel tool on the Zeiss Zen software.

2.3. Small molecule kinase inhibitor treatments

For asynchronous cell cycle experiments, cells were seeded into 6-well plates at 30% confluency for 24 hours. The asynchronous cells were treated with small molecule kinase inhibitors (Table 2.1) or Dimethyl Sulfoxide (DMSO) solvent control for 6- or 24-hours prior to being harvested as indicated in the figures. Cell cycle synchronised cells were released and seeded into 6-well plates at 25% confluency and treat with small molecule inhibitors or DMSO at 16 hours post G0 release and cells harvested 24 hours post G0 release. For apoptosis assays, cells were seeded onto 10 cm plates at 30% confluency then incubated for 24 hours. The cells were treated with small molecule kinase inhibitors or DMSO solvent control for 24 hours prior to being harvested.

Drug	Target	IC50	Concentration	Provider
Palbociclib (PD0332991) Isethionate	CDK4 CDK6	11 nM 16 nM	10 μM	Sigma Aldrich
PHA-767491	Cdc7	10 nM	10 μM	Sigma Aldrich
CVT-313	CDK2	0.5 μM	10 μM	Santa Cruz Biotechnology
Ro-3306	CDK1	20 nM	10 μM	Selleckchem
CDK2-IN-73	CDK2	44 nM	10 μM	Selleckchem
Roscovitine	CDK2	0.7 μM	30 μM	Sigma Aldrich; Selleckchem
XL-413 hydrochloride	Cdc7	3.4 nM	10 μM	Selleckchem
MG-132	26S Proteasome	0.1 μM	10 μM	Sigma Aldrich

Table 2.1. Small molecule inhibitors. The small molecule inhibitors used in experiments throughout this study, the main target that is inhibited, the IC50 in cell free assays, the concentration used in experiments and the supplier.

2.4. Protein harvesting and Sodium Dodecyl Polyacrylamide Gel Electrophoresis (SDS-PAGE)

2.4.1. Protein harvesting from 6-well cell culture plates

For protein harvesting from the 6-well plates used for small molecule drug treatment experiments, the media was removed from the wells and the cells were washed twice in 1x PBS. The cells were scrape harvested using a cell scraper in 4x SDS loading buffer (200 mM tris HCl pH 6.8, 27.7 mM SDS, 40% (v/v) glycerol, 1 mM DTT, bromophenol blue) with 1 mM

phenylmethanesulfonylfluoride (PMSF), a serine/threonine protease inhibitor. The samples were vortexed then boiled for 10 minutes at 95 °C and stored at -20 °C.

2.4.2. Protein harvesting from 10 cm cell culture plates

For protein harvesting from 10 cm plates used for transfected 3T3 cells, the media was removed, and the cells washed in 5 ml 1x PBS with 1 mM DTT. A further 5 ml of 1x PBS with 1 mM DTT was added to the cells and left on ice for 5 minutes. The PBS was removed, and the plates left on ice at a 45° angle for 5 minutes and any remaining PBS removed. The cells were scrape harvested using a cell scraper and the samples were added to 0.33 volumes of 4x SDS loading dye with 1 mM PMSF. The samples were the vortexed and boiled at for 10 minutes at 95 °C and stored at -20 °C.

2.4.3. Casting SDS-PAGE gels

The Bio-Rad Mini-PROTEAN® tetra handset system was used to cast polyacrylamide gels. Table 2.2 outlines the recipes used to prepare 10% and 6% resolving gels and 5% stacking gel. After the resolving gel was poured, drops of isopropanol were added to remove any bubbles and make the resolving gel level, this layer of isopropanol was removed once the resolving gel had set. The stacking gel was then poured on top of the resolving gel and a 15 well comb added. Once the gels were set, they were used immediately or wrapped in wet blue roll and kept at 4 °C until use.

Reagent	**10 % resolving gel**	**6 % resolving gel**	**5 % stacking gel**
40% Acrylamide	1.88 ml	3 ml	0.25 ml
1.5M Tris-HCl pH 8.8	1.88 ml	5.6 ml	-
0.5M Tris-HCl pH 6.8	-	-	0.5 ml
MilliQ water	3.6 ml	6.35 ml	1.21 ml
10% SDS	75 µl	75 µl	20 µl
10% APS	45 µl	120 µl	10 µl
TEMED	15 µl	20 µl	5 µl

Table 2.2. The recipe for various SDS-PAGE gels used in the project.

2.4.4. SDS-PAGE

Proteins in SDS-PAGE samples were resolved on 10% or 6% SDS-polyacrylamide gels. The gels were placed in a Mini-PROTEAN® Tetra Cell tank (Bio-Rad) filled with 1x Tris-Glycine-SDS PAGE buffer (TGS) (ThermoFisher). Samples were boiled for 10 minutes at 95 °C prior to loading into the gel. PageRuler™ Plus Prestained Protein Ladder (ThermoFisher) was used as the protein standard. The gel was run at 100 V until samples reached the resolving gel then the gel was run at 200 V until the sample dye front had run to the base of the resolving gel.

2.5. Western blotting

2.5.1. Protein transfer to Polyvinylidene (PVDF) membrane

The transfer of protein form SDS-PAGE gels to an Amersham Hybond PVDF 0.45 μm membrane (Sigma Aldrich) was achieved using a semi-dry electroblotting transfer unit (Sigma Aldrich). Eight sheets of blotting paper were soaked in transfer buffer (0.3 M Tris-Base (Sigma Aldrich), 10 μM CAPS, 0.02% SDS, 10% ethanol). The membrane was soaked in 100% ethanol to hydrate the membrane, then in transfer buffer for 5 minutes. The set-up for the transfer included four sheets of soaked blotting paper on the base with the soaked PVDF membrane on top followed by the SDS-PAGE gel then four more sheets of soaked blotting paper. The transfer unit was run at constant current of 63 mA per gel for 90 minutes.

2.5.2. Probing and developing membranes

After completion of the transfer, the PVDF membranes were blocked in blocking buffer (1x Tris Buffered Saline (TBS), 1% BSA (w/v), 0.1% Tween-20) for 1 hour on a roller then probed with a specific primary antibody (Table 2.3) diluted in blocking buffer and incubated at 4 °C overnight on a roller. Membranes were washed four times in blocking buffer for 5 minutes to remove excess primary antibody and incubated with a species-specific secondary antibody as indicated (Table 2.3) diluted in blocking buffer for 1 hour on a roller. The membranes were then washed four times in wash buffer (1x TBS, 0.1% Tween-20) for 5 minutes. To develop the blots, hydrogen peroxide and luminol enhancer solution (SuperSignal™ West Pico PLUS Chemiluminescent Substrate, ThermoFisher) were mixed together at a 1:1 ratio and added on to the blot to visualise the protein bands using the BIO-RAD ChemiDoc™ MP Imaging System.

Antibody	Provider	Code	Dilution	Antibody species
CIZ1	Covalabs	Copeland *et al.,* 2015	1:1000	Rabbit
UBR5	Abcam	Ab134089	1:1000	Rabbit
GFP	Sigma Aldrich	G6539	1:2000	Mouse
FLAG	Abcam	Ab1162	1:1000	Rabbit
β-Actin	Sigma Aldrich	A1978	1:10,000	Mouse
Anti-Rabbit IgG HRP	Abcam	ab6721	1:5000	Goat
Anti-Mouse IgG-HRP	Invitrogen	A28177	1:5000	Goat

Table 2.3. Primary and secondary antibodies used for western blotting. A list of the antibodies used, the provider and antibody code, the dilution used and the antibody species.

2.5.3. Standardising protein loads

Protein band intensities were quantified using the BIO-RAD Image Lab Software Version 6.1.0 build 7 Standard Edition. To balance the protein loads, western blotting was performed and standardised using actin band intensities using the following equation:
1/ (value/lowest actin value) x load volume of well.

Subsequently, protein levels were determined for actin and CIZ1. The quantity of CIZ1 was standardised to a relative abundance of the actin load control. The control was standardised to 1 and all other samples were standardised to the control to show relative differences in protein levels compared to the control. Replicate number for protein quantitation stated in figure legend.

2.6. Flow cytometry

For cell cycle analysis by flow cytometry, cells were labelled with EdU at a final concertation of 10 μM for 1 hour. The cells were trypsinised as described in section 2.1.1, neutralised in 5 ml of media, centrifuged (all centrifugation steps were carried out at 500 *x g* for 5 minutes) and the supernatant discarded. Cell pellets were resuspended in 3 ml of PBS, 1% w/v BSA and

cells extracted from buffer by centrifugation and the supernatant discarded. The pellets were resuspended in 100 μl of 4 % PFA and left at room temperature for 15 minutes. Cells were then centrifuged, cell pellets washed in 3 ml of PBS, 1% w/v BSA in 1x PBS then centrifuged and the pellets were stored at -20 °C until use or immediately processed for flow cytometry analysis. The pellets were washed 3 times in PBS, 1% w/v BSA and centrifuged between each wash, cells permeabilised in PBS, 0.5 % v/v Triton X-100 for 15 minutes then centrifuged, and the supernatant discarded. The samples were labelled with 500 μl of EdU labelling cocktail (430 μL of 1x Click-iT™ EdU reaction buffer, 20 μL Copper sulphate solution, 1.2 μL Alexafluorazide 488, 50 μL of 1x EdU Additive) from the Alexa Fluor 488 azide Click-iT™ EdU cell proliferation kit (Invitrogen). The cells were incubated in the dark for 30 minutes, washed 3 times in 0.1% Triton X-100 in 1x PBS and centrifuged between each wash. Samples were labelled with 5 μg/ml of Hoechst 33342 in PBS, 0.1% v/v Triton X-100 for 30 minutes in the dark on ice. The samples were analysed using the Beckman Coulter CytoFLEX using PB450 (450/45) for Hoechst staining and PE (585/42) for EdU staining. 10,000 events were collected for all samples and consistent gating applied.

2.7. Apoptosis assays

After 24-hour drug treatment (section 2.3), the media from the culture plate was collected into a 50 ml falcon tube. The cells were harvested by trypsinisation and added to the falcon tube containing the media. The cells were centrifuged at 500 x *g* for 5 minutes and the supernatant discarded, washed in 1 ml cold PBS and centrifuged at 500 x *g* for 5 minutes. The cells were resuspended in 1 μl of media and stained with 1 μg/ml propidium iodide (PI) and 0.1 μM YO-PRO-1™. The samples were incubated on ice for 30 minutes before being analysed with the Beckman Counter CytoFLEX using FITC (535/40) channel for YO-PRO-1 staining and PE (585/42) channel for PI staining. 10,000 events were collected for all samples and consistent gating applied.

YO-PRO-1 is a nucleic acid stain used to identify apoptotic cells. The ability of YO-PRO-1 to stain early apoptotic cells is based on the plasma membrane being generally preserved with increased permeability only for small cationic probes such as YO-PRO-1 (Wlodkowic *et al.,* 2009). The plasma membrane of early apoptotic cells is permeable to small, cations e.g., YO-PRO-1 and impermeable to larger cations including PI, a dead cell stain. Late apoptotic/

necrotic cells are permeable to YO-PRO-1 and PI as a result of the highly compromised plasma membrane. Live cells have an intact plasma membrane and are impermeant to YO-PRO-1 and PI (Fujisawa *et al.,* 2013; Wlodkowic *et al.,* 2009). The stains, therefore, identify live cells (YO-PRO-1^-/PI^-), early apoptotic cells (YO-PRO-1^+/ PI^-) and late apoptotic/ necrotic cells (YO-PRO-1^+/ PI^+).

2.8. E3 ligase plasmid purification

2.8.1. *E. coli* transformations

E. coli culture media LB broth (10 g Tryptone, 10 g NaCl, 5 g Yeast extract per litre MilliQ water) and LB agar (40 g/l LB agar (ThermoFisher)) were both autoclaved prior to use and handled in a laminar flow hood to ensure aseptic technique to prevent contamination.

Transformation of competent top 10 *Escherichia coli* cells was performed by adding 1 μL of each specific plasmid encoding the E3 ligases (UBR5, FBXO38 and UBE2O) to 50 μl competent cells, the cells were then incubated on ice for 30 minutes, heat-shocked for 1 minute at 42 °C and then transferred back to ice for 5 minutes. The addition of 200 μl of LB broth (Melford) to the competent cells was followed by incubation for 1 hour at 37 °C with shaking (50 rpm). After incubation, 100 μl of the sample was plated onto LB agar (ThermoScientific) plates supplemented with ampicillin (100 μg/ml) (Melford) and incubated overnight at 37 °C. The agar plates with colonies were stored at 4 °C and used within 2 months.

2.8.2. Plasmid purification

For transfection-grade plasmid purification, a single colony was picked from the LB agar plate and used to inoculate 10 ml of LB media supplemented with ampicillin (100 μg/ml) and incubated overnight at 37 °C, 130 rpm. The stationary phase cultures were harvested by centrifugation, 3000 x *g* for 20 minutes and the media removed. The plasmids were purified using the NucleoSpin® Plasmid Transfection-grade miniprep kit (Macherey-Nagel) according to manufacturer's instructions. Briefly, cell pellets were resuspended in 250 μl resuspension buffer followed by the addition of 250 μl of lysis buffer and the tube inverted gently 6-8 times, this was followed by the addition of 300 μl of neutralisation buffer. The tubes were inverted until the blue colour changed to an off-white precipitate. The tubes were centrifuged for 10

minutes at 17,000 x *g*, this step was repeated in case the supernatant was not clear. All subsequent centrifugation steps were at carried out at 11,000 *x g*. The supernatant was transferred to a NucleoSpin® Plasmid TG Column in a Collection Tube and centrifuged for 1 minute and the flow-through discarded. To the column, 650 μl of detoxification buffer was added and centrifuged for 1 minute and the flow-through discarded. The column was washed in 650 μL of wash buffer and centrifuged for 1 minute and the flow-through discarded. The column was centrifuged for a further minute. The NucleoSpin ® Plasmid TG Column was placed in a 1.5 ml microcentrifuge tube and 50 μl of elution buffer added and incubated for 1 minute at room temperature then centrifuged for 1 minute and the flow-through collected. The nucleic acid concentration was determined using UV absorbance spectroscopy with a Nanodrop™ 2000 (Thermo Scientific).

2.8.3. Ethanol precipitation of nucleic acid

To concentrate the purified plasmid stock, 0.1 volumes of 3 M sodium acetate (pH 5.2) followed by 3 volumes of 100% ethanol were added to the purified plasmid then mixed and stored at -20 °C overnight. The samples were centrifuged at 17,000 *x g* for 30 minutes at 4 °C and the supernatant discarded. The pellets were subsequently air dried for 15 minutes at room temperature to allow the evaporation of any remaining ethanol. The pellets were then resuspended in the desired volume of elution buffer and the nucleic acid concertation was determined using UV absorbance spectroscopy with a Nanodrop™ 2000 (Thermo Scientific).

2.9. Transfection of 3T3 cells

Amaxa® Cell Line Nucleofector ® Kit R (Lonza) was used for the transfection of E3 ligase plasmid into 3T3 cells. For asynchronous transfections, the 3T3 cells were grown to 70% confluence then harvested by trypsinisation and neutralised in 5 ml of media. The cells were centrifuged at 500 *x g* for 5 minutes and the supernatant discarded. To remove excess media, cells were centrifuged for an additional minute at 500 x *g* and the supernatant aspirated. The cell pellets were resuspended in 100 μl of Kit R solution with 5 μl of plasmid (total of 1.5 μg plasmid) plasmid DNA for overexpression of each E3 protein or 2 μl of the GFP control provided in Kit R and then transferred to electro cuvettes. To complete the transfection, the Lonza nucleofector 2b electroporation system was used on programme U-030. Transfected

cells were immediately transferred to media and plated onto 10 cm dishes and incubated for 48 hours prior to being harvested for western blot analysis, flow cytometry and EdU incorporation analysis. For transfection of synchronised 3T3 cells, the cells were transfected at the point of G0 release and incubated for 24 hours prior to western blot analysis.

2.10. Immunofluorescence

To determine transfection efficiency, immunofluorescence was used to identify FLAG-tagged E3 ligase constructs. Table 2.4 shows the antibodies used to complete the immunofluorescence.

Antibody	**Provider**	**Code**	**Dilution**	**Antibody species**
FLAG tag	Abcam	Ab1162	1:100-1:250	Rabbit
FALG tag	Sigma Aldrich	F2555	1:125-1:250	Rabbit
Alexa fluor 568 anti-rabbit IgG	Invitrogen	A11036	1:2000	Goat

Table 2.4. The antibodies used for immunofluorescence. A list of the antibodies used, the provider, antibody code, dilution and the antibody species.

Transfected cells were grown on autoclaved glass coverslips, the coverslips were transferred to a 24 well plate, washed 3 times in 1x PBS, fixed for 15 minutes in 4% PFA, then washed three times in 1x PBS. Next, 0.1% Triton-X 100 in 1x PBS was added to the coverslips for 20 minutes followed by 2 washes in antibody buffer (1x PBS, 0.1% v/v triton- X 100, 0.02 % w/v SDS and 1% w/v BSA). Primary antibodies were diluted in antibody buffer to a range of concentrations (Table 2.4) and 20 μl added to the coverslips, a minus primary antibody control was also prepared. Coverslips were incubated in a humidified chamber for 1 hour at 37 °C. The coverslips were washed 3 times in 1x PBS then 3 times in antibody buffer. The secondary antibody specific for the species of primary antibody (Table 2.4) was diluted in antibody buffer (1:2000) and 20 μl to added to the coverslips and incubated in a humidified chamber in the dark for 1 hour at 37 °C. The coverslips were washed 3 times in antibody buffer then 3 times in 1x PBS and mounted on Vectasheild containing DAPI. For GFP transfections, coverslips were fixed in 4% PFA then mounted onto Vectasheild containing DAPI. The coverslips were imaged the same day by fluorescence microscopy (Zeiss Scope.A1). GFP filter

set: excitation 470/40, beamsplitter FT496, emission BP 535/50. FLAG filter set: excitation BP550/25, beamsplitter FT570, emission BP 605/70. The following equation was used to determine GFP transfection efficiency: Transfection efficiency = (GFP positive cells / total cells) x 100. Merged images were generated using the add channel tool on the Zeiss Zen software.

2.11. Statistical analysis

The figures are presented as the mean ± the Standard Deviation (S.D.) for three or more experimental repeats as stated in the figure legends. Statistical significance was measured using the Mann Whitney test using Prism 9 Version 9.3.1 (350).

Chapter 3: Results

3.1. Regulation of CIZ1 by opposing CDK and UPS activities

CIZ1 overexpression has been associated with common cancer types including breast, prostate, gall bladder, colorectal and hepatocellular carcinoma. Previous work has shown CIZ1 protein levels to be reduced by inhibition of CDK2 and DDK which promotes ubiquitin proteasome system (UPS) mediated degradation of CIZ1 in mouse embryonic fibroblast (3T3 cells) (Pauzaite, 2019).

In this study, cells were treated with small molecule kinase inhibitors that target each cell cycle regulatory CDK and DDK to establish which kinase may target CIZ1 and be most appropriate as a potential target. The inhibitors used and their target are: PD0332991 (PD, also called palbociclib; cyclin D-CDK4/6 CDK), PHA-767491 (PHA; Dbf4-Cdc7), CVT-313, CDK2-IN-73 (both CDK2 inhibitors) and Ro-3306 (CDK1 inhibitor). PD0332991 (hereafter referred to as PD) is a highly selective inhibitor of CDK4/6 (Guarducci *et al.,* 2017). PHA-767491 (hereafter referred to as PHA) is a dual Cdc7/ CDK9 inhibitor but can also inhibit CDK2 (IC50 240 nM) and CDK1 (IC50 250 nM) at higher concentrations (Montagnoli *et al.,* 2008; Sasi *et al.,* 2014). CVT-313 is a selective CDK2 inhibitor and CDK2-IN-73 is a more potent CDK2 inhibitor (Brooks *et al.,* 1997; Coxon *et a.,* 2017). Ro-3306 is a CDK1 inhibitor but can also inhibit CDK2 (IC50 340 nM) and CDK4 (IC50 > 2000 nM) at higher concentrations (Vassilev *et al.,* 2006). The small molecule kinase inhibitors are ATP competitive inhibitors that interact with CDKs at the catalytic ATP site (Li *et al.,* 2015). MG132 is a proteasome inhibitor used in this study and works by blocking the proteolytic activity of the 26S proteasome (Han *et al.,* 2009).

In this study, PD, PHA and CVT-313 were used at a concentration of 10 μM based on previous work that showed this concentration to have an effect at the molecular level in 3T3 cells whilst leaving the cells phenotypically unchanged and viable (Pauzaite, 2019). Ro-3306 was used at a concentration of 10 μM based on published work using this inhibitor in 3T3 cells (Yoo *et al.,* 2017). There is limited published work using CDK2-IN-73, however, the concentration of 10 μM used is higher than the IC50. The aim of this section is to evaluate the efficacy of CDK and DDK inhibitors to reduce CIZ1 protein levels and determine the role of the UPS in CIZ1 regulation.

3.1.1. CIZ1 levels are reduced by kinase inhibition in asynchronous 3T3 cells

The working model for CIZ1 regulation (Figure 1.9) suggests CIZ1 stability is dependent on CDK- and DDK- mediated phosphorylation. To determine if CIZ1 protein levels can be reduced through CDK and or DDK inhibition, 3T3 cells were treated with small molecule kinase inhibitors. For this analysis, murine fibroblasts were used as this is the model system used to identify the putative regulators of CIZ1 (Pauzaite, 2019). 3T3 cells were treated with Dimethyl Sulfoxide (DMSO) as a solvent control, CDK4/6 inhibitor (PD), DDK inhibitor (PHA), CDK2 inhibitors (CVT-313 and CDK2-IN-73) and CDK1 inhibitor (Ro-3306), treatments used 10 μM of inhibitor for 24 hours. Treating asynchronous cells over a time course of 24 hours allows for a complete cell cycle and all cell cycle phases to be captured. The effect on CIZ1 protein levels were determined by western blotting (Figure 3.1).

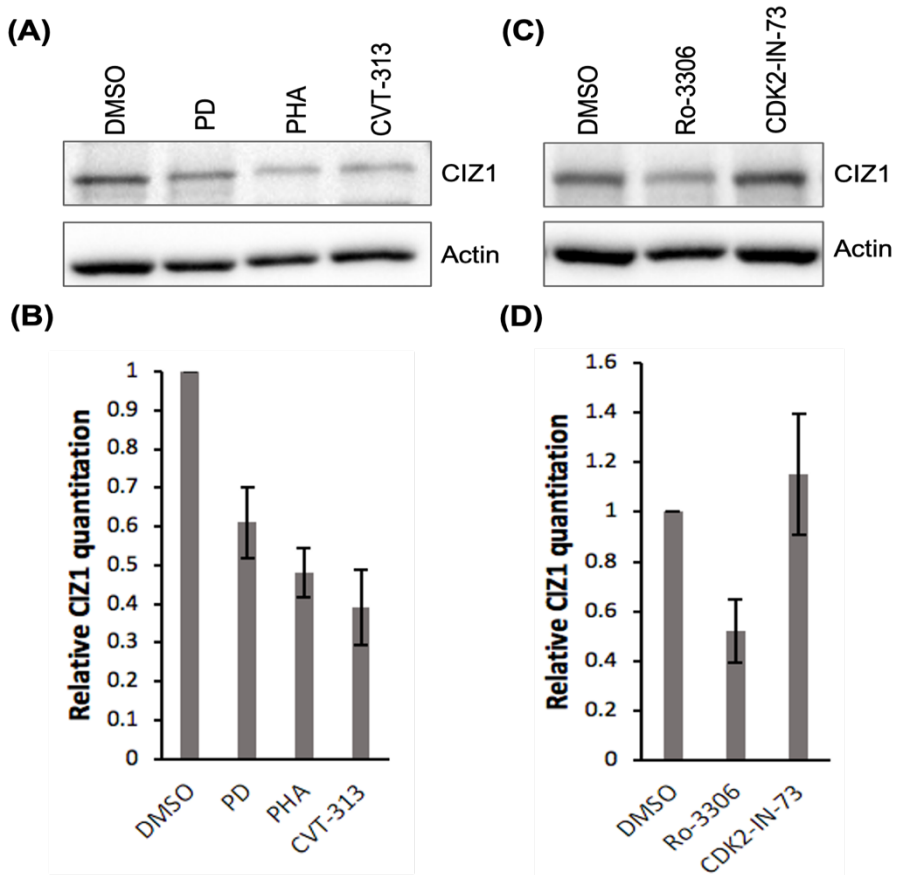

Figure 3.1. CIZ1 protein levels are reduced by the inhibition of CDK4/6, DDK, CDK2 and CDK1 in asynchronous 3T3 cells. (A) Western blot of asynchronous 3T3 cells treated with DMSO, PD, PHA and CVT-313 (all 10 μM) for 24 hours. Blots were probed with CIZ1 and Actin antibodies. **(B)** Quantitation of CIZ1 protein levels relative to actin load control for PD, PHA and CVT-313 standardised to DMSO control, data presented as mean ± S.D, n=3. Significance measured with Mann Whitney test, p = 0.1 for DMSO v PD, DMSO v PHA and DMSO v CVT-313. **(C)** as in A except for Ro-3306 and CDK2-IN-73. **(D)** as in B, but for Ro-3306 and CDK2-IN-73, p = 0.1 for DMSO v for Ro-3306 and p = 0.7 for DMSO v CDK2-IN-73.

Western blot analysis revealed a non-significant reduction in CIZ1 protein levels for PD, PHA and CVT-313 compared to the DMSO control (Figure 3.1. A, B). Ro-3306 also resulted in a non-significant reduction in CIZ1 proteins levels whereas CDK2-IN-73 treatment did not reduce CIZ1 levels compared to the control (Figure 3.1. C, D). CVT-313 caused the largest decrease in CIZ1 protein levels by 61%, followed by PHA, Ro-3306 and PD which led to a reduction by 52%, 48% and 39%, respectively. The results for CDK2-IN-73 are surprising as CDK2-IN-73 is a more potent CDK2 inhibitor than CVT-313 in vitro. The results demonstrate that inhibition of CDK4/6, DDK, CDK2 and CDK1 can reduce CIZ1 protein levels. The activities of the CDK complexes tested here span the entire cell cycle and more investigation is required to identify the role of each cyclin dependent kinases at different phases of the cell cycle.

3.1.2. CIZ1 levels are reduced by kinase inhibition in synchronised 3T3 cells

To assess if the effect of the kinase inhibitors is cell cycle phase dependent, 3T3 cells were synchronised by release from contact inhibition and serum starvation that forces cells in to G0. The cells were then released by reducing cell contacts, plating at low cell density and replacing media. Cells were subsequently treated with small molecule kinase inhibitors to determine the effect on CIZ1 protein levels specifically at late G1/S of the cell cycle. To confirm cell cycle synchronisation, entry in to S-phase was measured by monitoring the incorporation of EdU into nascent DNA 16-24 hours post release from quiescence (G0) (Figure 3.2. A, B). Synchronised 3T3 cells were treated with DMSO solvent control, CDK4/6 inhibitor (PD), DDK inhibitor (PHA), CDK2 inhibitors (CVT-313 and CDK2-IN-73) and CDK1 inhibitor (Ro-3306) 16 hours post release from G0 and harvested at 24 hours. This time course captures cells post-restriction point (15hr after release) and through the G1/ S transition (Coverley *et* al., 2002). The effect of kinase inhibition during late G1 phase on CIZ1 protein levels were determined by western blotting (Figure 3.2. C-F).

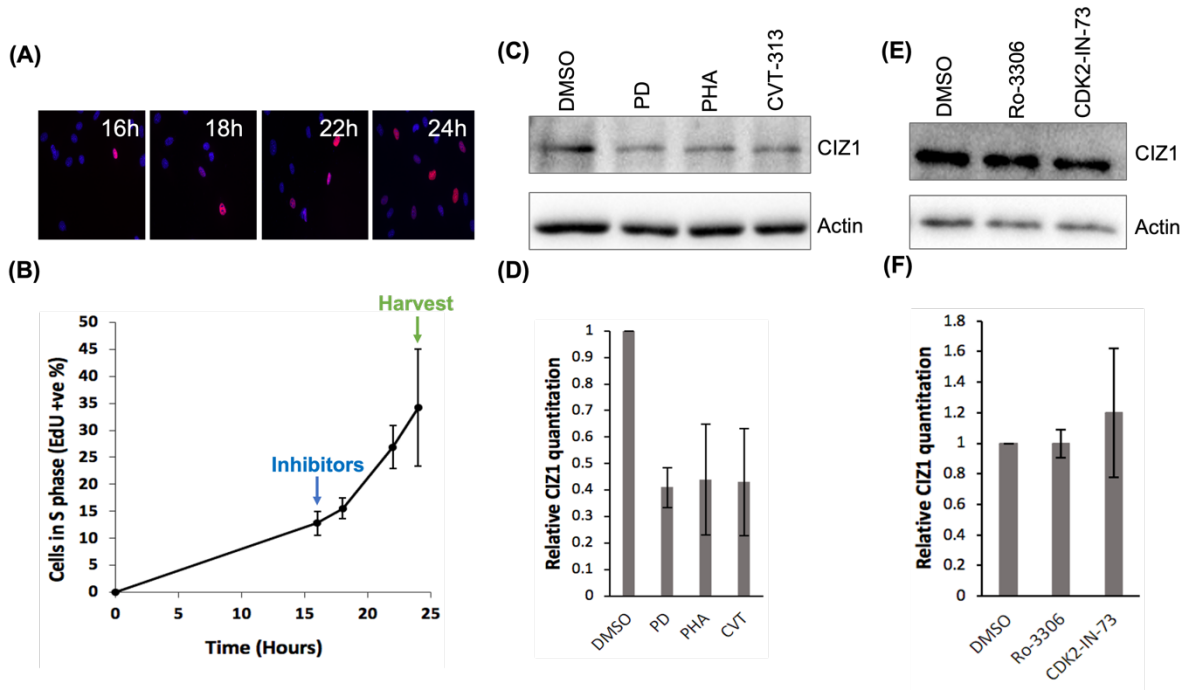

Figure 3.2. CIZ1 protein levels are reduced by the inhibition of CDK4/6, DDK, and CDK2 in late G1 3T3 cells. 3T3 cells were synchronised by release from G0. **(A)** Representative fluorescence microscope images show merged DNA stain (DAPI) and EdU 16-24 hours post release. **(B)** Percentage S phase cells (EdU positive) 16-24 hours post release presented as mean ± S.D., n=3. Blue arrow represents addition of inhibitors, green arrow represents the point the cells were harvested. **(C)** Western blot of cells treated with DMSO, PD, PHA and CVT-313 at a concentration of 10 μM 16-24 hours post release. Blots were probed with CIZ1 and Actin antibodies. **(D)** Quantitation of CIZ1 protein levels relative to actin load control for PD, PHA and CVT-313 standardised to DMSO control, data presented as mean ± S.D, n=3. Significance measured with Mann Whitney test, p = 0.1 for DMSO v PD, DMSO v PHA and DMSO v CVT-313. **(E)** As in C except for Ro-3306 and CDK2-IN-73. **(F)** as in D except for Ro-3306 and CDK2-IN-73. Significance measured with Mann Whitney test, p= 0.7 for DMSO v Ro-3306 and DMSO v CDK2-IN-73.

The increase in percentage S phase cells at 16-24 hours post release from G0 (Figure 3.2 A, B) demonstrates successful synchronisation of 3T3 cells with 35-40% of cells in S phase 24 hours post release. Western blot analysis revealed a non-significant reduction in CIZ1 protein levels for PD, PHA and CVT-313 compared to the DMSO control (Figure 3.2. C, D). PD, PHA and CVT-313 treatments all caused a similar reduction in CIZ1 protein levels by approximately 65%. CIZ1 protein levels were not affected by Ro-3306 or CDK2-IN-73 compared to the DMSO control (Figure 3.2. E, F), the findings for Ro-3306 are expected as CDK1 is inactive in G1/S due to the inhibitory phosphorylation by Wee1 (Potapova *et al.,* 2009). Although more repeats are required to support the findings, the asynchronous and synchronous data suggest that

CDK1 inhibition acts in G2 phase reducing CIZ1 levels, CDK2/DDK imply late G1 phase and CDK4/6 imply early G1 phase.

So far, the data has shown no effect of the CDK2 inhibitor CDK2-IN-73 on CIZ1 protein levels in asynchronous or synchronised 3T3 cells, this could potentially be due to insufficient inhibition of CDK2. The ability of CDK2-IN-73 to inhibit CDK2 was investigated further in synchronised 3T3 cells. The inhibition of CDK2 should lead to a reduction in S phase entry as activation of CDK2 initiates DNA synthesis (Lunn *et al.,* 2010). To determine if CDK2-IN-73 reduces S phase entry, 3T3 cells were synchronised by G0 release and monitored from G0-S. Synchronised cells were treated with DMSO solvent control and the CDK2 inhibitors CVT-313 and CDK2-IN-73 at a concertation of 10 μM 16-24 hours post release from G0. CLICK-IT EdU fluorescent labelling was used to measure EdU incorporation into nascent DNA 24 hours post release quantified as S phase cells (EdU positive) as a percentage of all cells (DAPI stained) (Figure 3.3).

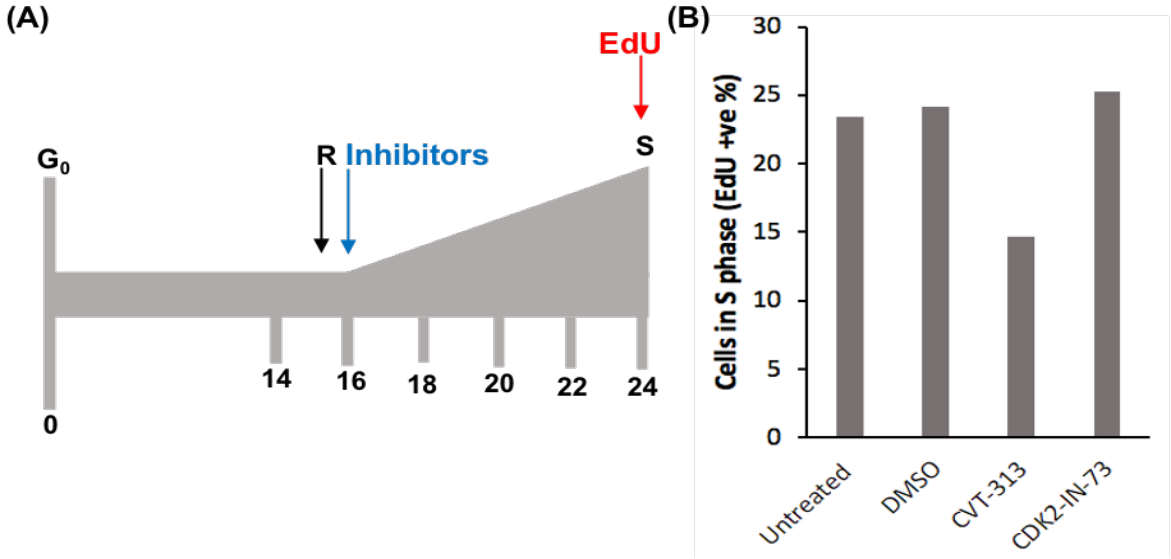

Figure 3.3. S phase entry is not reduced by CDK2-IN-73. 3T3 cells were synchronised by release from G0 and treated with DMSO, CVT-313 and CDK2-IN-73 at a concentration of 10 μM 16-24 hours post release. **(A)** Experimental overview. The timeline shows entry into S phase after release from G0 represented by the triangle, timing of restriction point (R), addition of inhibitors and EdU labelling. **(B)** Percentage S phase cells (EdU positive) 24 hours post release, n=1.

Entry into S phase was reduced by CVT-313 by 10 % compared to the DMSO control, however CDK2-IN-73 had no effect on S phase entry compared to the DMSO control. This is surprising as CDK2-IN-73 is a more potent CDK2 inhibitor than CVT-313 (IC50 values of 44 nM and 0.5

μM for CDK2-IN-73 and CVT-313, respectively) (Brooks *et al.,* 1997; Coxon *et al.,* 2017) therefore it would be expected that CDK2-IN-73 would have a similar effect or a more potent effect on S phase entry compared to CVT-313. This suggests that CDK2-IN-73 is not having an inhibitory effect on CDK2 in 3T3 cells and could explain the reason behind CDK2-IN-73 treatment not leading to a reduction in CIZ1 protein levels.

3.1.3. CIZ1 protein levels are post-translationally regulated by the ubiquitin proteasome system (UPS)

The data so far has shown that the inhibition of CDK4/6, DDK, CDK2 and CDK1 results in a non-significant reduction in CIZ1 protein levels. CIZ1 levels are reduced specifically at late G1/S in synchronised cells treated with CDK4/6, DDK and CDK2 inhibitors. The reduction in CIZ1 protein levels could potentially be a result of reduced progression through the cell cycle or an active degradation process such as proteasomal-mediated degradation. To determine the potential role of the proteasome in the regulation of CIZ1 protein levels, asynchronous 3T3 cells were treated with CDK4/6 inhibitor (PD), DDK inhibitor (PHA) and CDK2 inhibitor (CVT-313), in combination with the proteasome inhibitor MG132 at a concentration of 10 μM for 6 hours. The effect on CIZ1 protein levels were determined by western blotting (Figure 3.4).

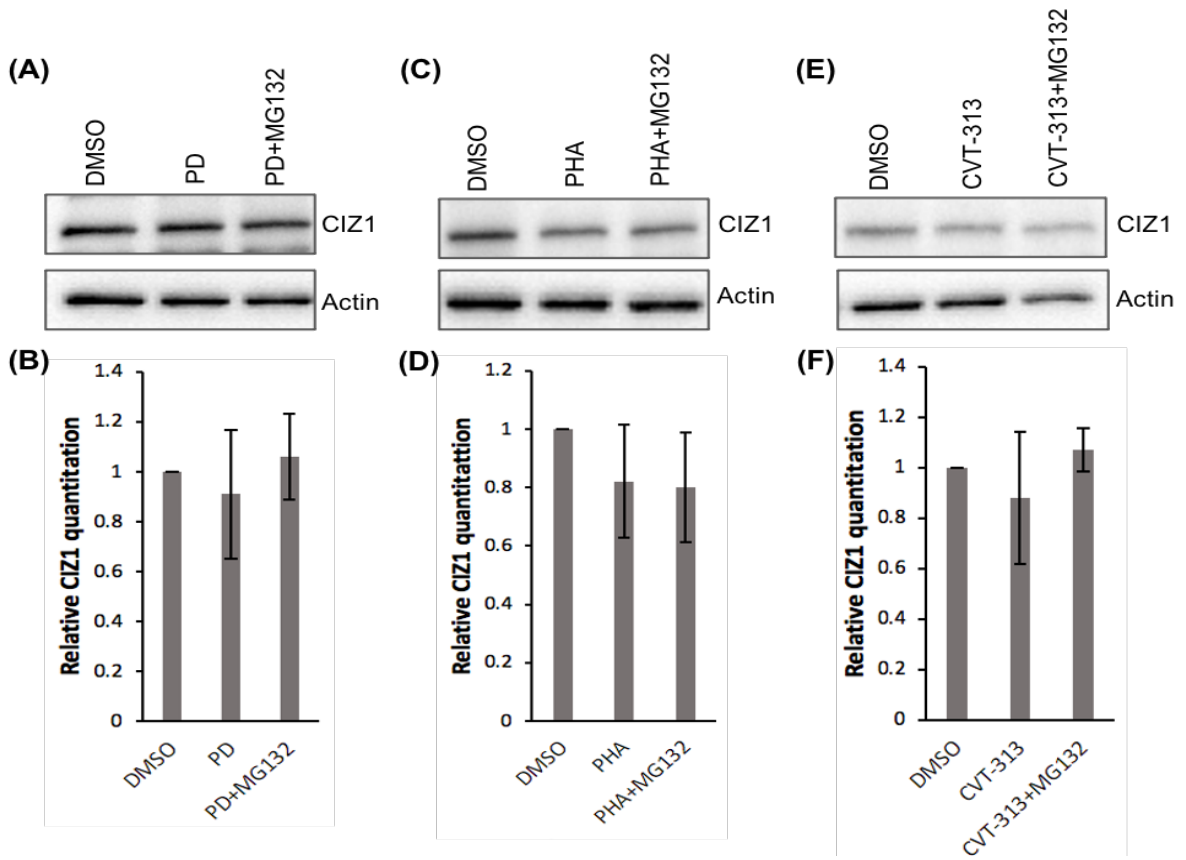

Figure 3.4. CIZ1 protein levels are minimally affected by proteasome inhibition in asynchronous 3T3 cells. (A) Western blot of asynchronous 3T3 cells treated with DMSO and PD±MG132 at a concertation of 10 μM for 6 hours. Blots were probed with CIZ1 and Actin antibodies. **(B)** Quantitation of CIZ1 protein levels relative to actin load control for PD±MG132 standardised to DMSO control, data presented as mean ± S.D, n=3. Significance measured with Mann Whitney test, p =0.7 for DMSO vs PD, p = 0.4 for PD vs PD+MG132 **(C)** as for A but for PHA±MG132. **(D)** as for B but for PHA±MG132, p = 0.7 for DMSO vs PHA, p=0.9 for PHA vs PHA+MG132. **(E)** as for A but for CVT-313±MG132. **(F)** as for B bur for CVT-313±MG132, p = 0.7 for DMSO vs CVT-313 and CVT-313 vs CVT-313+MG132.

This analysis revealed minimal change in CIZ1 protein levels for PD, PHA and CVT-313 treatments compared to DMSO control resulting in no observable effect of the proteasome inhibitor MG132. In earlier experiments, asynchronous 3T3 cells treated with PD, PHA and CVT-313 at 10 μM for 24 hours resulted in a non-significant reduction in CIZ1 protein levels (Figure 3.1). This suggests treatment of asynchronous cells with kinase inhibitors for 6 hours may not be sufficient time for the degradation of CIZ1. A further confounding effect may be due to cell cycle specific activity for each kinase inhibitor.

In earlier experiments, synchronised 3T3 cells in late G1 phase showed reductions in CIZ1 protein levels when treated with the small molecule kinase inhibitors PD, PHA and CVT-313 (Figure 3.2). To determine if kinase inhibition during late G1 phase promotes UPS mediated

degradation of CIZ1 protein levels, 3T3 cells were synchronised in G0 and released back into G1 phase. At 16 hours post release, cells were treated with DMSO solvent control, or CDK4/6 inhibitor (PD), DDK inhibitor (PHA) and CDK2 inhibitor (CVT-313) with or without the proteasomal inhibitor MG132. Cells were harvested 24 hours post release and the effect on CIZ1 protein levels were determined by western blotting (Figure 3.5).

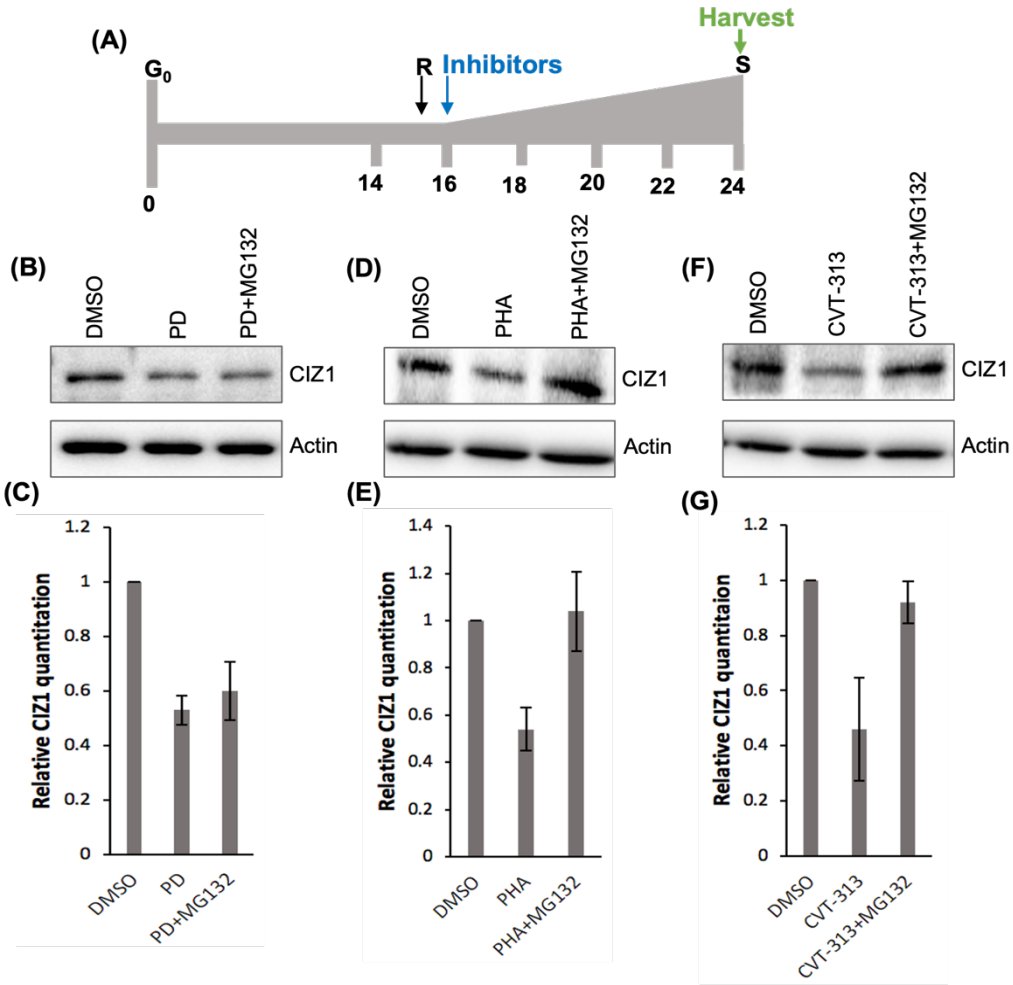

Figure 3.5. CIZ1 protein levels are recovered by proteasomal inhibition after DDK/ CDK2 inhibition in synchronised 3T3 cells. 3T3 cells were synchronised by release from G0. **(A)** Experimental overview. Timeline shows entry into S phase after G0 release represented by the triangle, timings of restriction point ©, addition of inhibitors and harvesting. **(B)** Western blot of cells treated with DMSO and PD±MG132 at a concentration of 10 μM 16-24 hours post release. Blots probed with CIZ1 and Actin antibodies. **(C)** Quantitation of CIZ1 protein levels relative to actin load control for PD±MG132 standardised to DMSO control, data presented as mean ± S.D, n=3. Significance measured with Mann Whitney test, p =0.1 for DMSO vs PD, p = 0.4 for PD vs PD+MG132. **(D)** as for B but for PHA±MG132. **(E)** as for C but for PHA±MG132, p = 0.1 for DMSO vs PHA and PHA vs PHA+MG132. **(F)** as for B but for CVT±MG132. **(G)** as for C but for CVT-313±MG132, p = 0.1 for DMSO vs CVT-313 and CVT-313 vs CVT-313+MG132.

Western blot analysis revealed a non-significant reduction in CIZ1 protein levels for PD compared to DMSO control and no change with the addition of the proteasome inhibitor

MG132 (Figure 3.5. B, C). PHA and CVT-313 treatment resulted in a non-significant reduction in CIZ1 protein levels compared to DMSO control and the addition of MG132 recovered CIZ1 protein levels to similar levels of control (Figure 3.5. D-G). Importantly, PD, PHA and CVT-313 treatments reduced CIZ1 protein levels by an amount consistent with earlier experiments in synchronised 3T3 cells (Figure 3.2). Although more repeats are required to support the findings, the data suggests that CIZ1 is regulated by the UPS and that this effect is enhanced by DDK and CDK2 inhibition but not CDK4/6 inhibition.

3.2. CIZ1 regulation by E3 ligases

Identification of the E3 ligases involved in the regulation of CIZ1 levels and characterisation of their function could provide a deeper understanding of the regulatory mechanisms that control CIZ1 activity. The model for CIZ1 regulation suggests that CIZ1 is regulated by opposing DDK/ CDK2 and UPS activities (Figure 3.6). The reduction in CIZ1 protein levels by CDK and DDK inhibition would be dependent on a functional UPS system. In addition, the model suggests that perturbation of CDK networks through small molecule inhibition of cyclin dependent kinases may reduce CIZ1 levels and this has potential clinical benefit in cancers that are reliant on CIZ1 overexpression (Pauzaite, 2019). In addition, the E3s that target CIZ1 for degradation could be used for patient stratification to determine if the patient has a functional UPS with the E3s that target CIZ1 and therefore would benefit from CDK/DDK inhibition therapy.

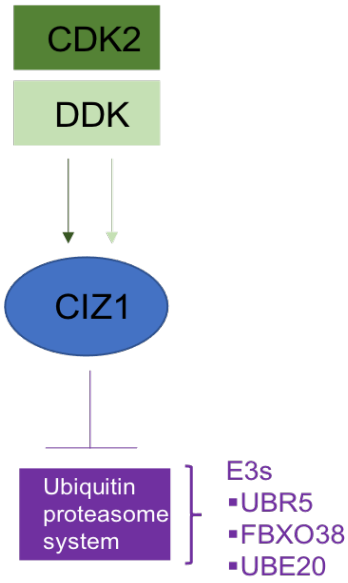

Figure 3.6. The proposed model for CIZ1 regulation by CDK/DDK and E3 ligase activities. CIZ1 levels are regulated by CDK2/DDK mediated phosphorylation which leads to stability and accumulation. Opposing regulation is by the UPS which degrades CIZ1, this is dependent on a functional UPS and the presence of the E3 ligase(s) that target CIZ1. The putative E3 ligases targeting CIZ1 include UBR5, FBXO38 and UBE2O.

Previous work has identified three putative E3 ligases that potentially regulate CIZ1 including Ubiquitin-protein ligase E3 component n- recognin 5 (UBR5), F-box only protein 38 (FBXO38) and E3-independent E2 ubiquitin-conjugation enzyme (UBE2O) (Pauzaite, 2019). The aim of this section is to characterise the activity of each E3 in the regulation of CIZ1 protein levels and cell cycle progression. The three putative E3 ligases will be transfected into asynchronous and synchronous 3T3 cells. Overexpression of an E3 ligase that regulates CIZ1 would be expected to show a reduction in CIZ1 levels, similar to previously published results using siRNA to target CIZ1 (Copeland et al., 2010). The depletion of CIZ1 in 3T3 cells using anti-CIZ1 siRNA has been shown to reduce the number of cells in S phase (Copeland *et al.,* 2010; Coverley *et al.,* 2005). Coverley *et al.,* (2005) observed this effect at 48 hours post-transfection with anti-CIZ1 siRNA. This section will investigate the potential role of three putative E3 ligases in the regulation of CIZ1 protein levels.

3.2.1. Characterising the potential role of UBR5 in regulating CIZ1 protein levels

UBR5 is a HECT E3 ligase and has been shown to have a role in cell cycle regulation (Shearer *et al.,* 2015), the potential role of UBR5 in regulating CIZ1 protein levels was evaluated. Asynchronous 3T3 cells were transfected with UBR5-GFP plasmid or GFP control and harvested 48 hours post-transfection. Transfection efficiency was determined by fluorescence microscopy and the expression of UBR5-GFP was also determined by western blotting (Figure 3.7). All downstream analysis has been completed 48 hours post-transfection based on CIZ1 depletion studies which found a reduction in S phase cells 48 hours post-transfection with anti-CIZ1 siRNA (Coverley *et al.,* 2005). Similar downstream analysis has been used in this study therefore the time course of 48 hours was chosen.

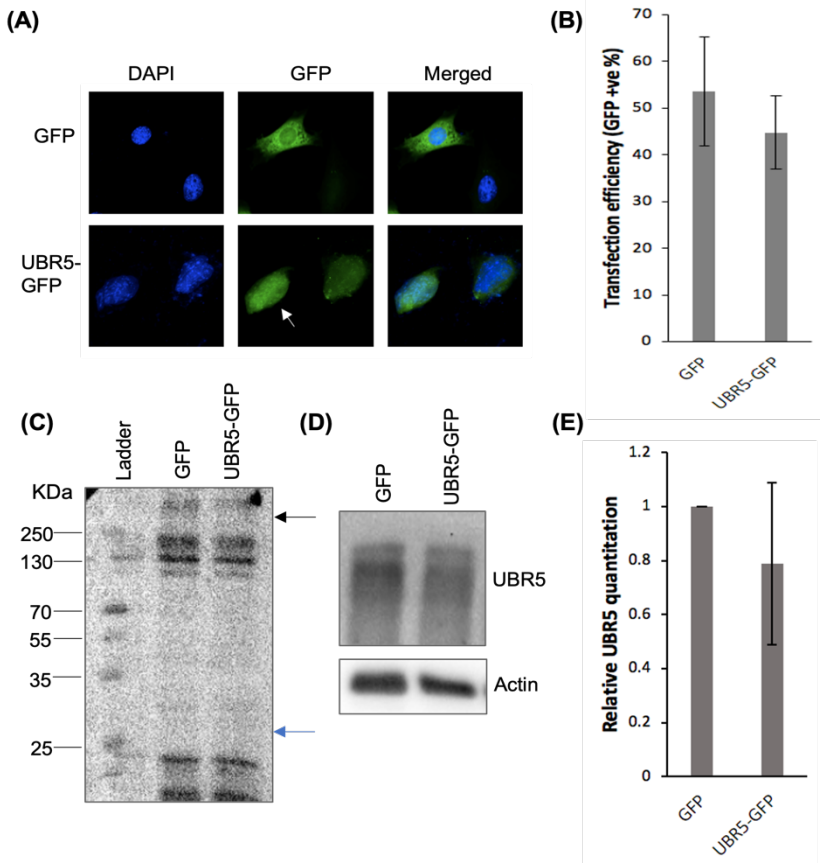

Figure 3.7. Validating GFP and UBR5-GFP expression in asynchronous 3T3 cells. Asynchronous 3T3 cells were transfected with GFP and UBR5-GFP and harvested 48 hours post transfection. **(A)** Representative fluorescence microscope images show DNA stain (DAPI), GFP and merged images. White arrow represents a cell scored as UBR5-GFP positive. **(B)** Percentage transfected cells (GFP positive) presented as mean ± S.D., n=5. **(C)** Western blot of transfected cells probed with GFP antibody. Blue arrow indicates expected molecular weight of GFP (27KDa) and black arrow indicates expected molecular weight for UBR5-GFP (3366KDa) **(D)** Western blot of transfected cells probed with UBR5 and Actin antibodies. **(E)** Quantitation of UBR5 protein levels relative to actin load control, data presented as mean ± S.D, n=3.

The fluorescence microscopy images show fluorescence in the green channel for GFP and UBR5-GFP transfected cells as expected (Figure 3.7. A). The images for GFP and UBR5-GFP transfected cells were taken at different exposure times based on signal to noise ratio. A lower level of fluorescence was detected in the UBR5-GFP transfected cells and therefore images were captured using a longer exposure time. A consideration for UBR5-GFP expression levels is that fusion tags can affect protein expression (Saiz-Baggettp *et al.,* 2017). Transfection efficiency was calculated as 50-60% for GFP control and 40-50% for UBR5-GFP (Figure 3.7. B). The white arrow indicates a cell that was scored as UBR5-GFP positive, however, a non-transfected control would be necessary to accurately determine the difference between autofluorescence and a UBR5-GFP positive cell and thereby allow a more accurate transfection efficiency to be calculated. Western blot analysis revealed non-specific binding of the GFP antibody and a weak signal, the band pattern for both GFP and UBR5-GFP transfections is similar with no distinct differences (Figure 3.7. C). This suggests there is non-specific binding of the GFP antibody. The western blot probed with UBR5 antibody revealed a small non-significant decrease in UBR5 protein levels in the UBR5-GFP transfected cells compared to GFP control (Figure 3.7. D, E) which would suggest unsuccessful transfection. However, UBR5 antibody validation would be required to ensure that the antibody is detecting UBR5 specifically. Additional controls including the quantitation of UBR5 mRNA levels are required to validate UBR5-GFP expression.

The effect of transfecting cells with UBR5-GFP plasmid on CIZ1 levels was determined by western blotting. The effect on the cell cycle profile was determined by measuring EdU incorporation into nascent DNA by fluorescence microscopy and multiparameter flow cytometry 48 hours post-transfection (Figure 3.8).

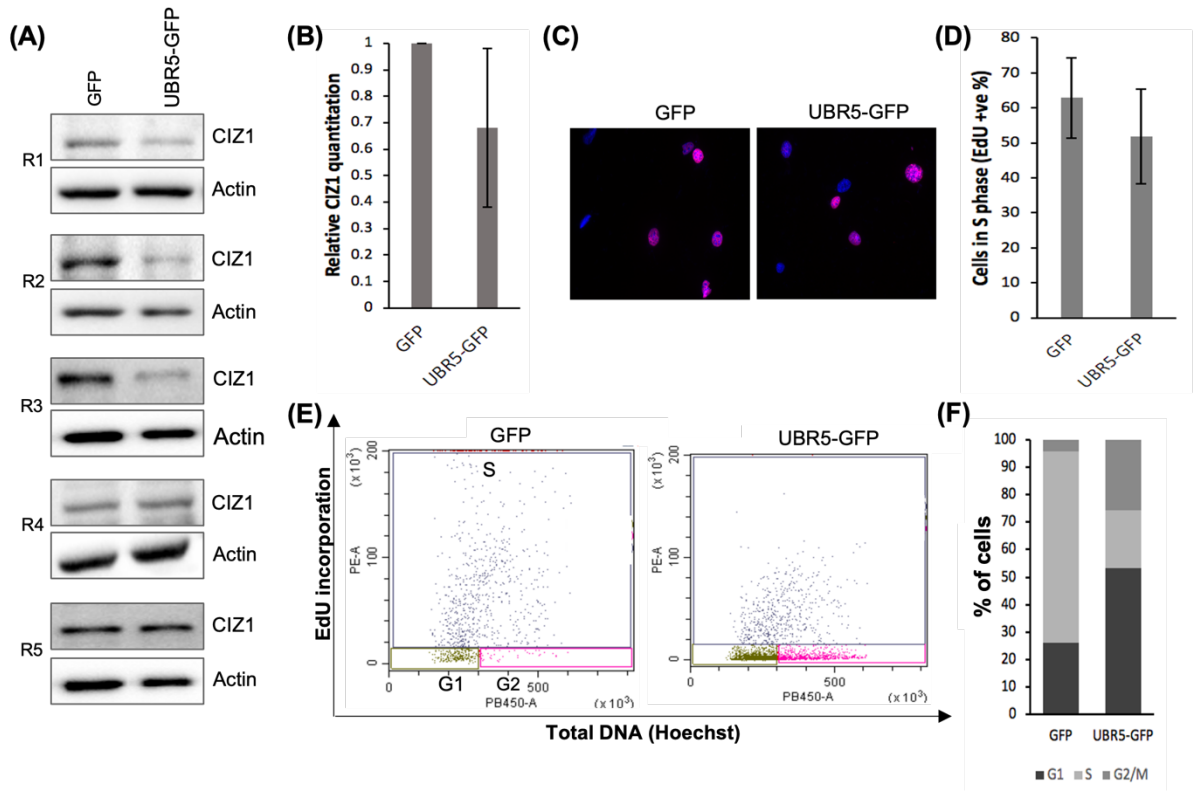

Figure 3.8. CIZ1 protein levels and DNA synthesis are reduced in 3T3 cells after transfection with UBR5-GFP. Asynchronous 3T3 cells were transfected with GFP and UBR5-GFP and harvested 48 hours post transfection. **(A)** Western blot of transfected cells probed with CIZ1 and Actin antibodies, five experimental repeats shown (R1-5). **(B)** Quantitation of CIZ1 protein levels relative to actin load control, data presented as mean ± S.D, n=5. Significance measured using Mann Whitney test, p = 0.127. **(C)** Representative fluorescence microscope images show merged DNA stain (DAPI) and EdU of transfected cells. **(D)** Percentage S phase cells (EdU positive) in relation to all DAPI stained cells, presented as mean ± S.D., n=5. Significance measured using Mann Whitney test, p = 0.198. **(E)** Multiparameter flow cytometry dot plot, EdU intensity (y axis) and Hoechst intensity (total DNA) (x axis) with G1, S and G2 populations labelled on the GFP control. **(F)** Quantitation of flow cytometry dot plot data, stacked bar chart shows percentage of cells in G1, S and G2/M as indicated.

Transfection of 3T3 cells with UBR5-GFP resulted in a reduction in CIZ1 levels compared to GFP control for three out of five experimental repeats (Figure 3.8. A). Repeats labelled R1, R2 and R3 show an average reduction in CIZ1 protein levels by approximately 48%. All repeats together show a non-significant reduction in CIZ1 protein levels by approximately 33% (Figure 3.8. B). Cells transfected with UBR5-GFP showed a non-significant reduction in percentage S phase cells by approximately 10% compared to GFP control (Figure 3.8. C, D). Flow cytometry analysis revealed a reduction in EdU signal intensity for UBR5-GFP transfected cells to GFP control (Figure 3.8. E) and quantitation revealed a reduction in percentage S phase by approximately 42% (Figure 3.8. F). The larger reduction in S phase cells observed by flow

cytometry analysis compared to fluorescence microscopy could be due to flow cytometry analysis measuring EdU intensity as opposed to fluorescence microscopy in which cells are simply scored as EdU positive or negative. As such flow cytometry can miss those cells that are in early S-phase with small diffuse replication foci and low overall fluorescence intensity. The reduction in EdU positive cells by both methods suggests a reduction in total replicating nuclei. In addition, the reduced fluorescence intensity for UBR5 transfected cells is consistent with less efficient initiation of DNA replication and reduced fork progression. Together, the results demonstrate a non-significant reduction in CIZ1 levels and EdU labelling after transfection with UBR5-GFP plasmid, however, further validation of UBR5-GFP overexpression would be required for conclusions to be drawn regarding the effect of UBR5 on CIZ1 regulation.

3.2.2. Detection of FBXO38-FLAG and UBE2O-FLAG expression by immunofluorescence and western blotting

To determine if FBXO38 and UBE2O E3 ligases regulate CIZ1 protein levels, asynchronous 3T3 cells were transfected with FBXO38-FLAG and UBE2O-FLAG plasmid. GFP was used as the control and GFP transfection efficiency was determined by fluorescence microscopy. Detection of FBXO38-FLAG and UBE2O-FLAG was determined by immunofluorescence microscopy 48 hours post-transfection. For the immunofluorescence, Anti-DDDDK tag (FLAG tag (abcam ab1162) primary antibody at a concertation of 1:100 and Alexa fluor 568 anti-rabbit secondary antibody at a concertation of 1:2000 was used. Initially, as a control, non-transfected asynchronous 3T3 cells were probed with primary and secondary antibody to determine primary antibody specificity. A minus primary antibody control was used to determine any cross-reactivity of the secondary antibody (Figure 3.9).

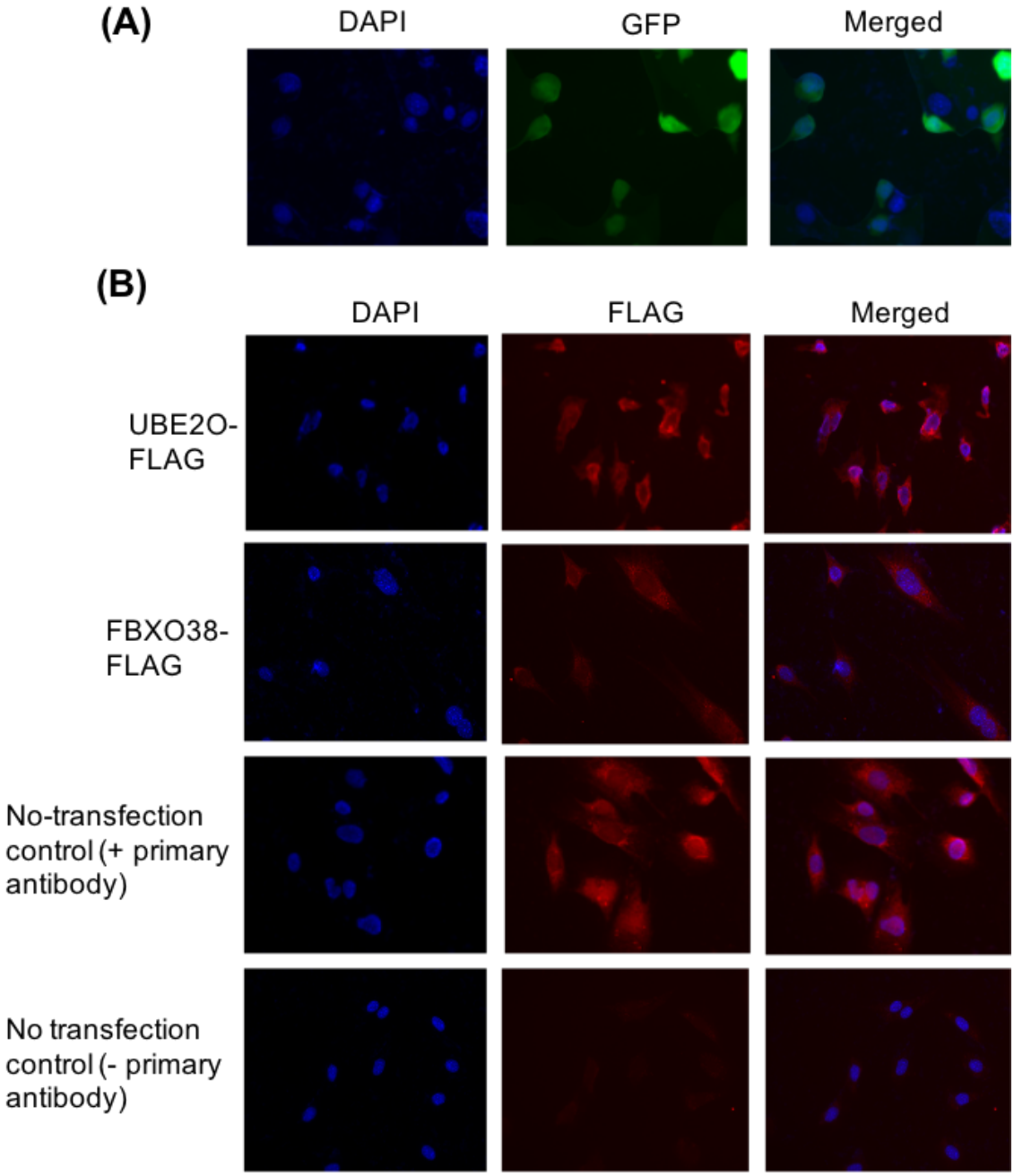

Figure 3.9. Validation of the anti-FLAG antibody by immunofluorescence. Asynchronous 3T3 cells were transfected with GFP, UBE2O-FLAG and FBXO38-FLAG and harvested 48 hours post transfection. **(A)** Representative fluorescence microscope images show DNA stain (DAPI), GFP and merged images for GFP-transfected control. **(B)** Representative immunofluorescence images showing DNA stain (DAPI), FLAG and merged images. Cells were treated with Anti-DDDDK tag (FLAG tag (abcam ab1162)) primary antibody (1:100) as indicated in the figure and Alexa fluor 568 anti-rabbit secondary antibody (1:2000).

Fluorescence microscopy of GFP-transfected control (Figure 3.9.A) was used to calculate transfection efficiency which was 44±3.5% (n=5) for FBXO38-FLAG transfection experiments and 48.9±8.1% (n=3) for UBE2O-FLAG transfection experiments. The immunofluorescence experiment showed the FLAG signal to be similar for UBE2O, FBXO38 and the non-transfected primary antibody control. The minus primary antibody control shows no detectable signal demonstrating that there is no cross-reactivity of the secondary antibody (Figure 3.9. B), this suggests there is non-specific binding of the primary antibody. As a result, transfection efficiency for UBE2O-FLAG and FBXO38-FLAG could not be calculated. To try and resolved the problem with non-specific binding of the primary antibody, a different primary antibody was used (Figure 3.10). The primary antibody Anti-FLAG (Sigma F2555) was used at a concentration of 1:125.

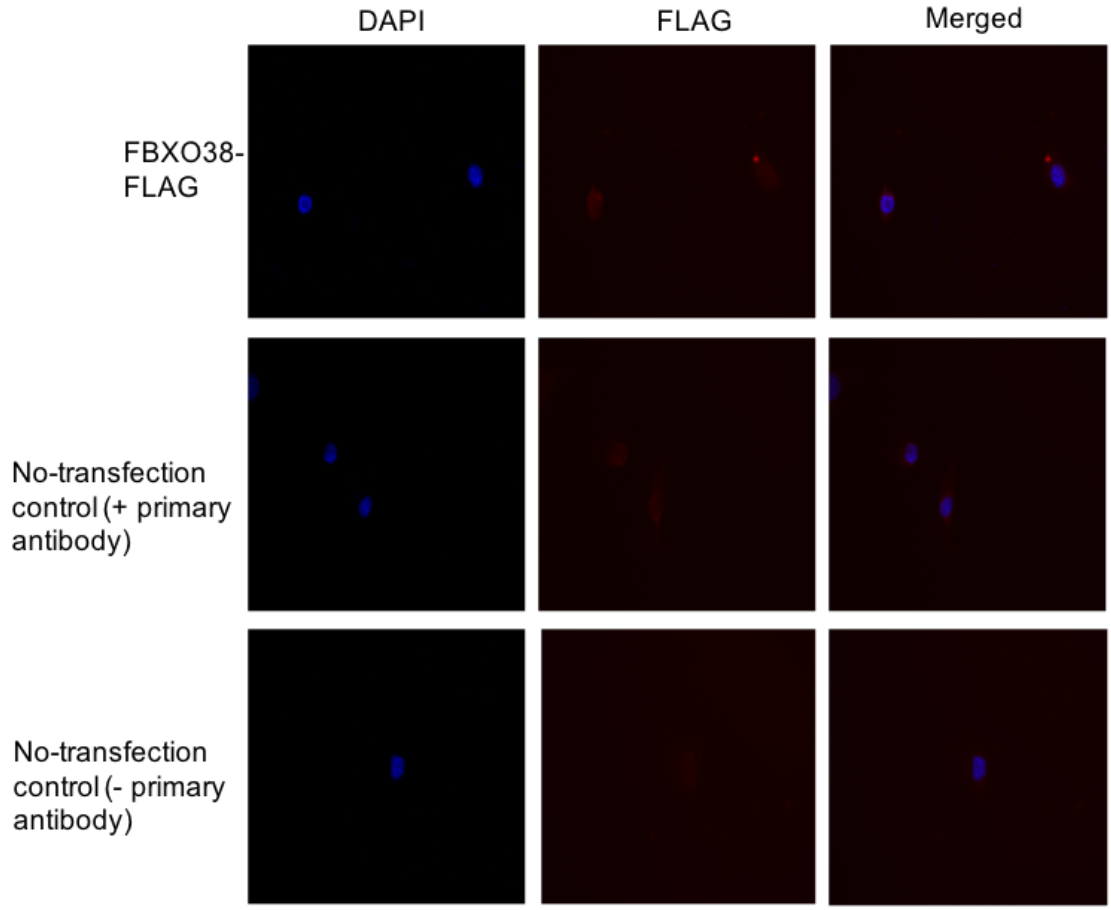

Figure 3.10. Detecting FBXO38-FLAG by immunofluorescence. Representative fluorescence images of asynchronous 3T3 cells transfected with FBXO38-FLAG harvested 48 hours post transfection or non-transfected cells showing DAPI, FLAG and merged images. Cells were treated with Anti-FLAG (Sigma F2555) primary antibody (1:125) as indicated in the figure and Alexa fluor 568 anti-rabbit secondary antibody (1:2000).

The immunofluorescence revealed no detectable signal for FLAG in the FBXO38-FLAG transfected cells or non-transfected controls. This suggests that the transfection may not have been successful and therefore the FLAG-tagged E3 construct can't be detected by immunofluorescence. Another explanation for the result includes a potential problem with the sensitivity of the primary antibody. As FBXO38-FLAG and UBE2O-FLAG were unable to be detected by immunofluorescence, protein samples were harvested 48 hours post transfection to detect FBXO38-FLAG and UBE2O-FLAG overexpression by western blot analysis (Figure 3.11).

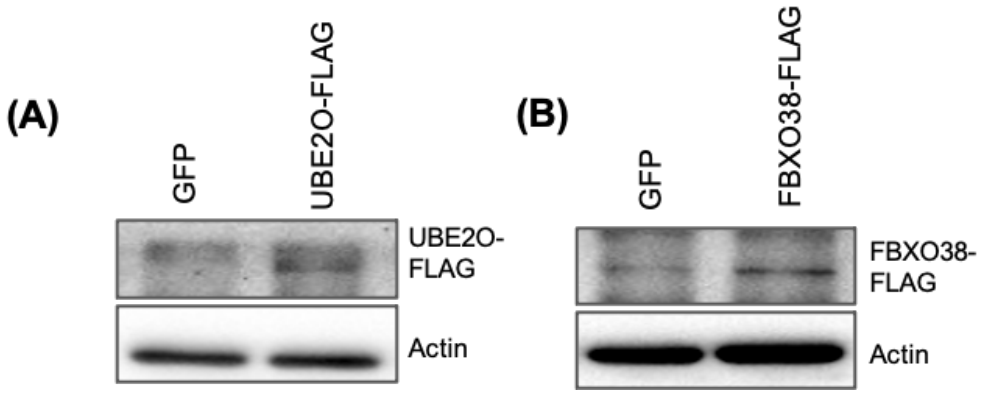

Figure 3.11. Detection of FBXO38-FLAG and UBE2O-FLAG by western blotting. (A) Western blot of asynchronous 3T3 cells transfected with GFP and UBE2O-FLAG, samples harvested 48 hours post transfection. Blots were probed with FLAG (ab1162 abcam) and Actin antibodies. **(B)** as for A but for GFP and FBXO38-FLAG transfected cells.

Western blot analysis revealed a faint band for UBE2O-FLAG and FBXO38-FLAG in the transfected cell populations suggesting that the expression of the constructs is very low, potentially as a result of low transfection efficiency. Furthermore, it could be possible that the anti-FLAG antibody concentration requires further optimisation. Additional controls including determination of transcript levels by quantitative reverse transcriptase PCR and optimisation of the transfection procedure are required to validate this approach and the observed results.

3.2.3. Characterising the potential role of FBXO38 in regulating CIZ1 protein levels

FBXO38 is an F-box protein, F-box proteins have many targets involved in cell cycle regulation (Bassermann *et al.,* 2014). To determine if FBXO38 has a potential role in the regulation of CIZ1 protein levels, asynchronous 3T3 cells were transfected with FBXO38-FLAG plasmid or GFP control and harvested 48 hours post transfection. Figure 3.11 demonstrates a low level

of FBXO38-FLAG in the transfected cell population and the effect on CIZ1 protein levels was determined by western blot analysis. The effect on the cell cycle profile was determined by measuring EdU incorporation into nascent DNA by fluorescence microscopy and multiparameter flow cytometry (Figure 3.12).

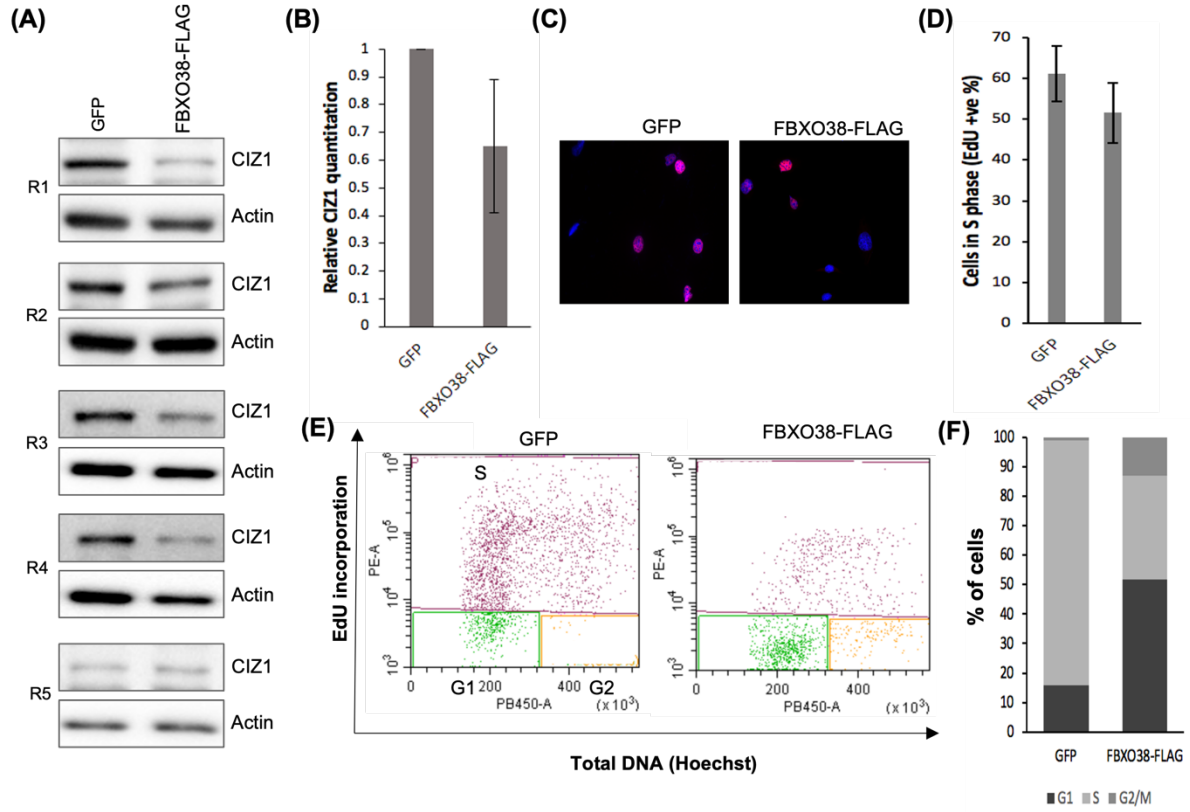

Figure 3.12. CIZ1 protein levels and DNA synthesis are reduced in 3T3 cells after transfection with FBXO38-FLAG. Asynchronous 3T3 cells were transfected with GFP and FBXO38-FLAG and harvested 48 hours post transfection. **(A)** Western blot of transfected cells probed with CIZ1 and Actin antibodies, five experimental repeats shown (R1-5). **(B)** Quantitation of CIZ1 protein levels relative to actin load control, data presented as mean ± S.D, n=5. Significance measured using Mann Whitney test, p = 0.127. **(C)** Representative fluorescence microscope images show merged DNA stain (DAPI) and EdU of transfected cells. **(D)** Percentage S phase cells (EdU positive) in relation to all DAPI stained cells, presented as mean ± S.D., n=5. Significance measured using Mann Whitney test, p = 0.0635**. (E)** Multiparameter flow cytometry dot plot, EdU intensity (y axis) and Hoechst intensity (total DNA) (x axis) with G1, S and G2 populations labelled on the GFP control dot plot. **(F)** Quantitation of flow cytometry dot plot data, stacked bar chart shows percentage of cells in G1, S and G2/M as indicated.

Transfection of 3T3 cells with FBXO38-FLAG resulted in a non-significant reduction in CIZ1 levels by 35% compared to GFP control, with four out of five experimental repeats showing a reduction in CIZ1 protein levels (Figure 3.12. A, B). This reduction in CIZ1 levels was associated with a non-significant reduction in percentage S phase cells by ~ 10% for FBXO38-FLAG transfected cells (Figure 3.12. C, D). Quantitation of flow cytometry results shows that

transfection of 3T3 cells with FBXO38-FLAG reduced the number of S-phase cells by approximately 45%, relative to GFP control (Figure 3.12. E, F). Together, the results demonstrate a non-significant reduction in CIZ1 levels and EdU labelling after transfection with FBXO38-FLAG plasmid, however, further validation of FBXO38-FLAG overexpression would be required for conclusions to be drawn regarding the effect of FBXO38 on CIZ1 regulation.

3.2.4. Characterising the potential role of UBE2O in regulating CIZ1 protein levels

UBE2O is a hybrid E2/ E3 and can mono-ubiquitinate, multi-ubiquitinate and polyubiquitinate substrates and therefore UBE2O can have roles in protein signalling, localisation and degradation (Ullah *et al.,* 2018). To determine if UBE2O has a potential role in the regulation of CIZ1 protein levels, asynchronous 3T3 cells were transfected with UBE2O-FLAG plasmid or GFP control and harvested 48 hours post-transfection. Figure 3.11 demonstrates a low level of UBE2O-FLAG in the transfected cell population and the effect on CIZ1 protein levels was determined by western blot analysis and the effect on the cell cycle profile was determined by measuring EdU incorporation into nascent DNA by fluorescence microscopy and multiparameter flow cytometry (Figure 3.13).

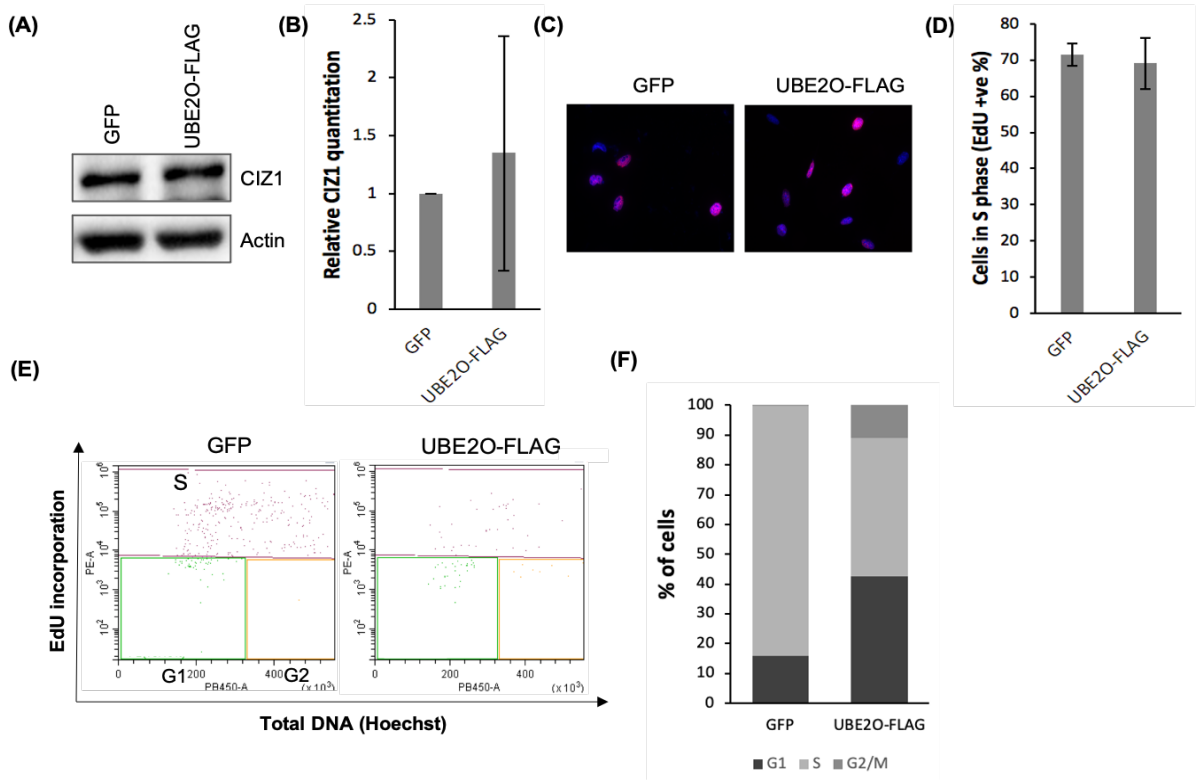

Figure 3.13. CIZ1 protein levels and DNA synthesis are not reduced in 3T3 cells after transfection with UBE2O-FLAG. Asynchronous 3T3 cells were transfected with GFP and UBE2O-FLAG and harvested 48 hours post transfection. **(A)** Western blot of transfected cells probed with CIZ1 and Actin antibodies. **(B)** Quantitation of CIZ1 protein levels relative to actin load control, data presented as mean ± S.D, n=3. Significance measured using Mann Whitney test, p = 0.7. **(C)** Representative fluorescence microscope images show merged DNA stain (DAPI) and EdU of transfected cells. **(D)** Percentage S phase cells (EdU positive) in relation to all DAPI stained cells, presented as mean ± S.D., n=3. Significance measured using Mann Whitney test, p = 0.7. **(E)** Multiparameter flow cytometry dot plot, EdU intensity (y axis) and Hoechst intensity (total DNA) (x axis) with G1, S and G2 populations labelled on the GFP control dot plot. **(F)** Quantitation of flow cytometry dot plot data, stacked bar chart shows percentage of cells in G1, S and G2/M as indicated.

Transfection of 3T3 cells with UBE2O-FLAG resulted in a small, non-significant increase in CIZ1 levels compared to GFP control (Figure 3.13. A, B). The large standard deviation could be a result of variation between the experimental repeats such as differences in transfection efficiency. EdU labelling by fluorescence microscopy showed minimal change in percentage S phase cells for UBE2O-FLAG transfected cells compared to GFP control (Figure 3.13. C, D). Flow cytometry analysis shows a low number of events on the dot plot (Figure 3.13. E), this was likely due to the low number of cells post-transfection. Flow cytometry analysis showed a reduction in EdU signal intensity by approximately 35% for UBE2O-FLAG transfected cells

compared to GFP control (Figure 3.13. F). The reduction in EdU intensity suggests less efficient DNA replication. The findings demonstrate a small increase in CIZ1 protein levels after transfection with UBE2O-FLAG, however, the overexpression of UBE2O-FLAG needs to be validated in future experiments to support this conclusion.

3.2.5. Characterising the potential role of UBR5 in regulating CIZ1 protein levels at G1/S

So far, the data suggests that CIZ1 protein levels may be regulated by CDK/ DDK activity at different phases throughout the whole cell cycle. The data for E3 transfection experiments in asynchronous 3T3 cells demonstrate that transfecting cells with UBR5-GFP or FBXO38-FLAG plasmids results in a non-significant decrease in CIZ1 protein levels. E3 transfection experiments were carried out in synchronised 3T3 cells to determine the effect on CIZ1 levels specifically at late G1/S. 3T3 cells were synchronised by release from G0. At the point of release from G0 the cells were transfected with UBR5-GFP or GFP control and protein samples harvested 24 hours post-transfection. The effect on CIZ1 protein levels was determined by western blot analysis. To determine the effect on DNA synthesis, CLICK-IT EdU fluorescent labelling was used to measure EdU incorporation into nascent DNA by fluorescence microscopy 16-24 hours post-release (Figure 3.14).

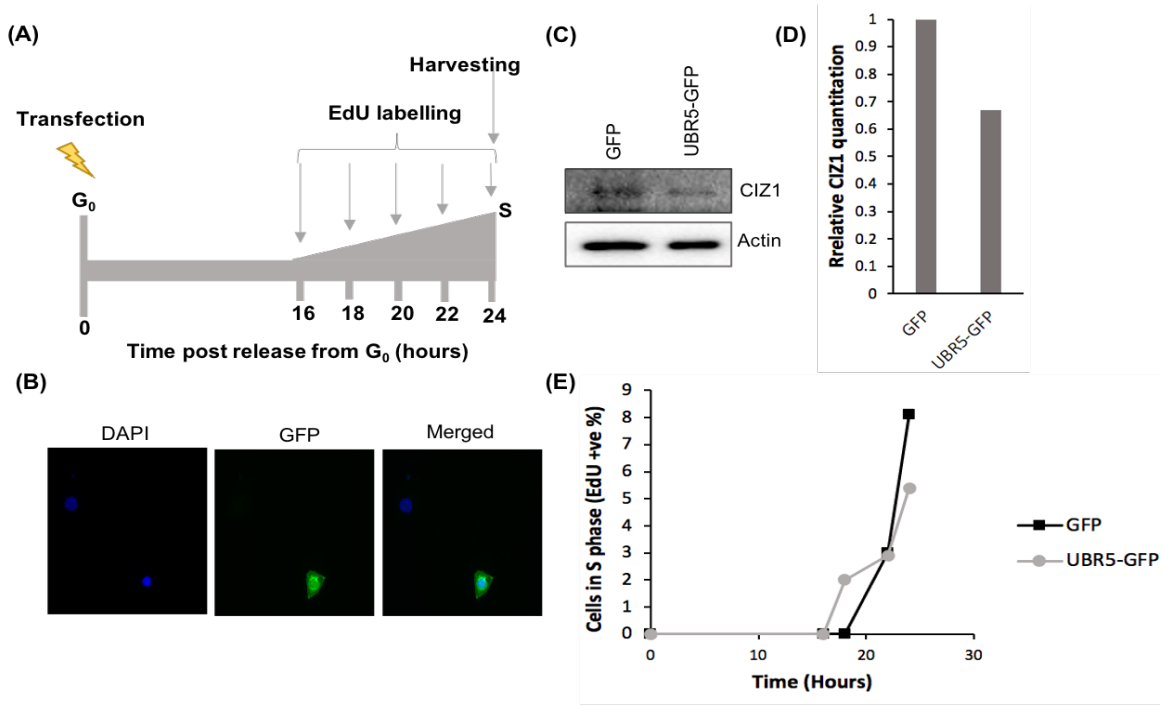

Figure 3.14. CIZ1 protein levels are reduced in synchronised 3T3 cells after transfection with UBR5-GFP. 3T3 cells were synchronised by release from G0, transfected at the point of release with UBR5-GFP or GFP control and harvested 24 hours post release. **(A)** Experimental overview. Timeline shows entry into S phase after G0 release represented by the triangle, timings of transfection, EdU labelling and protein harvesting. **(B)** Representative fluorescence microscope images show DNA stain (DAPI), GFP and merged images for GFP-transfected control. **(C)** Western blot of transfected cells probed with CIZ1 and Actin antibodies. **(D)** Quantitation of CIZ1 protein levels relative to actin load control, n=1. **(E)** Percentage S phase cells (EdU positive) in relation to all DAPI stained cells 16-24 hours post release, n=1.

Fluorescence microscopy of GFP-transfected control (Figure 3.14.B) was used to calculate transfection efficiency which was 71.4%. Transfection efficiency for UBR5-GFP could not be calculated due to the signal from the EdU labelling used to determine percentage S phase cells overlapping with the GFP signal. As both the EdU and GFP signal for UBR5-GFP transfected cells is nuclear, the overlap of signal made it difficult to determine transfection efficiency. Detection of UBR5-GFP was not possible by western blot, possibly due to unsuccessful transfection or due to the low cell number 24 hours post transfection meaning low levels of protein in the protein samples harvested. Western blot analysis revealed a reduction in CIZ1 protein levels by 33% for UBR5-GFP transfected cells compared to GFP control (Figure 3.14. C, D). The data is presented as n=1 due to obtaining a very low cell number 24 hours post transfection on other repeats resulting in no detectable signal on western blot analysis. The percentage cells in S phase for GFP-transfected and UBR5-transfected cells is similar 16-24 hours post transfection (Figure 3.14. E). At 24 hours post

transfection, approximately 8% of cells were in S phase for the GFP transfected control, this is lower than the 35-40% of cells in S phase 24 hours post release seen in figure 3.2. This suggests that the transfection process has affected cell cycle re-entry and therefore the effect of transfecting cells with UBR5-GFP on the cell cycle can't be determined. Further optimisation of synchronised cell transfections is required, including validation of UBR5-GFP overexpression, in order to gain further repeats to determine if UBR5 has an effect on CIZ1 protein levels at G1/S of the cell cycle.

3.2.6. Characterising the potential role of FBXO38 in regulating CIZ1 protein levels at G1/S

To determine if FBXO38 effects CIZ1 levels in G1 phase, 3T3 cells were synchronised by release from G0. At the point of release from G0 the cells were transfected with FBXO38-FLAG or GFP control and protein samples harvested 24 hours post transfection. The effect on CIZ1 protein levels was determined by western blot analysis. To determine the effect on DNA synthesis, CLICK-IT EdU fluorescent labelling was used to measure EdU incorporation into nascent DNA by fluorescence microscopy 16-24 hours post release (Figure 3.15).

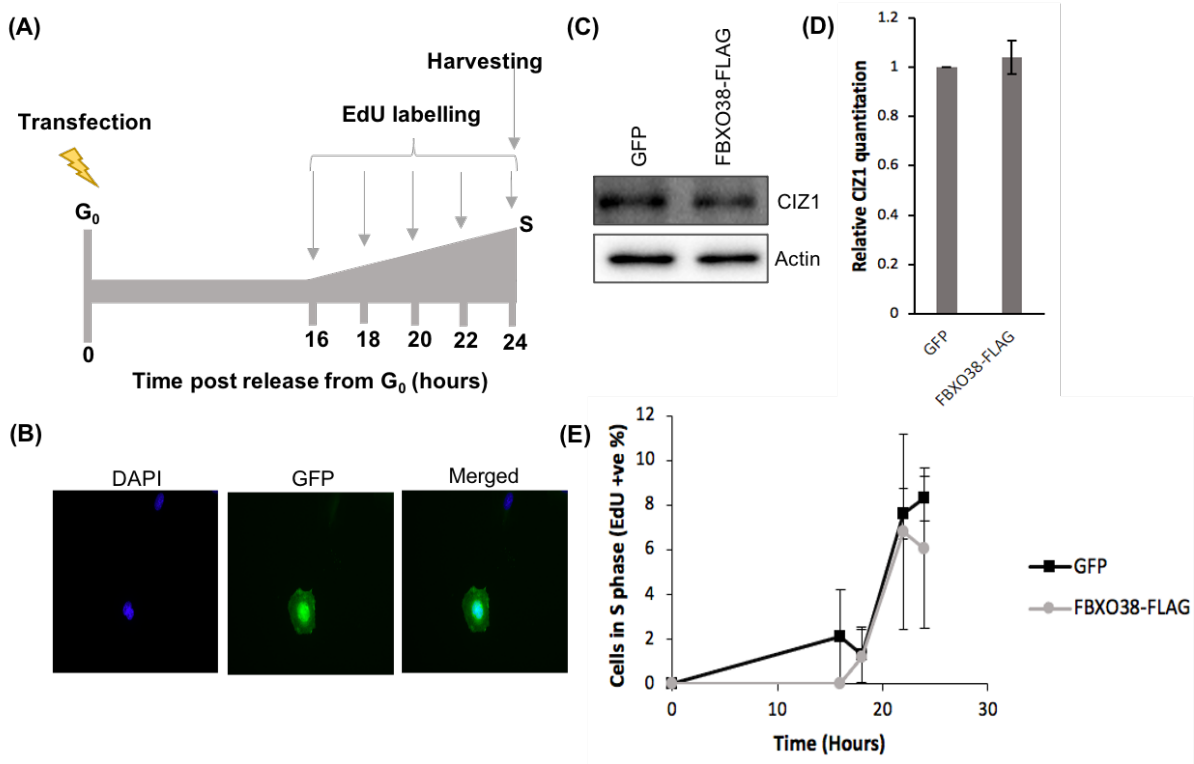

Figure 3.15. CIZ1 protein levels are not reduced in synchronised 3T3 cells after transfection with FBXO38-FLAG.. 3T3 cells were synchronised by release from G0, transfected at the point of release with FBXO38-FLAG or GFP control and harvested 24 hours post release. **(A)** Experimental overview. Timeline shows entry into S phase after G0 release represented by the triangle, timings of transfection, EdU labelling and protein harvesting. **(B)** Representative fluorescence microscope images show DNA stain (DAPI), GFP and merged images for GFP-transfected control. **(C)** Western blot of transfected cells probed with CIZ1 and Actin antibodies. **(D)** Quantitation of CIZ1 protein levels relative to actin load control, n=3. Significance measured using Mann Whitney test, p = 0.7. **(E)** Percentage S phase cells (EdU positive) in relation to all DAPI stained cells 16-24 hours post release, n=3.

Fluorescence microscopy of GFP-transfected control (Figure 3.15. B) was used to calculate transfection efficiency which was 69±6.4%, n=3. The overexpression of FBXO38-FLAG was not able to be detected by western blot using FLAG or FBXO38 antibodies, possibly due to unsuccessful transfection or due to the antibodies not being able to detect the protein at low levels as a result of low cell numbers 24 hours post-transfection. Western blot analysis revealed no significant change in CIZ1 protein levels in the FBXO38-FLAG transfected cells compared to GFP control (Figure 3.15. C, D). The percentage S phase cells for the GFP control was low 24 hours post-transfection (Figure 3.15. E) which is consistent with that seen in the synchronised UBR5 transfection experiments further suggesting that the transfection process has affected cell cycle re-entry. The data shows that transfecting cells with FBXO38-FLAG at

G1/ S has no effect on CIZ1 protein levels, however further optimisation of the synchronised transfection protocol is required in order to validate that FBXO38-FLAG is being overexpressed and to determine if FBXO38 overexpression has an effect on the cell cycle.

3.3. The ability of CDK/DDK inhibitors to induce apoptosis

So far, the data shows that inhibition of CDK4/6, DDK, CDK2 and CDK1 results in a non-significant reduction in CIZ1 levels. The overexpression of CIZ1 can contribute to several hallmarks of cancer including resisting cell death, anti-CIZ1 siRNA used to deplete CIZ1 levels has been shown to increase apoptosis in colorectal cancer cells (Yin *et al.,* 2013). The aim of this section is to evaluate the ability of CDK and DDK inhibitors to induce apoptosis in 3T3 cells and retinoblastoma positive cancer cell lines including prostate cancer (PC3) cells and primary and metastatic human colorectal carcinoma (SW480 and SW620, respectively) cell lines. The presence of Rb means the cells have a functional restriction point. In G1, CDK4/6 phosphorylates Rb leading to the release of E2F transcription factor and transcription of cyclin E and A leading to Rb hyperphosphorylation and passage through restriction point (Narasimha *et al.,* 2014). Under conditions where Rb is not phosphorylated, cells will not progress through G1/S which can lead to G1 arrest. Cell cycle arrest can be reversible, or apoptosis can be induced (Rubin, 2013). Inhibitors of CDK4/6 (PD), DDK (PHA and XL-413) and CDK2 (CVT-313 and Roscovitine) will be used in apoptosis assay studies to evaluate the ability to induce apoptosis in cancer cells. XL-413 is a Cdc7 inhibitor (Sasi *et al.,* 2014) and Roscovitine inhibits CDK2 in addition to CDK1, CDK5, CDK7 and CDK9 (Taylor *et al.,* 2004). These inhibitors were chosen due to preliminary work showing a reduction in CIZ1 levels and cellular proliferation in PC3, SW480 and SW620 cell lines (Pauzaite, 2019).

3.3.1. 3T3 cells

So far, the data on CDK inhibition shows that CIZ1 protein levels are reduced by CDK4/6, DDK, CDK2 and CDK1 inhibition in asynchronous 3T3 cells. Preliminary work has shown that inhibition of CDK4/6 (PD), DDK (PHA) and CDK2 (CVT-313) reduces S phase entry in 3T3 cells (Pauzaite, 2019). To determine if DDK/CDK inhibitors induce apoptosis in 3T3 cells, asynchronous 3T3 cells were treated with Dimethyl Sulfoxide (DMSO) solvent control, CDK4/6 inhibitor (PD-0332991 (PD), DDK inhibitor (PHA-767491 (PHA), CDK2 inhibitors (CVT-313 and

CDK2-IN-73) and CDK1 inhibitor (Ro-3306) at a concentration of 10 μM for 24 hours. Cells were labelled with YO-PRO-1 which can selectively pass the plasma membrane of apoptotic cells. Cells were also stained with propidium iodide (PI), a dead cell stain, which is a membrane impermeant dye. Samples were analysed by flow cytometry (Figure 3.16).

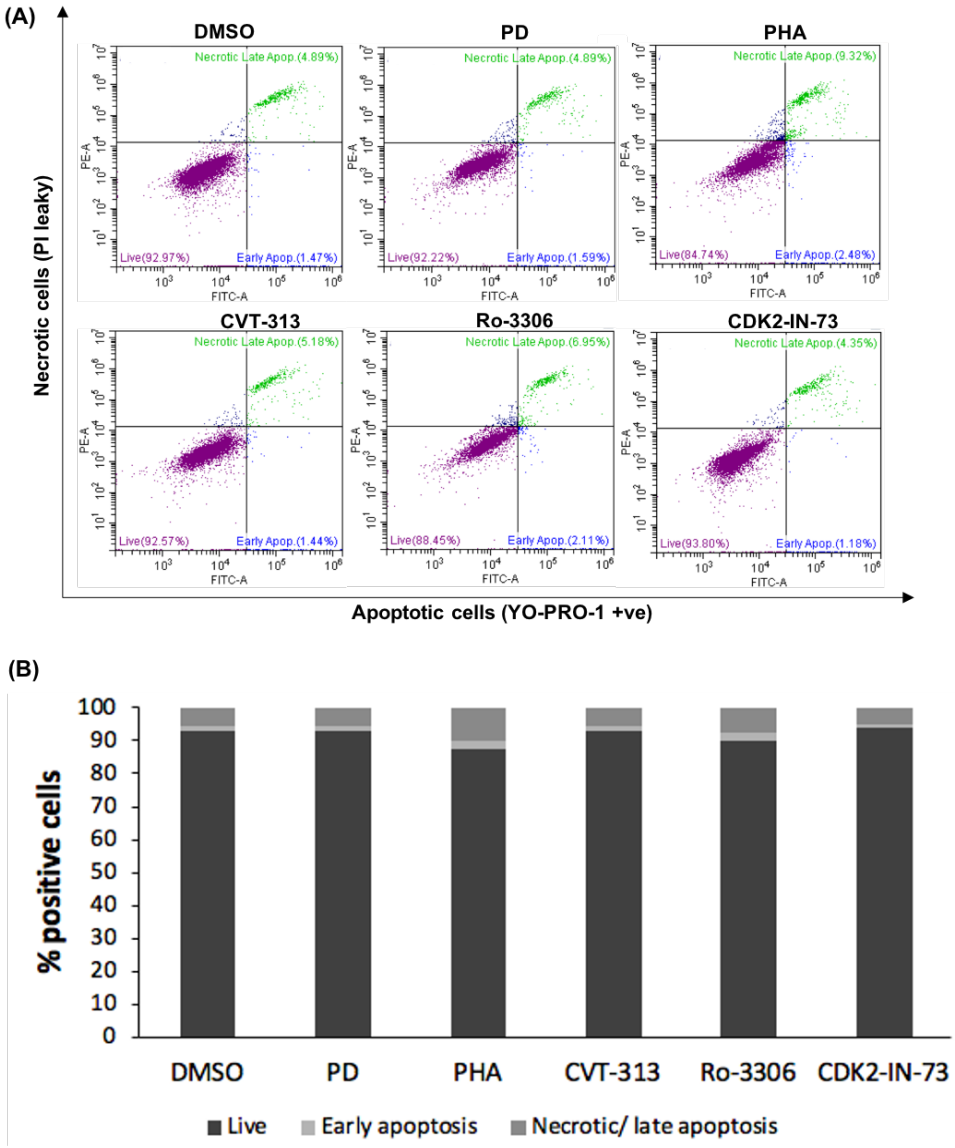

Figure 3.16. Quantitation of apoptotic cells after CDK and DDK inhibition in asynchronous 3T3 cells. Asynchronous 3T3 cells were treated with DMSO, PD, PHA, CVT, Ro-3306 and CDK2-IN-73 at a concertation of 10 μM for 24 hours, harvested and labelled with YO-PRO-1 and propidium iodide (PI). **(A)** Multiparameter flow cytometry dot plots, PI intensity (y axis) and YO-PRO-1intensity (x axis). Quadrant tool used to divide cell populations into live, early apoptotic and late apoptotic/ dead. Cells with low YO-PRO-1 and PI classified as live (purple), cells with high YO-PRO-1 and low PI classified as early apoptotic (blue) and cells with high YO-PRO-1 and PI classified as late apoptotic/ dead (green). **(B)** Quantitation of live, early apoptotic and late apoptotic/ dead cells.

Flow cytometry analysis revealed that treatment with PD, PHA, CVT, Ro-3306 and CDK2-IN-73 caused little change in early apoptotic and late apoptotic/ dead cells compared to the DMSO control. This suggests that the CDK and DDK inhibition for 24 hours may be causing cell cycle arrest as opposed to apoptosis. The results for PHA treatment show a small increase in late apoptotic/ dead cells compared to DMSO control by 4.43%, demonstrating a small proportion of cells being apoptotic with the majority remaining live. This suggests that the dual inhibition of Cdc7 and CDK9 increases apoptosis in 3T3 cells after 24-hours treatment.

3.3.2. Cancer cell lines

The ability of CDK and DDK inhibitors to induce apoptosis in Rb-positive cancer cells lines was assessed. Preliminary work found inhibition of DDK (PHA) and CDK2 (CVT-313 and Roscovitine) to significantly reduce CIZ1 protein levels in PC3 and SW480 cell lines and significantly reduce the number of cells in S phase in PC3, SW480 and SW620 cell lines (Pauzaite, 2019). To determine if small molecule kinase inhibition can induce apoptosis, PC3, SW480 and SW620 cells were treated with Dimethyl Sulfoxide (DMSO) solvent control, CDK4/6 inhibitor (PD), DDK inhibitors (PHA and XL-413) and CDK2 inhibitors (CVT-313 and Roscovitine) at a concentration of 10 μM (PD, PHA, CVT-313, XL-413) or 30μM (Roscovitine) for 24 hours and apoptosis followed using the Vybrant™ Apoptosis Assay Kit YO-PRO-1/ Propidium Iodide. Samples were analysed by flow cytometry (Figure 3.17).

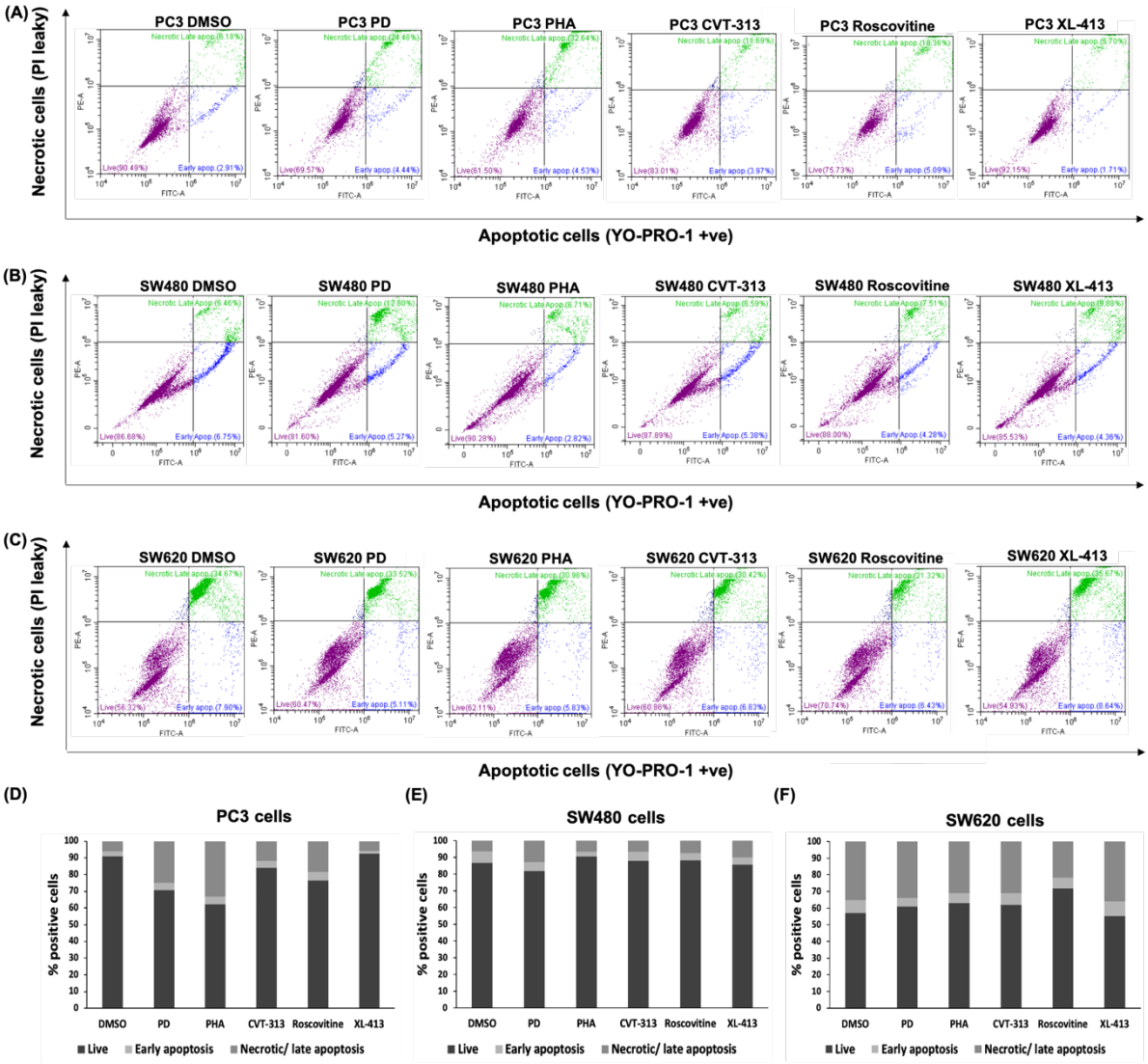

Figure 3.17. Quantitation of apoptotic cells after CDK and DDK inhibition in PC3, SW480 and SW620 cells. PC3, SW480 and SW620 cells were treated with DMSO, 10 μM PD, 10 μM PHA, 10 μM CVT-313, 30 μM Roscovitine and 10 μM XL-413 for 24 hours, harvested and labelled with YO-PRO-1 and propidium iodide (PI). **(A, B and C)** Multiparameter flow cytometry dot plots, PI intensity (y axis) and YO-PRO-1intensity (x axis). Quadrant tool used to divide cell populations into live, early apoptotic and late apoptotic/ dead. Cells with low YO-PRO-1 and PI classified as live (purple), cells with high YO-PRO-1 and low PI classified as early apoptotic (blue) and cells with high YO-PRO-1 and PI classified as late apoptotic/ dead (green). **(D, E and F)** Quantitation of live, early apoptotic and late apoptotic/ dead cells.

Treatment of PC3 cells with CDK and DDK inhibitors increased the number of late apoptotic/ dead cells, PHA caused the largest increase in late apoptotic/ dead cells by 26.8% followed by PD, Roscovitine and CVT-313 which caused an increase by 18.6%, 12.3% and 5.6%, respectively. The results suggest that the inhibition of CDK4/6, DDK and CDK2 are able to induce apoptosis in PC3 cells, however DDK inhibition with XL-413 does not induce apoptosis after treatment for 24 hours. These findings demonstrate a differential effect of the two DDK

inhibitors PHA and XL-413 that may reflect the off-target effects of each kinase, as they have very similar IC50 values for DDK in vitro (Koltun *et al.,* 2012; Montagnoli *et al.,* 2008). PD treatment increased the number of SW480 cells that were in late apoptosis/ dead by 6.3% suggesting inhibition of CDK4/6 may lead to an increase in apoptosis. All other kinase inhibitors did not increase apoptosis in SW480 and SW620 cells, however the high number of dead cells in the DMSO control for SW620 cells is not typically seen in this cell line (Ji *et al.,* 2011), and means it is difficult to accurately determine the effect of the inhibitors. The apoptosis assay should be repeated for SW620 cells to accurately evaluate the ability of CDK/DDK inhibition to induce apoptosis. Together, the results demonstrate that CDK4/6, DDK and CDK2 inhibitors increase apoptosis in PC3 cells with limited effect in SW480 and SW620 cells suggesting cell line dependence of CDK/DDK inhibitors to induce apoptosis in cancer cells.

Chapter 4: Discussion

4.1. CIZ1 levels are reduced by CDK/DDK inhibition

CIZ1 has a role in facilitating the initiation of DNA replication (Copeland *et al.,* 2010; Copeland *et al.,* 2015; Coverley *et al.,* 2005), this process must be highly regulated to ensure faithful replication of the genome. The overexpression of CIZ1 can promote tumourigenesis in a range of common cancers including breast, prostate, colorectal, gall bladder and hepatocellular carcinoma by contributing to the proliferation of cancer cells. The reduction of CIZ1 using siRNA and shRNA has been shown to reduce proliferation of cancer cells and reduce tumour size, these findings demonstrate that CIZ1 is a viable therapeutic target in cancer. (Den Hollander and Kumar, 2006; Den Hollander *et al.,* 2006, Lei *et al.,* 2016; Liu *et al.,* 2015; Wang *et al.,* 2014; Wu *et al.,* 2015; Yin *et al.,* 2013; Zhang *et al.,* 2014). There is evidence that CIZ1 may have a tumour suppressor function at normal levels. *CIZ1* (-/-) mouse embryonic fibroblasts show increased sensitivity to irradiation and increased susceptibility to viral oncogenesis (Nishibe *et al.,* 2013). CIZ1-null female mice display lymphoproliferative disorders based on the role of CIZ1 in X chromosome inactivation (Ridings-Figueroa *et al.,* 2017; Stewart *et al.,* 2019), this highlights the importance of regulation of CIZ1 proteostasis. The oncogenic role of CIZ1 overexpression emphasises the need to understand the molecular mechanisms that regulate CIZ1.

The molecular mechanisms that regulate CIZ1 have not been fully determined. The role of phosphorylation in regulating CIZ1 activity in the initiation of DNA replication provided the basis for investigating the role of kinase mediated phosphorylation in the regulation of CIZ1 proteostasis (Copeland *et al.,* 2010; Copeland *et al.,* 2015). Preliminary work has established a working model for CIZ1 regulation (Figure 1.9). The working model suggests that CIZ1 levels are regulated by opposing CDK/DDK phosphorylation and UPS mediated degradation. This model is based on the hypothesis that the CDK/DDK mediated phosphorylation of CIZ1 is required for stability and accumulation and protects from UPS mediated degradation. The model proposes that CIZ1 overexpression could result from an aberrant increase in kinase activity or loss of function/ down-regulation of the UPS. Furthermore, the model suggests that disturbing the equilibrium between phosphorylation and UPS mediated degradation could be used to reduce CIZ1 levels. Specifically, the use of CDK inhibitors, this would prevent the CDK-mediated phosphorylation of CIZ1 and facilitate UPS mediated degradation. The

modulation of CIZ1 levels could be of clinical benefit in tumours that are reliant on CIZ1 for growth.

The effect of CDK/DDK inhibition on CIZ1 protein levels was assessed through small molecule kinase inhibition studies. Asynchronous and synchronous 3T3 cells were treated with CDK/ DDK inhibitors at a concentration of 10 μM. As this is a high concentration of inhibitor, it is important to consider the potential off-target effects of the inhibitors when using them at this concentration, such as off-target effects on other CDKs as well as other kinases within the cell. Nevertheless, the inhibition of CDK4/6 (PD), DDK (PHA) and CDK2 (CVT-313) resulted in a non-significant reduction in CIZ1 protein levels in asynchronous and synchronised cells at the G1/S transition. Importantly, PHA has off-target effects and inhibits CDK2 with an IC50 of 240nM (Montagnoli *et al.,* 2008), this could contribute to the reduction in CIZ1 levels observed after treatment with PHA. This is consistent with previous work which found PHA to have inhibitory effects on CDK2 shown by a reduction of the phosphorylation of CIZ1 on the CDK2 phosphorylation site T293 (Pauzaite, 2019). Inhibition of CDK1 (Ro-3306) resulted in a non-significant reduction in CIZ1 levels in asynchronous cells but not in synchronised cells, this is consistent with CDK1 being inactive during G1/S (Moiseeva *et al.,* 2019; Potapova *et al.,* 2009). The preliminary findings using the CDK1 inhibitor suggest CIZ1 is regulated by CDK1-mediated phosphorylation, however, it has not yet been determined if CDK1 directly phosphorylates CIZ1. Together the findings suggest that CIZ1 may be regulated by CDK4/6, DDK and CDK2 during G1/S and CDK1 later in the cell cycle.

Treatment of 3T3 cells with the CDK2 inhibitor CDK2-IN-73 resulted in no change to CIZ1 protein levels or S phase entry, suggesting limited inhibition of CDK2. Importantly, the IC50 of CDK2-IN-73 (44 nM) was determined in cell-free assays. In cellular assays, CDK2-IN-73 at a concentration of 30 μM had no effect on the growth of retinoblastoma proficient tumour cell lines (Coxon *et al.,* 2017) suggesting that the potent inhibition of CDK2 seen in cell-free assays is unable to be translated to cellular assays. Furthermore, it is important to consider that different cell lines have different responsiveness to a given drug and this could explain why CDK2-IN-73 has shown no effect in 3T3 cells. Reasons why different cell lines can respond differently to a given drug include differences in drug transporters, alterations in the targeted pathway (upstream or downstream of target), alteration by mutation of the drug target and

efflux of the drug (Gottesman, 2002). To further determine if CDK2-IN-73 has any inhibitory effect on CDK2 in 3T3 cells, the phosphorylation of known CDK2 targets could be quantified after treatment with CDK2-IN-73. Although CDK2-IN-73 displayed no effect on CIZ1 protein levels in this study, the CDK2 inhibitor CVT-313 reduced CIZ1 levels, this supports previous work demonstrating that CDK2 contributes to CIZ1 regulation (Pauzaite, 2019). Together, the small molecule kinase inhibition studies support the working model for CIZ1 regulation as inhibition of DDK/ CDK2 resulted in a reduction in CIZ1 levels. However, the reduction in CIZ1 levels observed in the small molecule kinase inhibition studies was non-significant, therefore further repeats are required to support the findings from this study.

4.2. The reduction in CIZ1 levels after DDK/CDK2 inhibition can be recovered by inhibiting the proteasome

The potential role of the UPS in CIZ1 degradation following CDK/ DDK inhibition was assessed in asynchronous and synchronised cells. The inhibition of CDK4/6, DDK and CDK2 resulted in a more efficient reduction of CIZ1 levels in cells at the G1/S transition compared to asynchronous cells. In addition, proteasomal inhibition resulted in a more efficient reversal of CIZ1 degradation in cells at the G1/S transition. This is consistent with the phase of the cell cycle where the activity of the kinases is maximal. Furthermore, the treatment of asynchronous cells with kinase inhibitors for 6 hours may not be sufficient time for the degradation of CIZ1.

In synchronised cells, inhibition of DDK and CDK2 resulted in a non-significant reduction in CIZ1 levels, this effect was reversed by proteasomal inhibition. Inhibition of CDK4/6 with PD resulted in a non-significant reduction in CIZ1 levels, however this effect was not reversed by proteasomal inhibition. This suggests that there are potentially two distinct mechanisms, either proteasome independent or dependent, that mediate the reduction in CIZ1 protein levels observed after CDK4/6 inhibition and DDK/CDK2 inhibition, respectively. CDK4/6 inhibition may be affecting cells that have not passed restriction point. In quiescent release experiments cells re-enter the cell cycle in a pre-restriction point state with hypophosphorylated Rb (Moser *et al.,* 2018; Spencer *et al.,* 2013), 40-50% of cells release into the cell cycle, the remainder stay in G0/G1. It may be that inhibition of CDK4/6 promotes stalling of some cells in a pre-restriction point state not seen in control cells. Therefore,

inhibition of CDK4/6 may reduce the number of cells that enter S-phase and prevent CIZ1 accumulation. Therefore, proteasome inhibition would have no effect on CIZ1 protein levels that are reduced by inhibition of CDK4/6. The second potential mechanism for CIZ1 reduction includes UPS-mediated degradation as proteasomal inhibition successfully recovered CIZ1 levels reduced by DDK/CDK2 inhibition. Importantly, PD would not affect the activity of DDK and CDK2, suggesting that it is the DDK/CDK2 mediated phosphorylation of CIZ1 that provides the protection from UPS mediated degradation. Although more repeats are required to support the findings, the data suggests that DDK and CDK2 inhibition facilitates the proteasomal-mediated degradation of CIZ1 and supports the working model for CIZ1 regulation (Figure 1.9).

The working model for CIZ1 regulation (Figure 1.9) suggest that dysregulation of DDK or CDK kinase or UPS activity could lead to the loss of tight control of CIZ1 levels, an aberrant increase in kinases activity or loss of function/ down regulation of the UPS can result in CIZ1 overexpression and promote tumourigenesis. The ability of CDK inhibitors to potentially facilitate the UPS mediated degradation of CIZ1 provides an avenue for reducing CIZ1 levels in CIZ1-dependent cancers. The working model suggests that CDK inhibitors could be repurposed to shift the equilibrium of CIZ1 regulation towards UPS mediated degradation. The degradation of CIZ1 after kinase inhibition would be dependent on a functional UPS, this highlights the importance of identifying the E3 ligases that potentially target CIZ1 for degradation.

4.3. Characterisation of the putative E3 ligases that potentially regulate CIZ1 protein levels

The ubiquitin proteasome system is a protein degradation system, K48-linked poly-ubiquitylation of protein substrates mediates proteasomal degradation (Morimoto and Shirakawa, 2016). The activities of E1 ubiquitin-activating enzymes, E2 ubiquitin-conjugating enzymes and E3 ubiquitin ligases are required in the processes of attaching ubiquitin to the target substrate (Stewart *et al.,* 2016; Streich and Lima, 2014). The role of the E3 ligase is to provide high substrate specificity (Galdeano, 2017; Weber *et al.,* 2019). Previous work identified three putative E3 ligases that may regulate CIZ1 including UBR5, FBXO38 and UBE2O (Pauzaite, 2019). Here, to characterise the E3 ligases that may target CIZ1 for

degradation, 3T3 cells were transfected with UBR5-GFP, FBXO38-FLAG or UBE2O-FLAG plasmid and the effect on CIZ1 levels was determined.

A major limitation with the transfection experiments was validating the expression of the E3s. For UBR5-GFP, UBR5 expression was unable to be detected by western blot using anti-GFP and anti-UBR5 antibodies. For FBXO38-FLAG and UBE2O-FLAG, the expression of these E3s was unable to be detected by immunofluorescence using anti-FLAG antibodies, however, the western blot data suggested a very low level of expression of the E3s based on a faint band on the blot. It is important to consider the different possibilities for these findings. For example, when using antibodies, detection problems can arise due to problems with antibody sensitivity and specificity as well as not using optimal antibody concentrations. It is important to validate the antibodies in future work, for example by using positive and negative controls to ensure the antibody can detect the target protein. Furthermore, it is also important to consider that the difficulty in validating E3 expression may simply be due to limited success of transfections as 3T3 cells are a cell line that is difficult to transfect (Cao *et al.,* 2019). In addition, other factors that may have influenced transfection efficiency include cell viability, cell density, passage number, and quality of the plasmid DNA (Fus-Kujawa *et al.,* 2021; Kucharski *et al.,* 2021). For synchronised transfection experiments, validation of E3 expression was unsuccessful, in addition, the ability of cells to re-enter the cell cycle after release from G0 was limited. This is likely due to contact inhibition, serum starvation, and transfection all being stress-inducing thereby limiting the ability of cells to successfully re-enter the cell cycle. This demonstrates the need for optimisation of the transfection protocol.

Although there was difficulty validating the expression of the E3s, the findings from this study show that transfecting cells with UBR5-GFP or FBXO38-FLAG plasmid resulted in a non-significant reduction in CIZ1 protein levels and the number of cells in S phase, furthermore UBR5 appeared to have an effect at G1/S whilst FBXO38 did not. In contrast, transfecting cells with UBE2O-FLAG did not affect CIZ1 levels but resulted in a non-significant reduction in the number of cells in S phase. It is also important to consider that the E3s target other proteins involved in the cell cycle (Cipolla *et al.,* 2019; Munoz *et al.,* 2007; Shearer *et al.,* 2015; Ullah *et al.,* 2018) which could have an effect on cell cycle profile. These findings are preliminary and future studies would need to both validate E3 expression and investigate the effect on

CIZ1 levels in asynchronous and synchronous cells before valid conclusions can be made regarding the potential role of each of the E3s in the regulation of CIZ1 protein levels.

4.4. Cytotoxic effects of CDK/DDK inhibitors

CDK and DDK inhibitors have been shown to reduce CIZ1 protein levels in this study. The depletion of CIZ1 has previously been observed to induce apoptosis in cancer cells (Yin *et al.,* 2013). The ability of CDK and DDK inhibitors to induce apoptosis was assessed in 3T3 cells and retinoblastoma positive cancer cell lines. Rb proficient cells have a functional restriction point, therefore under conditions of Rb hypophosphorylation the cells can arrest in G1 (Rubin, 2013; Yen and Sturgill, 1998).

The apoptosis assays revealed that CDK and DDK inhibitors had limited effect on inducing apoptosis in 3T3 cells. Previous work in 3T3 cells has shown kinase inhibition to reduce S phase entry (Pauzaite, 2019), together this suggests that the inhibitors cause cell cycle arrest in G1. DDK inhibition (PHA) resulted in a small increase in late apoptotic/ dead cells, the more potent effect of PHA compared to the other inhibitors is consistent with previous work which found PHA treatment to be the most efficient at reducing S phase entry in 3T3 cells (Pauzaite, 2019). The findings could be attributed to the inhibitory effects of PHA on CDK2 with an IC50 of 240nM (Montagnoli *et al.,* 2008). The ability of PHA to induce apoptosis may be a result of inhibition of CDK9. CDK9 phosphorylates RNA Polymerase II, therefore inhibition of CDK9 can affect transcription resulting in a depletion of proteins (Parua *et al.,* 2020; Natoni *et al.,* 2013). Overall, kinase inhibition has limited effect on increasing apoptosis in 3T3 cells and instead may induce cell cycle arrest.

The CDK and DDK inhibitors displayed differential effects on increasing apoptosis in PC3, SW480 and SW620 cancer cell lines. In prostate cancer cells (PC3), treatment with CDK4/6 (PD), DDK (PHA) and CDK2 inhibitors (CVT-313 and roscovitine) increased the number of late apoptotic/ dead cells compared to the control demonstrating a cytotoxic effect. The DDK inhibitor XL-413 had no effect on increasing apoptosis. PHA and XL-413 inhibit DDK with an IC50 of 10nM and 3.4nM, respectively (Koltun *et al.,* 2012; Montagnoli *et al.,* 2008). The ability of PHA to increase apoptosis could reflect the off-target effects on CDK2 in addition to the ability of PHA to inhibit CDK9 (Montagnoli *et al.,* 2008). The two CDK inhibitors roscovitine

and CVT-313 increased apoptosis, however roscovitine had a more potent effect, this is consistent with published work suggesting that the inhibition of CDK9 by roscovitine is important for the increase in apoptosis in PC3 cells (Mohapatra *et al.,* 2009). These findings demonstrate that kinase inhibition is effective at increasing apoptosis in PC3 cells. PC3 cells are androgen independent, prostate cancers are typically androgen-dependent to begin with and androgen deprivation therapy can increase the rate of apoptosis in androgen-responsive prostate cancer cells. Patients can develop androgen-independent prostate cancer in which androgen deprivation is unable to increase the rate of apoptosis (Saraon *et al.,* 2014). Published work supporting the findings from this study demonstrate the ability of CDK inhibitors to induce apoptosis in PC3 cells due to the effect of CDK inhibitors on caspase activation (Arisan *et al.,* 2014). Together, the findings demonstrate possible clinical applications of kinase inhibitors in prostate cancer.

Treatment of primary and metastatic colorectal cancer cells (SW480 and SW620, respectively) with kinase inhibitors had minimal effect on increasing the rate of apoptosis. The CDK4/6 inhibitor caused a small increase in apoptosis in SW480 cells, this finding is consistent with published work demonstrating CDK4 inhibition can lead to an increase in the number of SW480 cells in sub-G1 (Tetsu and McCormick, 2003). Previous work has shown DDK and CDK2 inhibition to reduce S phase entry in SW480 and SW620 cells (Pauzaite, 2019) suggesting possible G1 arrest in response to kinase inhibitors. DDK and CDK2 inhibitors reduce CIZ1 protein levels in SW480 cells, however growth and proliferation appear to be independent of CIZ1, this is in contrast to PC3 cells which are dependent on CIZ1 for cellular proliferation and viability (Pauzaite, 2019). Differences between the cell lines has also been observed in this study which found DDK and CDK inhibitors to increase apoptosis in PC3 cells with limited effect in SW480 cells. Together, the findings demonstrate that kinase inhibition could be used to reduce CIZ1 protein levels in PC3 cells with possible clinical applications.

4.5. Implications of the work

The work has evaluated the efficacy of CDK/DDK inhibitors to reduce CIZ1 levels and the role of the UPS in the degradation of CIZ1. The findings from this study support the working model in which CDK/ DDK inhibitors can reduce CIZ1 levels. Future studies need to validate these

findings and demonstrate that the effect can be translated to cancer cells. Furthermore, the data from apoptosis assays suggests possible clinical applications of CDK inhibitors, in particular the ability of CDK inhibitors to increase apoptosis in prostate cancer cells. Further repeats of CDK inhibition studies are required in asynchronous and synchronous cells to validate which DDK/ CDKS can be inhibited to effectively reduce CIZ1 levels. The advancements in the selectivity of CDK inhibitors has increased the efficacy of their use in cancer treatment (Asghar *et al.,* 2015). Palbociclib is an FDA approved CDK4/6 inhibitor and used as first-line treatment for advanced post-menopausal $ER^+/HER2^-$ breast cancer (Beaver *et al.,* 2015). Abemaciclib (Verzonio) and ribociclib (Kisqali) are also FDA approved CDK4/6 inhibitors and used in the treatment of $HR^+/HER2^-$ advanced or metastatic breast cancer (Eggersmann *et al.,* 2019). The current use of CDK inhibitors in cancer treatment demonstrates that CDKs are a viable drug target.

The findings from this study suggest that CIZ1 levels can be reduced by inhibition of DDK/ CDK2 and this is dependent on a functional UPS. If future work could support these findings, the E3s that target CIZ1 could be used as biomarkers for patient stratification when determining which patients would benefit from CDK inhibitors as a strategy to reduce CIZ1 levels. This highlights the importance of optimisation of asynchronous and synchronous transfection experiments in future work, in addition to the use of alternative experimental strategies to characterise the E3s that potentially target CIZ1. Together with CDK/ DDK inhibition studies, this would help to determine which CDK/DDKs and E3s regulate CIZ1 and thereby help to understand how CDK/ DDKS can be effectively targeted in cancer.

4.6. Future directions

To progress this area of research further, future experiments should address the limitations of this study and aim to further increase understanding of how CIZ1 protein levels are regulated. In this study, 3T3 cells were used as the model cell line as this is the model system used to identify the putative regulators of CIZ1 (Pauzaite, 2019). However, it is important to keep in mind that 3T3 cells are fibroblastic. Solid tumours, including those mentioned throughout this project, are generally of epithelial origin, therefore it may be beneficial for future studies to use epithelial cells as the model cells, for example, Human Embryonic Kidney (HEK) cells.

For the CDK inhibition experiments, a limitation was that inhibition of the DDK/CDKs was not validated. It would be beneficial for future experiments to have additional controls in order to validate inhibition of the CDKs following DDK/ CDK inhibitor treatment. This could be achieved by looking at the phosphorylation status of known targets of the DDK/ CDKs following the addition of the inhibitors. Furthermore, future studies should determine whether the DDK/ CDKs can be inhibited using a lower concentration of inhibitor than 10 μM in order to reduce off-target effects associated with using a high concentration.

Some experiments in this study used synchronised cells in order to specifically look at CIZ1 levels at G1/S. The synchronisation of cells was checked by following the number of cells entering S-phase after release from quiescence. This was achieved by monitoring EdU incorporation into nascent DNA 16-24 hours after G0 release. This technique does not directly measure if cells entered G0 following contact inhibition and serum starvation. This could be achieved by measuring the levels of p27 or cyclin D as they are both often used as markers of quiescence. Alternatively, flow cytometry could be used to determine the percentage of cells in G0/G1 (Matson *et al.,* 2019). This would help to validate whether cells successfully entered G0 following contact inhibition and serum starvation. Furthermore, the transfection of synchronised cells had limited success in this study, possibly due to the cells undergoing several stress-inducing processes such as contact inhibition and serum starvation followed by transfection. Future studies could try to transfect the cells with plasmid then synchronise the cells, this may be less stress-inducing and thereby increase the chance of the synchronised transfections being successful.

For the E3 transfection experiments, a major limitation was validating the expression of the E3s. An important consideration when validating UBR5-GFP expression by fluorescence microscopy is that a non-transfected control would be required in order to determine the level of autofluorescence of 3T3 cells. This is important as different exposure times were used when imaging GFP and UBR5-GFP transfected cells, therefore it is important to consider autofluorescence, as well as channel bleed through, when using longer exposure times. It may be beneficial for future studies to use confocal microscopy to image the transfected cells as autofluorescence and cross-talk between two fluorophores are typically reduced using

confocal microscopy (Jonkman *et al.,* 2020). In addition to fluorescence microscopy, this study used techniques such as western blotting and immunofluorescence to detect E3 expression. The success of these methods is dependent on antibodies that can successfully detect the target protein. Future studies could look at validating the expression of the E3s through the use of a different technique that is not reliant on an antibody for detection. For example, quantitative PCR (qPCR) could be used to quantify transcript abundance of the E3s following transfection. In addition to possible problems with detection methods, it is also important to consider that the difficulty in validating E3 expression may be a result of the transfections having limited success with potentially only very low transfection efficiency. Therefore, optimisation of the transfection protocol or use of a model cell line that is considered easy to transfect would be beneficial in the future. HEK293 cells are considered a cell line that is easy to transfect (Yuan *et al.,* 2018). Validating E3 expression is important so conclusions can be made regarding the potential role of the E3s in regulating CIZ1 levels.

In this study, the transfection experiments were performed to determine if any of the E3(s) have a potential role in the regulation of CIZ1 protein levels, however, this type of experiment does not determine if any of the E3s directly ubiquitylate CIZ1. This could be achieved in future experiments by overexpressing the E3s and evaluating CIZ1 ubiquitination using denaturing immunoprecipitation, this technique disrupts protein-protein interactions and leaves only covalent bonds thereby allowing retrieval of ubiquitylated target protein (Hasanov *et al.,* 2017). Therefore, this technique can be used to determine if any of the putative E3s specifically ubiquitylate CIZ1.

Finally, future studies should investigate the role of other potential regulators on CIZ1 levels. It is possible that the regulation of CIZ1 also involves the activities of phosphatases and de-ubiquitinating enzymes (DUBs). Previous work has shown that protein phosphatase 1 (PP1) and protein phosphatase 2A (PP2A) are involved in the de-phosphorylation of CIZ1 (Pauzaite, 2019). Identification of the DUBs involved in CIZ1 regulation could be achieved by biochemical approaches including *in vitro* deubiquitylation assays. Deregulation of phosphatase or DUB activity could promote CIZ1 accumulation, therefore phosphatases and DUBs may also represent therapeutic targets for reducing CIZ1 levels.

4.7. Concluding remarks

To conclude, this work has found that CIZ1 protein levels can be reduced by inhibition of CDK4/6, DDK, CDK2 and CDK1. Furthermore, inhibition of DDK and CDK2 potentially facilitate the UPS-mediated degradation of CIZ1. The E3 transfection studies highlighted problems that need troubleshooting in future work, in particular, validation of E3 expression. Despite this, preliminary findings show that transfecting 3T3 cells with UBR5-GFP or FBXO38-FLAG can reduce CIZ1 levels, however, valid conclusions regarding their role in CIZ1 regulation are unable to be made without validation of their expression. The findings from the apoptosis assays demonstrate a cytotoxic effect of DDK and CDK inhibitors in PC3 cells which demonstrates the potential clinical applications of kinase inhibitors in cancer cells. Together, the findings from this study suggest that the molecular pathways that regulate CIZ1 could be manipulated to reduce CIZ1 levels, however, the findings are preliminary and future work is essential to both validate the findings from this study and progress the research further.

References

Abbas, T. and Dutta, A., (2011). CRL4Cdt2. *Cell Cycle*, **10**(2), pp.241-249.

Abbas, T. and Dutta, A., (2017). Regulation of Mammalian DNA Replication via the Ubiquitin-Proteasome System. *Advances in Experimental Medicine and Biology*, **10**(42) pp.421-454.

Ainscough, J., Rahman, F., Sercombe, H., Sedo, A., Gerlach, B. and Coverley, D., (2007). C-terminal domains deliver the DNA replication factor Ciz1 to the nuclear matrix. *Journal of Cell Science*, **120**(1), pp.115-124.

Alao, J., (2007). The regulation of cyclin D1 degradation: roles in cancer development and the potential for therapeutic invention. *Molecular Cancer*, **6**(1), p.24.

Alfieri, C., Zhang, S. and Barford, D., (2017). Visualizing the complex functions and mechanisms of the anaphase promoting complex/cyclosome (APC/C). *Open Biology*, **7**(11), p.170204.

Amador, V., Ge, S., Santamaría, P., Guardavaccaro, D. and Pagano, M., (2007). APC/CCdc20 Controls the Ubiquitin-Mediated Degradation of p21 in Prometaphase. *Molecular Cell*, **27**(3), pp.462-473.

Arisan, E., Obakan, P., Coker-Gurkan, A., Calcabrini, A., Agostinelli, E. and Unsal, N., (2014). CDK Inhibitors Induce Mitochondria-mediated Apoptosis Through the Activation of Polyamine Catabolic Pathway in LNCaP, DU145 and PC3 Prostate Cancer Cells. *Current Pharmaceutical Design***, 20**(2), pp.180-188.

Asghar, U., Witkiewicz, A., Turner, N. and Knudsen, E., (2015). The history and future of targeting cyclin-dependent kinases in cancer therapy. *Nature Reviews Drug Discovery*, **14(**2), pp.130-146.

Bajar, B., Lam, A., Badiee, R., Oh, Y., Chu, J., Zhou, X., Kim, N., Kim, B., Chung, M., Yablonovitch, A., Cruz, B., Kulalert, K., Tao, J., Meyer, T., Su, X. and Lin, M., (2016). Fluorescent indicators for simultaneous reporting of all four cell cycle phases. *Nature Methods*, **13**(12), pp.993-996.

Balaji, V. and Hoppe, T., (2020). Regulation of E3 ubiquitin ligases by homotypic and heterotypic assembly. *F1000Research***, 6**(9), p.88.

Baldwin, G., (2009). Phosphorylation of cyclin-dependent kinase 2 peptides enhances metal binding. *Biochemical and Biophysical Research Communications*, **379**(1), pp.151-154.

Bard, J., Goodall, E., Greene, E., Jonsson, E., Dong, K. and Martin, A., (2018). Structure and Function of the 26S Proteasome. *Annual Review of Biochemistry*, **87**(1), pp.697-724.

Bassermann, F., Eichner, R. and Pagano, M., (2014). The ubiquitin proteasome system — Implications for cell cycle control and the targeted treatment of cancer. *Biochimica et Biophysica Acta (BBA) - Molecular Cell Research*, **1843**(1), pp.150-162.

Beaver, J., Amiri-Kordestani, L., Charlab, R., Chen, W., Palmby, T., Tilley, A., Zirkelbach, J., Yu, J., Liu, Q., Zhao, L., Crich, J., Chen, X., Hughes, M., Bloomquist, E., Tang, S., Sridhara, R., Kluetz, P., Kim, G., Ibrahim, A., Pazdur, R. and Cortazar, P., (2015). FDA Approval: Palbociclib for the Treatment of Postmenopausal Patients with Estrogen Receptor–Positive, HER2-Negative Metastatic Breast Cancer. *Clinical Cancer Research*, **21**(21), pp.4760-4766.

Bell, S. and Dutta, A., (2002). DNA Replication in Eukaryotic Cells. *Annual Review of Biochemistry*, **71**(1), pp.333-374.

Bell, S. and Stillman, B., (1992). ATP-dependent recognition of eukaryotic origins of DNA replication by a multiprotein complex. *Nature*, **357(**6374), pp.128-134.

Benanti, J., (2012). Coordination of cell growth and division by the ubiquitin–proteasome system. *Seminars in Cell & Developmental Biology*, **23**(5), pp.492-498.

Blagosklonny, M. and Pardee, A., (2002). The Restriction Point of the Cell Cycle. *Cell Cycle*, **1**(2), pp.102-109.

Bochis, O., Fetica, B., Vlad, C., Achimas-Cadariu, P. and Irimie, A., (2015). The importance of ubiquitin E3 ligases, SCF and APC/C, in human cancers. *Medicine and Pharmacy Reports*, **88(**1), pp.9-14.

Boutros, R., Dozier, C. and Ducommun, B., (2006). The when and wheres of CDC25 phosphatases. *Current Opinion in Cell Biology*, 1**8**(2), pp.185-191.

Brooks, E., Gray, N., Joly, A., Kerwar, S., Lum, R., Mackman, R., Norman, T., Rosete, J., Rowe, M., Schow, S., Schultz, P., Wang, X., Wick, M. and Shiffman, D., (1997). CVT-313, a Specific and Potent Inhibitor of CDK2 That Prevents Neointimal Proliferation. *Journal of Biological Chemistry*, **272**(46), pp.29207-29211.

Canavese, M., Santo, L. and Raje, N., (2012). Cyclin dependent kinases in cancer. *Cancer Biology & Therapy*, **13**(7), pp.451-457.

Cao, Y., Ma, E., Cestellos-Blanco, S., Zhang, B., Qiu, R., Su, Y., Doudna, J. and Yang, P., (2019). Nontoxic nanopore electroporation for effective intracellular delivery of biological macromolecules. *Proceedings of the National Academy of Sciences*, **116**(16), pp.7899-7904.

Cappell, S., Mark, K., Garbett, D., Pack, L., Rape, M. and Meyer, T., (2018). EMI1 switches from being a substrate to an inhibitor of APC/CCDH1 to start the cell cycle. *Nature*, **558**(7709), pp.313-317.

Chari, A., Mazumder, A. and Jagannath, S., (2010). Proteasome inhibition and its therapeutic potential in multiple myeloma. *Biologics: Targets & Therapy*, **4**(4), pp.273-287.

Chen, D., Frezza, M., Schmitt, S., Kanwar, J. and P. Dou, Q., (2011). Bortezomib as the First Proteasome Inhibitor Anticancer Drug: Current Status and Future Perspectives. *Current Cancer Drug Targets*, **11**(3), pp.239-253.

Choudhury, R., Bonacci, T., Arceci, A., Lahiri, D., Mills, C., Kernan, J., Branigan, T., DeCaprio, J., Burke, D. and Emanuele, M., (2016). APC/C and SCF cyclin F Constitute a Reciprocal Feedback Circuit Controlling S-Phase Entry. *Cell Reports*, **16**(12), pp.3359-3372.

Chow, J. and Poon, R., (2012). The CDK1 inhibitory kinase MYT1 in DNA damage checkpoint recovery. *Oncogene*, **32**(40), pp.4778-4788.

Cipolla, L., Bertoletti, F., Maffia, A., Liang, C., Lehmann, A., Cohn, M. and Sabbioneda, S., (2019). UBR5 interacts with the replication fork and protects DNA replication from DNA polymerase η toxicity. *Nucleic Acids Research*, **47**(21), pp.11268-11283.

Copeland, N., Sercombe, H., Ainscough, J. and Coverley, D., (2010). Ciz1 cooperates with cyclin-A–CDK2 to activate mammalian DNA replication in vitro. *Journal of Cell Science*, **123**(7), pp.1108-1115.

Copeland, N., Sercombe, H., Wilson, R. and Coverley, D., (2015). Cyclin A/CDK2 phosphorylation of CIZ1 blocks replisome formation and initiation of mammalian DNA replication. *Journal of Cell Science*, **128**(8), pp.1518-1527.

Cotton, T. and Lechtenberg, B., (2020). Chain reactions: molecular mechanisms of RBR ubiquitin ligases. *Biochemical Society Transactions*, **48**(4), pp.1737-1750.

Coverley, D., Higgins, G., West, D., Jackson, O. T., Dowle, A., Haslam, A., Ainscough, E., Chalkley, R., & White, J. (2017). A quantitative immunoassay for lung cancer biomarker CIZ1b in patient plasma. *Clinical biochemistry*, ***50*(**6), pp.336–343.

Coverley, D., Laman, H. and Laskey, R., (2002). Distinct roles for cyclins E and A during DNA replication complex assembly and activation. *Nature Cell Biology*, **4**(7), pp.523-528.

Coverley, D., Marr, J. and Ainscough, J., (2005). Ciz1 promotes mammalian DNA replication. *Journal of Cell Science*, **118**(1), pp.101-112.

Coxon, C., Anscombe, E., Harnor, S., Martin, M., Carbain, B., Golding, B., Hardcastle, I., Harlow, L., Korolchuk, S., Matheson, C., Newell, D., Noble, M., Sivaprakasam, M., Tudhope, S., Turner, D., Wang, L., Wedge, S., Wong, C., Griffin, R., Endicott, J. and Cano, C., (2017). Cyclin-Dependent Kinase (CDK) Inhibitors: Structure–Activity Relationships and Insights into the CDK-2 Selectivity of 6-Substituted 2-Arylaminopurines. *Journal of Medicinal Chemistry*, **60**(5), pp.1746-1767.

Dang, F., Nie, L. and Wei, W., (2020). Ubiquitin signalling in cell cycle control and tumorigenesis. *Cell Death & Differentiation*, **28**(2), pp.427-438.

De Boer, L., Oakes, V., Beamish, H., Giles, N., Stevens, F., Somodevilla-Torres, M., DeSouza, C. and Gabrielli, B., (2008). Cyclin A/cdk2 coordinates centrosomal and nuclear mitotic events. *Oncogene*, **27**(31), pp.4261-4268.

Delmolino, L., Saha, P. and Dutta, A., (2001). Multiple Mechanisms Regulate Subcellular Localization of Human CDC6. *Journal of Biological Chemistry*, **276**(29), pp.26947-26954.

Deng, L., Meng, T., Chen, L., Wei, W. and Wang, P., (2020). The role of ubiquitination in tumorigenesis and targeted drug discovery. *Signal Transduction and Targeted Therapy*, **5**(1), p.11.

Den Hollander, P. and Kumar, R., (2006). Dynein Light Chain 1 Contributes to Cell Cycle Progression by Increasing Cyclin-Dependent Kinase 2 Activity in Estrogen-Stimulated Cells. *Cancer Research*, **66**(11), pp.5941-5949.

Den Hollander, P., Rayala, S., Coverley, D. and Kumar, R., (2006). Ciz1, a Novel DNA-Binding Coactivator of the Estrogen Receptor α, Confers Hypersensitivity to Estrogen Action. *Cancer Research*, **66**(22), pp.11021-11029.

DePamphilis, M., de Renty, C., Ullah, Z. and Lee, C., (2012). "The Octet": Eight Protein Kinases that Control Mammalian DNA Replication. *Frontiers in Physiology*, **3**(368), pp.1-20.

De Poot, S., Tian, G. and Finley, D., (2017). Meddling with Fate: The Proteasomal Deubiquitinating Enzymes. *Journal of Molecular Biology*, **429**(22), pp.3525-3545.

Ding, L., Cao, J., Lin, W., Chen, H., Xiong, X., Ao, H., Yu, M., Lin, J. and Cui, Q., (2020). The Roles of Cyclin-Dependent Kinases in Cell-Cycle Progression and Therapeutic Strategies in Human Breast Cancer. *International Journal of Molecular Sciences*, **21**(6), p.1960.

Eggersmann, T., Degenhardt, T., Gluz, O., Wuerstlein, R. and Harbeck, N., (2019). CDK4/6 Inhibitors Expand the Therapeutic Options in Breast Cancer: Palbociclib, Ribociclib and Abemaciclib. *BioDrugs*, **33**(2), pp.125-135.

Evrin, C., Clarke, P., Zech, J., Lurz, R., Sun, J., Uhle, S., Li, H., Stillman, B. and Speck, C., (2009). A double-hexameric MCM2-7 complex is loaded onto origin DNA during licensing of eukaryotic DNA replication. *Proceedings of the National Academy of Sciences*, **106**(48), pp.20240-20245.

Fragkos, M., Ganier, O., Coulombe, P. and Méchali, M., (2015). DNA replication origin activation in space and time. *Nature Reviews Molecular Cell Biology*, **16**(6), pp.360-374.

Fujisawa, S., Romin, Y., Barlas, A., Petrovic, L., Turkekul, M., Fan, N., Xu, K., Garcia, A., Monette, S., Klimstra, D., Erinjeri, J., Solomon, S., Manova-Todorova, K. and Sofocleous, C., (2013). Evaluation of YO-PRO-1 as an early marker of apoptosis following radiofrequency ablation of colon cancer liver metastases. *Cytotechnology*, **66**(2), pp.259-273.

Fujita, T., Liu, W., Doihara, H. and Wan, Y., (2008). Regulation of Skp2-p27 Axis by the Cdh1/Anaphase-Promoting Complex Pathway in Colorectal Tumorigenesis. *The American Journal of Pathology*, **173**(1), pp.217-228.

Fus-Kujawa, A., Prus, P., Bajdak-Rusinek, K., Teper, P., Gawron, K., Kowalczuk, A. and Sieron, A., (2021). An Overview of Methods and Tools for Transfection of Eukaryotic Cells in vitro. *Frontiers in Bioengineering and Biotechnology*, **9**(701031), pp.1-15.

Galdeano, C., (2017). Drugging the undruggable: targeting challenging E3 ligases for personalized medicine. *Future Medicinal Chemistry*, **9**(4), pp.347-350.

Gavet, O. and Pines, J., (2010). Progressive Activation of CyclinB1-Cdk1 Coordinates Entry to Mitosis. *Developmental Cell*, **18**(4), pp.533-543.

Georges, A., Coyaud, E., Marcon, E., Greenblatt, J., Raught, B. and Frappier, L., (2019). USP7 Regulates Cytokinesis through FBXO38 and KIF20B. *Scientific Reports*, **9**(1), p.2724.

Gerard, C. and Goldbeter, A., (2009). Temporal self-organization of the cyclin/Cdk network driving the mammalian cell cycle. *Proceedings of the National Academy of Sciences*, **106**(51), pp.21643-21648.

Gin, P., Yin, L., Davies, B., Weinstein, M., Ryan, R., Bensadoun, A., Fong, L., Young, S. and Beigneux, A., (2008). The Acidic Domain of GPIHBP1 Is Important for the Binding of Lipoprotein Lipase and Chylomicrons. *Journal of Biological Chemistry*, **283**(43), pp.29554-29562.

Gottesman, M., (2002). Mechanisms of Cancer Drug Resistance. *Annual Review of Medicine*, **53**(1), pp.615-627.

Grant, G. and Cook, J., (2017). The Temporal Regulation of S Phase Proteins During G1. *Advances in Experimental Medicine and Biology*, **10**(42), pp.335-369.

Grice, G. and Nathan, J., (2016). The recognition of ubiquitinated proteins by the proteasome. *Cellular and Molecular Life Sciences*, **73**(18), pp.3497-3506.

Guarducci, C., Bonechi, M., Boccalini, G., Benelli, M., Risi, E., Di Leo, A., Malorni, L. and Migliaccio, I., (2017). Mechanisms of Resistance to CDK4/6 Inhibitors in Breast Cancer and Potential Biomarkers of Response. *Breast Care*, **12**(5), pp.304-308.

Han, Y., Moon, H., You, B. and Park, W., (2009). The effect of MG132, a proteasome inhibitor on HeLa cells in relation to cell growth, reactive oxygen species and GSH. *Oncology Reports*, **22**(1), pp.215-221.

Hanahan, D. and Weinberg, R., (2011). Hallmarks of Cancer: The Next Generation. *Cell*, **144**(5), pp.646-674.

Hasanov, E., Chen, G., Chowdhury, P., Weldon, J., Ding, Z., Jonasch, E., Sen, S., Walker, C. and Dere, R., (2017). Ubiquitination and regulation of AURKA identifies a hypoxia-independent E3 ligase activity of VHL. *Oncogene*, **36**(24), pp.3450-3463.

Hein, J., Garvanska, D., Nasa, I., Kettenbach, A. and Nilsson, J., (2021). Coupling of Cdc20 inhibition and activation by BubR1. *Journal of Cell Biology*, **220**(5), p. 202012081.

Heller, R., Kang, S., Lam, W., Chen, S., Chan, C. and Bell, S., (2011). Eukaryotic Origin-Dependent DNA Replication In Vitro Reveals Sequential Action of DDK and S-CDK Kinases. *Cell*, **146**(1), pp.80-91.

Higgins, G., Roper, K., Watson, I., Blackhall, F., Rom, W., Pass, H., Ainscough, J. and Coverley, D., (2012). Variant Ciz1 is a circulating biomarker for early-stage lung cancer. *Proceedings of the National Academy of Sciences*, **109**(45), pp.3128-3135.

Hormaechea-Agulla, D., Kim, Y., Song, M. and Song, S., (2018). New Insights into the Role of E2s in the Pathogenesis of Diseases: Lessons Learned from UBE2O. *Molecules and Cells*, **41**(3), pp.168-178.

Hwang, H. and Clurman, B., (2005). Cyclin E in normal and neoplastic cell cycles. *Oncogene*, **24**(17), pp.2776-2786.

Jackman, M., Marcozzi, C., Barbiero, M., Pardo, M., Yu, L., Tyson, A., Choudhary, J. and Pines, J., (2020). Cyclin B1-Cdk1 facilitates MAD1 release from the nuclear pore to ensure a robust spindle checkpoint. *Journal of Cell Biology*, **219**(6), p.201907082.

Ji, Z., Tang, Q., Zhang, J., Yang, Y., Liu, Y. and Pan, Y., (2011). Oridonin-induced apoptosis in SW620 human colorectal adenocarcinoma cells. *Oncology Letters*, **2**(6), pp.1303-1307.

Jin, J., Cardozo, T., Lovering, R., Elledge, S., Pagano, M. and Harper, J., (2004). Systematic analysis and nomenclature of mammalian F-box proteins. *Genes & Development*, **18**(21), pp.2573-2580.

Jonkman, J., Brown, C., Wright, G., Anderson, K. and North, A., (2020). Tutorial: guidance for quantitative confocal microscopy. *Nature Protocols*, **15**(5), pp.1585-1611.

Kernan, J., Bonacci, T. and Emanuele, M., (2018). Who guards the guardian? Mechanisms that restrain APC/C during the cell cycle. *Biochimica et Biophysica Acta (BBA) - Molecular Cell Research*, **1865**(12), pp.1924-1933.

Kim, T., Lara-Gonzalez, P., Prevo, B., Meitinger, F., Cheerambathur, D., Oegema, K. and Desai, A., (2017). Kinetochores accelerate or delay APC/C activation by directing Cdc20 to opposing fates. *Genes & Development*, **31**(11), pp.1089-1094.

Klug, A., (2010). The Discovery of Zinc Fingers and Their Applications in Gene Regulation and Genome Manipulation. *Annual Review of Biochemistry*, **79**(1), pp.213-231.

Koepp, D., Schaefer, L., Ye, X., Keyomarsi, K., Chu, C., Harper, J. and Elledge, S., (2001). Phosphorylation-Dependent Ubiquitination of Cyclin E by the SCFFbw7 Ubiquitin Ligase. *Science*, **294**(5540), pp.173-177.

Koltun, E., Tsuhako, A., Brown, D., Aay, N., Arcalas, A., Chan, V., Du, H., Engst, S., Ferguson, K., Franzini, M., Galan, A., Holst, C., Huang, P., Kane, B., Kim, M., Li, J., Markby, D., Mohan, M., Noson, K., Plonowski, A., Richards, S., Robertson, S., Shaw, K., Stott, G., Stout, T., Young, J., Yu, P., Zaharia, C., Zhang, W., Zhou, P., Nuss, J., Xu, W. and Kearney, P., (2012). Discovery of XL413, a potent and selective CDC7 inhibitor. *Bioorganic & Medicinal Chemistry Letters*, **22**(11), pp.3727-3731.

Kucharski, M., Mrowiec, P. and Ocłoń, E., (2021). Current standards and pitfalls associated with the transfection of primary fibroblast cells. *Biotechnology Progress*, **37**, p.3152.

Lara-Gonzalez, P., Westhorpe, F. and Taylor, S., (2012). The Spindle Assembly Checkpoint. *Current Biology*, **22**(22), pp.966-R980.

Lee, D. and Bell, S., (1997). Architecture of the yeast origin recognition complex bound to origins of DNA replication. *Molecular and Cellular Biology*, **17**(12), pp.7159-7168.

Lei, L., Wu, J., Gu, D., Liu, H. and Wang, S., (2016). CIZ1 interacts with YAP and activates its transcriptional activity in hepatocellular carcinoma cells. *Tumor Biology*, **37**(8), pp.11073-11079.

Li, M. and Zhang, P., (2009). The function of APC/CCdh1 in cell cycle and beyond. *Cell Division*, **4**(1), p.2.

Li, Y., Zhang, J., Gao, W., Zhang, L., Pan, Y., Zhang, S. and Wang, Y., (2015). Insights on Structural Characteristics and Ligand Binding Mechanisms of CDK2. *International Journal of Molecular Sciences*, **16**(12), pp.9314-9340.

Lin, K., Park, H. and Guan, K., (2017). Regulation of the Hippo Pathway Transcription Factor TEAD. *Trends in Biochemical Sciences*, **42**(11), pp.862-872.

Liu, E., Li, X., Yan, F., Zhao, Q. and Wu, X., (2004). Cyclin-dependent Kinases Phosphorylate Human Cdt1 and Induce Its Degradation. *Journal of Biological Chemistry*, **279**(17), pp.17283-17288.

Liu, L., Wong, C., Gong, B. and Yu, J., (2017). Functional significance and therapeutic implication of ring-type E3 ligases in colorectal cancer. *Oncogene*, **37**(2), pp.148-159.

Liu, Q., Niu, N., Wada, Y. and Liu, J., (2016). The Role of Cdkn1A-Interacting Zinc Finger Protein 1 (CIZ1) in DNA Replication and Pathophysiology. *International Journal of Molecular Sciences*, **17**(2), p.212.

Liu, T., Ren, X., Li, L., Liang, K., Yu, H., Ren, H., Zhou, W., Jing, H. and Kong, C., (2015). Ciz1 promotes tumorigenicity of prostate carcinoma cells. *Frontiers in Bioscience*, **20**(4), pp.705-715.

Lu, Z. and Hunter, T., (2010). Ubiquitylation and proteasomal degradation of the p21Cip1, p27Kip1and p57Kip2CDK inhibitors. *Cell Cycle*, **9**(12), pp.2342-2352.

Lunn, C., Chrivia, J. and Baldassare, J., (2010). Activation of Cdk2/Cyclin E complexes is dependent on the origin of replication licensing factor Cdc6 in mammalian cells. *Cell Cycle*, **9**(22), pp.4533-4541.

Malumbres, M., (2014). Cyclin-dependent kinases. *Genome Biology*, **15**(6), p.122.

Matson, J., House, A., Grant, G., Wu, H., Perez, J. and Cook, J., (2019). Intrinsic checkpoint deficiency during cell cycle re-entry from quiescence. *Journal of Cell Biology*, **218**(7), pp.2169-2184.

Meissner, B., Kridel, R., Lim, R., Rogic, S., Tse, K., Scott, D., Moore, R., Mungall, A., Marra, M., Connors, J., Steidl, C. and Gascoyne, R., (2013). The E3 ubiquitin ligase UBR5 is recurrently mutated in mantle cell lymphoma. *Blood*, **121**(16), pp.3161-3164.

Méndez, J., Zou-Yang, X., Kim, S., Hidaka, M., Tansey, W. and Stillman, B., (2002). Human Origin Recognition Complex Large Subunit Is Degraded by Ubiquitin-Mediated Proteolysis after Initiation of DNA Replication. *Molecular Cell*, **9**(3), pp.481-491.

Meng, X., Liu, X., Guo, X., Jiang, S., Chen, T., Hu, Z., Liu, H., Bai, Y., Xue, M., Hu, R., Sun, S., Liu, X., Zhou, P., Huang, X., Wei, L., Yang, W. and Xu, C., (2018). FBXO38 mediates PD-1 ubiquitination and regulates anti-tumour immunity of T cells. *Nature*, **564**(7734), pp.130-135.

Metzger, M., Pruneda, J., Klevit, R. and Weissman, A., (2014). RING-type E3 ligases: Master manipulators of E2 ubiquitin-conjugating enzymes and ubiquitination. *Biochimica et Biophysica Acta (BBA) - Molecular Cell Research*, **1843**(1), pp.47-60.

Mitsui, K., Matsumoto, A., Ohtsuka, S., Ohtsubo, M. and Yoshimura, A., (1999). Cloning and Characterization of a Novel p21Cip1/Waf1-Interacting Zinc Finger Protein, Ciz1. *Biochemical and Biophysical Research Communications*, **264**(2), pp.457-464.

Mohapatra, S., Chu, B., Zhao, X., Djeu, J., Cheng, J. and Pledger, W., (2009). Apoptosis of metastatic prostate cancer cells by a combination of cyclin-dependent kinase and AKT inhibitors. *The International Journal of Biochemistry & Cell Biology*, **41**(3), pp.595-602.

Moiseeva, T., Qian, C., Sugitani, N., Osmanbeyoglu, H. and Bakkenist, C., (2019). WEE1 kinase inhibitor AZD1775 induces CDK1 kinase-dependent origin firing in unperturbed G1- and S-phase cells. *Proceedings of the National Academy of Sciences*, **116**(48), pp.23891-23893.

Montagnoli, A., Valsasina, B., Croci, V., Menichincheri, M., Rainoldi, S., Marchesi, V., Tibolla, M., Tenca, P., Brotherton, D., Albanese, C., Patton, V., Alzani, R., Ciavolella, A., Sola, F., Molinari, A., Volpi, D., Avanzi, N., Fiorentini, F., Cattoni, M., Healy, S., Ballinari, D., Pesenti, E., Isacchi, A., Moll, J., Bensimon, A., Vanotti, E. and Santocanale, C., (2008). A Cdc7 kinase inhibitor restricts initiation of DNA replication and has antitumor activity. *Nature Chemical Biology*, **4**(6), pp.357-365.

Morimoto, D. and Shirakawa, M., (2016). The evolving world of ubiquitin: transformed polyubiquitin chains. *Biomolecular Concepts*, **7**(3), pp.157-167.

Moser, J., Miller, I., Carter, D. and Spencer, S., (2018). Control of the Restriction Point by Rb and p21. *Proceedings of the National Academy of Sciences*, **115**(35), pp.8219-8227.

Munoz, M., Saunders, D., Henderson, M., Clancy, J., Russell, A., Lehrbach, G., Musgrove, E., Watts, C. and Sutherland, R., (2007). The E3 Ubiquitin Ligase EDD Regulates S-Phase and G2/M DNA Damage Checkpoints. *Cell Cycle*, **6**(24), pp.3070-3077.

Nakayama, K. and Nakayama, K., (2005). Regulation of the cell cycle by SCF-type ubiquitin ligases. *Seminars in Cell & Developmental Biology*, **16**(3), pp.323-333.

Narasimha, A., Kaulich, M., Shapiro, G., Choi, Y., Sicinski, P. and Dowdy, S., (2014). Cyclin D activates the Rb tumor suppressor by mono-phosphorylation. *eLife*, **3**(4), p.02872.

Natoni, A., Coyne, M., Jacobsen, A., Rainey, M., O'Brien, G., Healy, S., Montagnoli, A., Moll, J., O'Dwyer, M. and Santocanale, C., (2013). Characterization of a Dual CDC7/CDK9 Inhibitor in Multiple Myeloma Cellular Models. *Cancers*, **5**(4), pp.901-918.

Nishibe, R., Watanabe, W., Ueda, T., Yamasaki, N., Koller, R., Wolff, L., Honda, Z., Ohtsubo, M. and Honda, H., (2013). CIZ1, a p21Cip1/Waf1-interacting protein, functions as a tumor suppressor in vivo. *Federation of European Biochemical Societies* (*FEBS) Letters*, **587**(10), pp.1529-1535.

O'Brien, P., Davies, M., Scurry, J., Smith, A., Barton, C., Henderson, M., Saunders, D., Gloss, B., Patterson, K., Clancy, J., Heinzelmann-Schwarz, V., Scolyer, R., Zeng, Y., Williams, E., Scurr, L., DeFazio, A., Quinn, D., Watts, C., Hacker, N., Henshall, S. and Sutherland, R., (2008). The E3 ubiquitin ligase EDD is an adverse prognostic factor for serous epithelial ovarian cancer and modulates cisplatin resistance in vitro. *British Journal of Cancer*, **98**(6), pp.1085-1093.

Parker, M., Botchan, M. and Berger, J., (2017). Mechanisms and regulation of DNA replication initiation in eukaryotes. *Critical Reviews in Biochemistry and Molecular Biology*, **52**(2), pp.107-144.

Parua, P., Kalan, S., Benjamin, B., Sansó, M. and Fisher, R., (2020). Distinct Cdk9-phosphatase switches act at the beginning and end of elongation by RNA polymerase II. *Nature Communications*, **11**(4338), pp.1-13.

Pauzaite, T., (2019). Identification and analysis of the signalling networks that regulate Ciz1 levels in normal and cancer cell lines. PhD, Lancaster University.

Pauzaite, T., Thacker, U., Tollitt, J. and Copeland, N., (2016). Emerging Roles for Ciz1 in Cell Cycle Regulation and as a Driver of Tumorigenesis. *Biomolecules*, **7**(4), p.1.

Peyressatre, M., Prével, C., Pellerano, M. and Morris, M., (2015). Targeting Cyclin-Dependent Kinases in Human Cancers: From Small Molecules to Peptide Inhibitors. *Cancers*, **7**(1), pp.179-237.

Piezzo, M., Cocco, S., Caputo, R., Cianniello, D., Gioia, G., Lauro, V., Fusco, G., Martinelli, C., Nuzzo, F., Pensabene, M. and Laurentiis, M., (2020). Targeting Cell Cycle in Breast Cancer: CDK4/6 Inhibitors. *International Journal of Molecular Sciences*, **21**(18), p.6479.

Potapova, T., Daum, J., Byrd, K. and Gorbsky, G., (2009). Fine Tuning the Cell Cycle: Activation of the Cdk1 Inhibitory Phosphorylation Pathway during Mitotic Exit. *Molecular Biology of the Cell*, **20**(6), pp.1737-1748.

Qiao, X., Liu, Y., Prada, M., Mohan, A., Gupta, A., Jaiswal, A., Sharma, M., Merisaari, J., Haikala, H., Talvinen, K., Yetukuri, L., Pylvänäinen, J., Klefström, J., Kronqvist, P., Meinander, A., Aittokallio, T., Hietakangas, V., Eilers, M. and Westermarck, J., (2020). UBR5 Is Coamplified with MYC in Breast Tumors and Encodes an Ubiquitin Ligase That Limits MYC-Dependent Apoptosis. *Cancer Research*, **80**(7), pp.1414-1427.

Qiao, X., Zhang, L., Gamper, A., Fujita, T. and Wan, Y., (2010). APC/C-Cdh1. *Cell Cycle*, **9**(19), pp.3904-3912.

Quereda, V., Porlan, E., Cañamero, M., Dubus, P. and Malumbres, M., (2015). An essential role for Ink4 and Cip/Kip cell-cycle inhibitors in preventing replicative stress. *Cell Death & Differentiation*, **23**(3), pp.430-441.

Rahman, F., Ainscough, J., Copeland, N. and Coverley, D., (2007). Cancer-associated missplicing of exon 4 influences the subnuclear distribution of the DNA replication factor CIZ1. *Human Mutation*, **28**(10), pp.993-1004.

Randell, J., Bowers, J., Rodríguez, H. and Bell, S., (2006). Sequential ATP Hydrolysis by Cdc6 and ORC Directs Loading of the Mcm2-7 Helicase. *Molecular Cell*, **21**(1), pp.29-39.

Ridings-Figueroa, R., Stewart, E., Nesterova, T., Coker, H., Pintacuda, G., Godwin, J., Wilson, R., Haslam, A., Lilley, F., Ruigrok, R., Bageghni, S., Albadrani, G., Mansfield, W., Roulson, J., Brockdorff, N., Ainscough, J. and Coverley, D., (2017). The nuclear matrix protein CIZ1 facilitates localization of Xist RNA to the inactive X-chromosome territory. *Genes & Development*, **31**(9), pp.876-888.

Riera, A., Barbon, M., Noguchi, Y., Reuter, L., Schneider, S. and Speck, C., (2017). From structure to mechanism—understanding initiation of DNA replication. *Genes & Development*, **31**(11), pp.1073-1088.

Rieser, E., Cordier, S. and Walczak, H., (2013). Linear ubiquitination: a newly discovered regulator of cell signalling. *Trends in Biochemical Sciences*, **38**(2), pp.94-102.

Rubenstein, E. and Hochstrasser, M., (2010). Redundancy and variation in the ubiquitin-mediated proteolytic targeting of a transcription factor. *Cell Cycle*, **9**(21), pp.4282-4285.

Rubin, S., (2013). Deciphering the retinoblastoma protein phosphorylation code. *Trends in Biochemical Sciences*, **38**(1), pp.12-19.

Saiz-Baggetto, S., Méndez, E., Quilis, I., Igual, J. and Bañó, M., (2017). Chimeric proteins tagged with specific 3xHA cassettes may present instability and functional problems. *Public Library of Science*, **12**(8), p.e0183067.

Saraon, P., Drabovich, A., Jarvi, K. and Diamandis, E., (2014). Mechanisms of Androgen-Independent Prostate Cancer. *The Journal of the International Federation of Clinical Chemistry and Laboratory Medicine*, **25**(1), pp.42-54.

Sasi, N., Tiwari, K., Soon, F., Bonte, D., Wang, T., Melcher, K., Xu, H. and Weinreich, M., (2014). The Potent Cdc7-Dbf4 (DDK) Kinase Inhibitor XL413 Has Limited Activity in Many Cancer Cell Lines and Discovery of Potential New DDK Inhibitor Scaffolds. *Public Library of Science,* **9**(11), p.113300.

Saurabh, K., Shah, P., Doll, M., Siskind, L. and Beverly, L., (2020). UBR-box containing protein, UBR5, is over-expressed in human lung adenocarcinoma and is a potential therapeutic target. *BioMed Central Cancer*, **20**(1), p.824.

Scheffner, M. and Kumar, S., (2014). Mammalian HECT ubiquitin-protein ligases: Biological and pathophysiological aspects. *Biochimica et Biophysica Acta (BBA) - Molecular Cell Research*, **1843**(1), pp.61-74.

Schrader, E., Harstad, K. and Matouschek, A., (2009). Targeting proteins for degradation. *Nature Chemical Biology*, **5**(11), pp.815-822.

Serman, T. and Gack, M., (2019). FBXO38 Drives PD-1 to Destruction. *Trends in Immunology*, **40**(2), pp.81-83.

Shearer, R., Iconomou, M., Watts, C. and Saunders, D., (2015). Functional Roles of the E3 Ubiquitin Ligase UBR5 in Cancer. *Molecular Cancer Research***, 13**(12), pp.1523-1532.

Skaar, J., Pagan, J. and Pagano, M., (2013). Mechanisms and function of substrate recruitment by F-box proteins. *Nature Reviews Molecular Cell Biology*, **14**(6), pp.369-381.

Skaar, J., Pagan, J. and Pagano, M., (2014). SCF ubiquitin ligase-targeted therapies. *Nature Reviews Drug Discovery*, **13**(12), pp.889-903.

Soucy, T., Smith, P., Milhollen, M., Berger, A., Gavin, J., Adhikari, S., Brownell, J., Burke, K., Cardin, D., Critchley, S., Cullis, C., Doucette, A., Garnsey, J., Gaulin, J., Gershman, R., Lublinsky, A., McDonald, A., Mizutani, H., Narayanan, U., Olhava, E., Peluso, S., Rezaei, M., Sintchak, M., Talreja, T., Thomas, M., Traore, T., Vyskocil, S., Weatherhead, G., Yu, J., Zhang, J., Dick, L., Claiborne, C., Rolfe, M., Bolen, J. and Langston, S., (2009). An inhibitor of NEDD8-activating enzyme as a new approach to treat cancer. *Nature*, **458**(7239), pp.732-736.

Spencer, S., Cappell, S., Tsai, F., Overton, K., Wang, C. and Meyer, T., (2013). The Proliferation-Quiescence Decision Is Controlled by a Bifurcation in CDK2 Activity at Mitotic Exit. *Cell*, **155**(2), pp.369-383.

Stern, B. and Nurse, P., (1996). A quantitative model for the cdc2 control of S phase and mitosis in fission yeast. *Trends in Genetics*, **12**(9), pp.345-350.

Stewart, E., Turner, R., Newling, K., Ridings-Figueroa, R., Scott, V., Ashton, P., Ainscough, J. and Coverley, D., (2019). Maintenance of epigenetic landscape requires CIZ1 and is corrupted in differentiated fibroblasts in long-term culture. *Nature Communications*, **10**(1), pp.1-13.

Stewart, M., Ritterhoff, T., Klevit, R. and Brzovic, P., (2016). E2 enzymes: more than just middle men. *Cell Research*, **26**(4), pp.423-440.

Streich, F. and Lima, C., (2014). Structural and Functional Insights to Ubiquitin-Like Protein Conjugation. *Annual Review of Biophysics*, **43**(1), pp.357-379.

Sumner, C., d'Ydewalle, C., Wooley, J., Fawcett, K., Hernandez, D., Gardiner, A., Kalmar, B., Baloh, R., Gonzalez, M., Züchner, S., Stanescu, H., Kleta, R., Mankodi, A., Cornblath, D., Boylan, K., Reilly, M., Greensmith, L., Singleton, A., Harms, M., Rossor, A. and

Houlden, H., (2013). A Dominant Mutation in FBXO38 Causes Distal Spinal Muscular Atrophy with Calf Predominance. *The American Journal of Human Genetics*, **93**(5), pp.976-983.

Sun, J., Fernandez-Cid, A., Riera, A., Tognetti, S., Yuan, Z., Stillman, B., Speck, C. and Li, H., (2014). Structural and mechanistic insights into Mcm2–7 double-hexamer assembly and function. *Genes & Development*, **28**(20), pp.2291-2303.

Sun, J., Kawakami, H., Zech, J., Speck, C., Stillman, B. and Li, H., (2012). Cdc6-Induced Conformational Changes in ORC Bound to Origin DNA Revealed by Cryo-Electron Microscopy. *Structure*, **20**(3), pp.534-544.

Swarts, D., Stewart, E., Higgins, G. and Coverley, D., (2018). CIZ1-F, an alternatively spliced variant of the DNA replication protein CIZ1 with distinct expression and localisation, is overrepresented in early stage common solid tumours. *Cell Cycle*, **17**(18), pp.2268-2283.

Symeonidou, I., Taraviras, S. and Lygerou, Z., (2012). Control over DNA replication in time and space. *Federation of European Biochemical Societies* (*FEBS) Letters*, **586**(18), pp.2803-2812.

Takeda, D. and Dutta, A., (2005). DNA replication and progression through S phase. *Oncogene*, **24**(17), pp.2827-2843.

Tanaka, K., (2009). The proteasome: Overview of structure and functions. *Proceedings of the Japan Academy, Series B*, **85**(1), pp.12-36.

Tanaka, S. and Araki, H., (2013). Helicase Activation and Establishment of Replication Forks at Chromosomal Origins of Replication. *Cold Spring Harbor Perspectives in Biology*, **5**(12), pp.a010371-a010371.

Tanaka, S., Nakato, R., Katou, Y., Shirahige, K. and Araki, H., (2011). Origin Association of Sld3, Sld7, and Cdc45 Proteins Is a Key Step for Determination of Origin-Firing Timing. *Current Biology*, **21**(24), pp.2055-2063.

Taylor, S., Kinchington, P., Brooks, A. and Moffat, J., (2004). Roscovitine, a Cyclin-Dependent Kinase Inhibitor, Prevents Replication of Varicella-Zoster Virus. *Journal of Virology*, **78**(6), pp.2853-2862.

Tetsu, O. and McCormick, F., (2003). Proliferation of cancer cells despite CDK2 inhibition. *Cancer Cell*, **3**(3), pp.233-245.

Thibaudeau, T. and Smith, D., (2019). A Practical Review of Proteasome Pharmacology. *Pharmacological Reviews*, **71**(2), pp.170-197.

Ullah, K., Zubia, E., Narayan, M., Yang, J. and Xu, G., (2018). Diverse roles of the E2/E3 hybrid enzyme UBE2O in the regulation of protein ubiquitination, cellular functions, and disease onset. *The Federation of European Biochemical Societies Journal*, **286**(11), pp.2018-2034.

Vassilev, L., Tovar, C., Chen, S., Knezevic, D., Zhao, X., Sun, H., Heimbrook, D. and Chen, L., (2006). Selective small-molecule inhibitor reveals critical mitotic functions of human CDK1. *Proceedings of the National Academy of Sciences*, **103**(28), pp.10660-10665.

Vermeulen, K., Van Bockstaele, D. and Berneman, Z., (2003). The cell cycle: a review of regulation, deregulation and therapeutic targets in cancer. *Cell Proliferation*, **36**(3), pp.131-149.

Wang, D., Wang, K., Yan, D., Liu, J., Wang, B., Li, M., Wang, X., Liu, J., Peng, Z., Li, G. and Yu, Z., (2014). Ciz1 is a novel predictor of survival in human colon cancer. *Experimental Biology and Medicine*, **239**(7), pp.862-870.

Wang, Y., Brady, K., Caiello, B., Ackerson, S. and Stewart, J., (2019). Human CST suppresses origin licensing and promotes AND-1/Ctf4 chromatin association. *Life Science Alliance*, **2**(2), p.e201800270.

Warder, D. and Keherly, M., (2003). Ciz1, Cip1 interacting zinc finger protein 1 binds the consensus DNA sequence ARYSR(0–2)YYAC. *Journal of Biomedical Science*, **10**(4), pp.406-417.

Watanabe, N., Arai, H., Nishihara, Y., Taniguchi, M., Watanabe, N., Hunter, T. and Osada, H., (2004). M-phase kinases induce phospho-dependent ubiquitination of somatic Wee1 by SCF -TrCP. *Proceedings of the National Academy of Sciences*, **101**(13), pp.4419-4424.

Weber, J., Polo, S. and Maspero, E., (2019). HECT E3 Ligases: A Tale With Multiple Facets. *Frontiers in Physiology*, **10**(370), pp.1-8.

Weroha, S., Lingle, W., Hong, Y., Li, S. and Li, J., (2010). Specific Overexpression of Cyclin E·CDK2 in Early Preinvasive and Primary Breast Tumors in Female ACI Rats Induced by Estrogen. *Hormones and Cancer*, **1**(1), pp.34-43.

Wlodkowic, D., Skommer, J. and Darzynkiewicz, Z., (2009). Flow Cytometry-Based Apoptosis Detection. *Methods in Molecular Biology*, (559), pp.19-32.

Wu, J., Lei, L., Gu, D., Liu, H. and Wang, S., (2016). CIZ1 is upregulated in hepatocellular carcinoma and promotes the growth and migration of the cancer cells. *Tumor Biology*, **37**(4), pp.4735-4742.

Xu, G. and Jaffrey, S., (2011). The new landscape of protein ubiquitination. *Nature Biotechnology*, **29**(12), pp.1098-1100.

Xu, G. and Jaffrey, S., (2013). Proteomic identification of protein ubiquitination events. *Biotechnology and Genetic Engineering Reviews*, **29**(1), pp.73-109.

Yanagi, K., Mizuno, T., You, Z. and Hanaoka, F., (2002). Mouse Geminin Inhibits Not Only Cdt1-MCM6 Interactions but Also a Novel Intrinsic Cdt1 DNA Binding Activity. *Journal of Biological Chemistry*, **277**(43), pp.40871-40880.

Yen, A. and Sturgill, R., (1998). Hypophosphorylation of the RB Protein in S and G2 as Well as G1 during Growth Arrest. *Experimental Cell Research*, **241**(2), pp.324-331.

Yin, J., Wang, C., Tang, X., Sun, H., Shao, Q., Yang, X. and Qu, X., (2013). CIZ1 regulates the proliferation, cycle distribution and colony formation of RKO human colorectal cancer cells. *Molecular Medicine Reports*, **8**(6), pp.1630-1634.

Yoo, B., Kang, D., Park, C., Kang, K. and Bae, C., (2017). CKAP2 phosphorylation by CDK1/cyclinB1 is crucial for maintaining centrosome integrity. *Experimental & Molecular Medicine*, **49**(7), pp.e354-e354.

Yuan, J., W. Xu, W., Jiang, S., Yu, H. and Fai Poon, H., (2018). The Scattered Twelve Tribes of HEK293. *Biomedical and Pharmacology Journal*, **11**(2), pp.621-623.

Zhang, D., Wang, Y., Dai, Y., Wang, J., Suo, T., Pan, H., Liu, H., Shen, S. and Liu, H., (2015). CIZ1 promoted the growth and migration of gallbladder cancer cells. *Tumor Biology*, **36**(4), pp.2583-2591.

Zhang, W., Cao, L., Sun, Z., Xu, J., Tang, L., Chen, W., Luo, J., Yang, F., Wang, Y. and Guan, X., (2016). Skp2 is over-expressed in breast cancer and promotes breast cancer cell proliferation. *Cell Cycle*, **15**(10), pp.1344-1351.

Zhao, M., Auerbach, A., D'Costa, A., Rapoport, A., Burger, A., Sausville, E., Stass, S., Jiang, F., Sands, A., Aguilera, N. and Zhao, X., (2009). Phospho-p70S6K/p85S6K and cdc2/cdk1 Are Novel Targets for Diffuse Large B-Cell Lymphoma Combination Therapy. *Clinical Cancer Research*, **15**(5), pp.1708-1720.

Zhou, X., Liu, Q., Wada, Y., Liao, L. and Liu, J., (2018). CDKN1A-interacting zinc finger protein 1 is a novel biomarker for lung squamous cell carcinoma. *Oncology Letters*, **15**(1), pp.183-188.

Zhou, Z., Lujan, S., Burkholder, A., Garbacz, M. and Kunkel, T., (2019). Roles for DNA polymerase δ in initiating and terminating leading strand DNA replication. *Nature Communications*, **10**(3992), pp.1-10.